RESEARCH ON THE DEVELOPMENT OF POLYMERS FOR THE FORMATION OF DYNAMIC MEMBRANES

by

NA DOWLER, RD SANDERSON, AJ VAN REENEN, and EP JACOBS

FINAL REPORT TO THE
WATER RESEARCH COMMISSION

BY THE
INSTITUTE FOR POLYMER SCIENCE
UNIVERSITY OF STELLENBOSCH

PART 1:
COPOLYMERS OF 2,5-FURANDIONE. SYNTHESIS, CHARACTERIZATION AND PROPERTIES IN DYNAMIC MEMBRANE APPLICATIONS

WRC PROJECT: 143
DEC 1986

RESEARCH ON THE DEVELOPMENT OF POLYMERS FOR THE FORMATION OF DYNAMIC MEMBRANES

THIS PROJECT WAS FUNDED BY THE WATER RESEARCH COMMISSION AND CARRIED OUT AT THE INSTITUTE FOR POLYMER SCIENCE AT THE UNIVERSITY OF STELLENBOSCH

THE REPORT IS PRESENTED IN TWO PARTS:

PART 1:
COPOLYMERS OF 2,5-FURANDIONE. SYNTHESIS, CHARACTERIZATION AND PROPERTIES IN DYNAMIC MEMBRANE APPLICATIONS

PART 2:
THE SYNTHESIS, CHARACTERIZATION AND PROPERTIES OF ZIRCONIUM-CHELATING POLYMERS FOR DYNAMIC MEMBRANE APPLICATIONS

ACKNOWLEDGEMENT

The Steering Comittee, co-opted members and referees for this project consisted of the following persons:

Dr CF Schutte	Water Research Commission (Chairman)
Prof CA Buckley	University of Natal
Mr NA Dowler	University of Stellenbosch
Prof W Engelbrecht	University of Stellenbosch
Dr PF Fuls	National Institute for Water Research
Dr OO Hart	Water Research Commission
Mrs MJ Hurndall	University of Stellenbosch
Mr EP Jacobs	University of Stellenbosch
Mr PE Odendaal	Water Research Commission
Dr HS Pienaar	University of Stellenbosch
Dr LS Rayner	University of Stellenbosch
Dr RD Sanderson	University of Stellenbosch
Prof DF Schneider	University of Stellenbosch
Mr DB Smit	Bakke Industries (Pty) Ltd
Mr AJ van Reenen	University of Stellenbosch
Mr PW Weideman	Water Research Commission (Secretary)

The financing of the project by the Water Research Commission and the contribution by the members of the Steering Committee are acknowledged gratefully.

REPORT ON THE RESEARCH ON THE DEVELOPMENT OF POLYMERS FOR THE FORMATION OF DYNAMIC MEMBRANES.

PART 1. COPOLYMERS OF 2,5-FURANDIONE. SYNTHESIS, CHARACTERIZATION AND PROPERTIES IN DYNAMIC MEMBRANE APPLICATIONS

N.A DOWLER, R.D. SANDERSON AND A.J VAN REENEN

EXECUTIVE SUMMARY.

1. INTRODUCTION

The objectives of this study were to (i) synthesize a number of polyelectrolytes which contain maleic aid functionality in aqueous solution and to characterize these polymers; (ii) evaluate these polymers in terms of their ability to form composite dynamic membranes in conjunction with hydrous zirconia membranes; (iii) determine the properties of the membranes formed as functions of time, variation in pH and salt concentration.

From these values it was hoped to derive values for membrane effective charge density and homogeneity index. Futher, the aim was to explaine the properties determined in (iii) above in terms of the chemistry and structures of the polymers concerned and to identify polymers having improved properties when compared to those of poly(acrylic acid) which is the current accepted polymer for this application.

2. POLYMERS

2.1 Synthesis

No useful homopolymers of maleic anhydride were synthesized; only oligomeric products were formed. The following copolymers were produced:

(a) Poly(maleic anhydride-alt-vinyl acetate): four copolymers having different molecular masses.

(b) Poly(maleic anhydride-alt-vinyl alcohol): four copolymers by the hydrolysis of the corresponding vinyl acetate copolymers.

(C) Poly(maleic anhydride-alt-acrylic acid): four copolymers prepared in organic solvent.

(d) Poly(maleic anhydride-co-itaconic acid): one copolymer polymerized in organic solvent.

(e) Poly(maleic anhydride-co-itaconic acid): four copolymers of different molecular masses polymerized in aqueous media.

(f) Poly(maleic anhydride-co-sodium vinyl sulphonate): three copolymers of low molecular mass.

(g) Poly(maleic anhydride-co-glycidyl methacrylate) which crosslinked during polymerization.

The copolymers of itaconic acid, prepared in aqueous media, are novel. A terpolymer of maleic anhydride, itaconic acid and styrene, prepared in organic solvents is, however, described.

2.2 Characterization.

With the exception of two MA/IA copolymers of high molecular mass and the crosslinked MA/GMA copolymers, all copolymers were characterized by dilute solution viscometry using 0,5 mole.dm^{-3} sodium sulphate solution as solvent at 40°C. The intrinsic viscosities were consistent with the predicted molecular mass progression. Attempts to determine M_w values by the use of GPC techniques were unsuccessful due to interactions of the polymers with the column packing. The compositions of a number of representative copolymers were determined by pH titration.

2.3 Evaluation of Properties.

The copolymers which were water-soluble were used to form composite dynamic membranes in combination with hydrous zirconia membranes, using MILLIPORE ultrafiltration membranes as supports. Insights were gained into the mechanism of dynamic membrane formation, and into the role of molecualr mass and chemical structure on the development of properties during formation.

The permanence properties of the membranes were evaluated and explained in terms of chelation properties of the copolymers, and the effects of pH on properties were determined and discussed with reference to chemical structures.

A number of selected polymer membranes were further evaluated for property changes at various salt concentrations, which enabled variables such as effective charge density and micro-homogeneity index to be established for these membranes.

A theory was outlined to explain the differences in microstructure observed in these membranes by reference to the chemistry of the copolymers concerned.

Three copolymers were identified as having performance properties which were significantly better than those of the hydrous zirconia poly(acrylic acid) combination.

These were:

(a) ZrO_2/MA/VA-3
(b) ZrO_2/MA/VOH-4
(c) ZrO_2/MA/AA-4

ABSTRACT

Copolymers were prepared with 2,5-furandione (I) and each of the following co-monomers:

ethenyl acetate (II), 2-propenoic acid (III), methylene butanedioic acid (IV), sodium ethene sulphonate (V).

The (I - IV) copolymers were prepared by free-radical reactions in both organic and aqueous media. The (I - II) copolymers were subjected to alkaline hydrolysis to yield the ethenyl alcohol (VI) copolymer (I - VI). The copolymers were characterized by viscometry in 0,5 M sodium sulphate as solvent at 40°C, but attempts to determine molecular mass by GPC methods, using the same solvent, were unsuccessful. The copolymer compositions were determined by pH titration techniques. Dual composite dynamic membranes were prepared from the copolymers on hydrous zirconia membranes, using "Millipore" ultra-filters as supports. The properties of composite membranes formed from the (I - II), (I - III) and (I - VI) copolymers, as determined by Lonsdale's A^2/B figure of merit as a criterion, were superior to those of a composite membrane formed from poly (2-propenoic acid) of M_w = 148 000. Selected membranes were evaluated for effective charge density ($\bar{X}$) and membrane charge micro-homogeneity index (b). The values of ($\bar{X}$) were found to be equal or greater, and the values of (b) significantly lower, than the values determined for the poly(2-propenoic acid) composite membrane.

An explanation is suggested based on the concepts of ion clusters and micelle formation.

CONTENTS

LIST OF TABLES

LIST OF FIGURES

CHAPTER 3

CHAPTER 4

CHAPTER 5

APPENDIX E

CHAPTER 1

INTRODUCTION

1.1 GENERAL OVERVIEW

The availability of adequate supplies of quality water for agricultural, consumer and industrial uses is one of the pre-requisites for a viable modern economy. South Africa's rapidly expanding population, together with increasing demands from the agricultural and industrial sectors, is placing a strain on the available resources. The periodic droughts which affect the sub-continent have highlighted supply weaknesses in a number of areas and, although present resources are estimated to be adequate for the next 30 years, it is apparent that a long-term strategy is needed for conservation of these resources.

One of the areas of concern is that of pollution of natural water supplies by industrial effluents, and the discharge of these effluents into the sewerage reticulation system.

These practices are becoming increasingly less acceptable and legislation governing industrial effluent disposal will undoubtedly become more stringent in the future. This must result in more attention being paid to extensive treatment of effluents to restore the water to re-use standards.

A feature of the last decade has been that energy costs have increased much more rapidly than capital investment costs and this relationship is unlikely to be radically upset in the near future. As a result, energy-efficient means of effluent treatment have gained prominence, with reverse osmosis (RO) techniques becoming increasingly important.

Within the general sphere of RO techniques, dynamic membrane

systems have shown particular promise in the areas of treatment of effluents difficult to treat by conventional membranes and traditional techniques. A comparison of dynamic membrane with conventional RO membrane systems indicates the following major advantages of dynamic membranes:

(1) Greater resistance to fouling by organic contaminants.
(2) Higher fluxes than those of conventional membranes.
(3) Easy, low-cost regeneration of membranes in situ.
(4) Ability to operate at temperatures of up to 95°C with good efficiency and long membrane life.
(5) Wide pH tolerance.

Dynamic membranes have shown promise, both in terms of performance and cost effectiveness, in a number of large-scale applications. Examples are the treatment of effluents from polymer plants, wool-scouring facilities and textile-dyeing plants. The field of dynamic membranes has been the object of a considerable research effort over the last 20 years, principally in the area of engineering development and applications research on the original hydrous zirconia - poly(acrylic acid) composite membrane system. Little research work has been performed on polyelectrolytes other than poly(acrylic acid).

1.2 OBJECTIVES

The number of polyelectrolytes which have been evaluated in composite dynamic membrane applications is quite small. The overall objective of the research programme reported in this thesis was to investigate the potential use of polymers containing the maleic acid group in such dynamic membranes. In general terms, polymers for this application must satisfy three requirements:

(1) The polymers must react chemically in some way with the underlying hydrous zirconia membrane to form a composite.

(2) The polymers must themselves form a coherent membrane film.

(3) The composite membrane formed must exhibit better rejection properties than the hydrous zirconia membrane alone.

Maleic anhydride was chosen as a component of all copolymers to be synthesized as its aqueous chemistry (as the maleic acid moiety) indicated that strong chelation to zirconium was to be expected, thus fulfilling the first of these requirements. Maleic acid groups not involved in chelation would be partly ionized at neutral pH, producing a negatively charged membrane having salt-rejection properties. Copolymerization with co-monomers, containing groups shown to produce effective salt rejection in other membrane systems, was used as a means of improving performance in terms of the second and third requirements.

The objectives of this study may therefore be stated in the following terms:

(A) Synthesize a number of polyelectrolytes which contain maleic acid functionality when in solution and characterize these polymers in respect of molecular mass and composition.

(B) Evaluate these polymers in terms of their ability to form composite dynamic membranes with hydrous zirconia sublayers.

(C) Determine the properties of the membranes formed, in respect of salt-rejecting and flux properties, as a function of time, pH and salt concentration. Additionally, composite membrane properties are to be evaluated, specifically

(1) membrane micro-homogeneity index;
(2) membrane fixed-charge index;
(3) thermodynamically effective fixed-charge density.

(D) Attempt to relate polymer structure and molecular mass to membrane performance.

(E) Identify copolymers containing maleic acid functionality, that form composite dynamic membranes having improved properties when compared with poly(acrylic acid), which is the accepted present state-of-the-art polymer.

CHAPTER 2

HISTORICAL BACKGROUND

2.1 REVERSE OSMOSIS

2.1.1 INTRODUCTION

The terms reverse osmosis and hyperfiltration are used to describe a pressure-driven process for the separation of water, partially or essentially purified, from an electrolyte solution by use of a semipermeable membrane. This definition is limited to aqueous systems which is the area of interest here, but its scope may be extended to include solvents other than water and contaminants other than electrolytes.

The terms quoted above are in common use to describe the same process and a short discussion of the relative merits of each is needed at this stage. Hyperfiltration is the term that is most commonly used by United States authors and journals and is a logical extension of the series of filtration, microfiltration, ultrafiltration, describing processes for separating materials of particle sizes down to colloidal dimensions from the supporting solvent by means of a direct filtration or sieving process. However, with aqueous solutions the dimensions of the ionic species present are of the same order as that of the water solvent and the sieving mechanism clearly can not apply. Transport of ionic species and solvent molecules in so-called hyperfiltration membranes is clearly by a different mechanism and this term is considered to be inappropriate and will not be used further.

If one considers a perfectly selective semipermeable membrane having pure solvent on one side and an electrolyte solution on the other, solvent will, in a constant-volume system, be transported through the membrane to the electrolyte and a

pressure differential will be established across the membrane. Solvent flux will cease when the differential pressure equals the osmotic pressure of the electrolyte solution. Application to the electrolyte side of pressure greater than this osmotic pressure results in a solvent flux from the electrolyte solution to the pure solvent; this flux of solvent from solution under pressure is the basis of the reverse osmosis (RO) process. In practice, membranes are not perfectly selective and some solute will be transported across the membrane. As a result, the pressure necessary to attain the RO condition is less than the osmotic pressure of the electrolyte and is equal to the difference between the osmotic pressures of the solutions on either side of the membrane. In practical cases, applied pressures are much higher than this to enable technologically adequate solvent fluxes to be obtained.

It is considered that the term reverse osmosis most accurately describes this process of flux of solvent from the electrolyte under pressure and will be used in subsequent discussion.

2.1.2 HISTORICAL PERSPECTIVE

The behaviour of semipermeable membranes and the osmotic pressure phenomenon have been known and studied for many years. In the mid-19th century l'Hermite[1] advanced a theory of osmosis, based upon observations of biological membranes, in which was embodied concepts of preferential solvent absorption in membranes which still have some relevance. At about the same time Traube[2], working with artificial membranes suggested a mechanism based upon sieving processes.

Some results of further work in this field by Pfeffer[3] on sucrose solutions were used by Van't Hoff[4] in the development of his theory of osmotic pressure. In the 1930s, Cellophane, that is, regenerated cellulose, membranes were studied extensively by McBain et al[5,6] who described the inverse relationship between rejection and salt concentration, and introduced the concept of a

Donnan equilibrium to give a qualitative explanation of the results.

The first suggestions that such membranes could be used for desalination purposes were made in the late 1950s by Reid[7] and Breton[7,8], who experimented with cellulose acetate (CA) membranes. These workers demonstrated that CA membranes could give a 98% rejection of salts at sea water concentration, but rather low water fluxes. These membranes were uncharged and rejection was not concentration-dependent. Practical membranes of this type, giving permeation rates of up to two orders of magnitude greater were developed by Loeb and Sourirajan[9] using a novel casting process, which was patented.[10]

The use of ion exchangers in RO processes was first studied by McKelvey et al[11] using commercially available electrodialysis membranes. High-rejection membranes had low fluxes and rejection depended on concentration, in accordance with ion exchange theory. The membranes were prepared from organic polymers modified to give the required ionic groups. In principle, inorganic ion exchange materials should function as desalination membranes and some work (using electrodialysis membranes) was performed by Berger et al[12] on membranes formed from zirconium phosphate and a number of hydrous oxides, including that of zirconium. McKelvey and Milne[13] also demonstrated that certain natural minerals having ion exchange properties such as bentonite clays and shales, exhibited rejection properties when formed into a consolidated layer; this system was examined also by Srivastava et al[14]. Salt rejection by treated porous glass membranes containing ionic groups was investigated by Kraus et al[15] and by Elmer[16]. Unfired "Vycor" glasses were shown to exhibit rejection which increased to about 55% at high pH[15]. Etching by acid of one side of a porous glass membrane resulted in higher rejection. Such membranes are reported to be seriously affected by the presence of Ca^{2+} ions which cause irreversible degradation of the glass structure.

The general field of reverse osmosis processes was comprehensively reviewed in a book by Sourirajan in 1970[17] and the thermodynamic theory of reverse osmosis was later well reviewed by Dresner and Johnson.[18]

In the period since about 1970, a large number of publications on RO membranes have appeared and no attempt will be made to cover the subject comprehensively here. However, the literature relating to permanent ("conventional") membranes with fixed charges on their surfaces will be reviewed, as membranes of such an ion exchange type bear some similarity in their chemistry and properties to the dynamic membrane systems which are the principal object of this study.

2.1.2.1 Permanent fixed-charge (ion exchange) membranes

Inorganic ion exchangers in membrane form, including clays, shales and inorganic glasses have been discussed under 2.1.2 above and this section will deal with the historical development of organic ion exchange membranes based on polyelectrolytes.

An early mention of membranes of this nature is contained in a publication by Sachs and Lonsdale[19] who cast poly(acrylic acid) on the surface of a polysulphone ultrafiltration membrane to form a composite membrane with salt-rejection properties approaching those of the CA membranes of the Loeb-Sourirajan type.

Sachs and Zisner[20] examined a number of similar polyelectrolyte composite membranes and made the very important point that such charged, hydrophilic membranes resist organic fouling and are useful in the treatment of sewage effluents.

Other polyelectrolytes examined included poly(vinyl methyl ether)[21] and vinyl acetate copolymers[22] but these showed only transient improvements due to the loss of the supplementary coating. Insolubilization of the coating membrane by ionic

methods was reported by Tadahiro et al[23]. Huang et al[24] have reported the ionic crosslinking of poly(acrylic acid) and a Toray patent[25] covers the ionic crosslinking of partially saponified poly(vinyl acetate). Dalton, Pienaar and Sanderson[26] used ionic crosslinking to produce a variety of poly(vinylacetate) copolymers. Homogeneous polyelectrolyte membranes of sulphonated polystyrene, poly(acrylic acid-co-maleic acid) and poly(1,2-dimethyl-5-vinyl pyridinium methyl sulphate) were crosslinked with metal ions.[27] Homogeneous poly(acrylic acid) membranes ionically crosslinked with Al^{3+} ions are described by Habert[28] and Dickson[38]. A homogeneous poly(styrene-alt-maleic anhydride) membrane (saponified) is also described[29] and a thin-skin asymmetric RO membrane formed from poly(vinyl alcohol) crosslinked by Cu^{2+} ions has been reported.[30]

Interpolymer membranes consisting of a matrix polymer having a polyelectrolyte crosslinked to the matrix have been described by a number of authors. Polyelectrolytes insolublized in this manner include poly(styrene sulphonic acid)[31,32,33] and sodium polystyrene sulphonate.[34]

The surfaces of membranes can be modified chemically to enhance their performance. Aromatic polyamide membranes containing pendent -COOH groups were reported to have superior rejection properties.[35]

Grafting of polyelectrolyte moities to membrane surfaces is a further technique which has received attention. Hence a poly(butadiene) to which 10,3% of maleic anhydride was grafted was converted into a crosslinked membrane with good salt-rejection properties.[36] Other polymers grafted onto membranes are poly(styrene sulphonates), poly(vinyl pyridine) and poly(acrylate esters) which were grafted onto polyethylene membranes[37].

2.2 DYNAMIC MEMBRANES

2.2.1 GENERAL REVIEW

In 1965, during the course of filtration experiments at the Oak Ridge National Laboratory, A.E. Marcinowsky observed that, when sodium chloride solution containing a small amount of thorium tetrachloride was circulated under pressure over a porous silver frit, there was a rapid decrease in permeation. At the same time some of the salt was rejected and the salt concentration in the permeate decreased. The rejection of the salts continued to increase over a period of days while the rate of permeation (or flux) declined. After some days the rejection of the thorium salt had increased to about 100% and the sodium chloride rejection had stabilized. The use of salts of ferric iron and zirconium as membranes were also studied and reported upon. Subsequent work at the same institution showed that a number of other additives such as organic polyelectrolytes, ground ion exchange resin beads and natural polymeric materials such as humic acids also exhibited rejection properties[40,41].

The most successful additives were those which would be expected to form films having ion exchange properties, and their reverse osmosis properties were consistent, at least qualitatively, with the ion exchange hypothesis. Amongst the materials examined were the hydrous oxides of Al^{3+}, Fe^{3+}, Sn^{4+}, Zr^{4+} and Th^{4+} and synthetic polyelectrolytes such as poly(styrene sulphonic acid) and poly(methyl vinyl ether-co-maleic anhydride).

The advantages of these membranes were given as high fluxes (often an order of magnitude better than those of cellulose acetate membranes) and their ability to be formed in situ and maintained by the addition of small amounts of the active substance to the feed. Rejection by dynamic membranes decreased with increase in salt concentration and was generally substantially lower than that achieved with cellulose acetate membranes. Rejection was pH-dependent since the effective charge

varied with pH. The most popular material for use in dynamic membranes was the hydrous oxide of Zr^{4+}, usually manufactured by boiling zirconium oxychloride solutions. This hydrous oxide is cationic at low pH and anionic at high pH, with a minimum in charge density at about pH 7 and it exhibits rather low rejection at normal feed-water pH. The presence of polyvalent counter-ions such as those of calcium and magnesium, and of sulphate ions reduced performance to a major degree.

These problems were addressed by Johnson et al who recognised that dynamic membranes formed from polyacrylic acid (PAA) had rather better properties in the neutral pH range than most other materials [42]. During the course of their work with polyacrylic acid they discovered that when a hydrous oxide membrane, formed dynamically, was exposed to an acid solution containing PAA, a layer of PAA appeared to become attached to the hydrous oxide membrane. When a base was added, the PAA was not removed[43]. The dual-layer membrane which was formed was superior in most respects to any dynamic membrane previously produced, and this development was the crucial step in the development of practical dynamic membrane systems.

At this time, however, little was known of either the mechanisms of formation of dynamic membranes or of rejection by such membranes, and during the following decade these problems were investigated. In 1977, Freilich and Tanny[44] reported on a study of the kinetics of growth of a hydrous zirconium dynamic membrane and concluded that a model based upon a two-stage process was a good fit. The first stage involved "pore-filling" of the substrate followed by the growth of a conventional filter cake on the membrane surface. These authors also commented that small quantities of oil or grease in the system had a highly adverse effect on the reproducibility of results.

The mechanism of deposition of the polyacrylic acid layer on the surface was studied by Tanny and Johnson[45]; their results indicated that the polyacrylic acid enters the pores of the

preformed hydrous zirconium membrane and does not form a surface layer.

In the same year Freilich and Tanny[46] published their results concerning the structure of a dynamic membrane as a function of support pore size and crossflow velocity. They concluded that support pore size was not critical but that the membrane structure was controlled principally by the crossflow velocity. Scanning electron microscope studies on hydrous zirconium membranes indicated thickness to be 8-30 micrometres and equivalent pore radius to be about 20 Angstroms. Tanny also published a comprehensive review[47] in the same year categorizing types of dynamic membranes. Igawa et al[48] also examined dual-layer membranes containing aluminium and zirconium hydrous oxides, and confirmed Freilich and Tanny's findings that most of the supplementary polyelectrolyte was within the pore structure.

As mentioned previously, support materials for the initial membrane formation do not appear to have a major effect on membrane properties. In the initial studies at Oak Ridge, reported by Johnson et al in 1972[43] commercial ultrafiltration membrane ("Acropor" and "Millipore") films were used wrapped around porous stainless steel tubes, together with porous carbon and ceramic tubes. The use of porous stainless steel tubes of 5 micrometre pore size with the use of various particulate filter-aids is also reported.[49] The tendency in recent years has been towards the use of porous stainless steel tubes of pore size less than one micrometre in commercial plants because of the excellent long-term stability and durability of this material.

2.2.2 Organic Polyelectrolytes

Considering only the dynamic dual-layer membrane system, the number of polyelectrolytes evaluated has been rather small. The original work on this system[43] involved the use of polyacrylic acid (PAA). In this study PAAs of molecular mass from 5×10^3 to

about $1x10^7$ were examined and it was determined that, under the set of formation conditions used, observed rejection (R_{obs}) was significantly dependent on PAA molecular mass.

As an example, using as a support a 0,1 micrometre pore size "Millipore" membrane observed rejection at a molecular mass of 5×10^3 was 70%, rising to about 93% at molecular mass 5×10^4 and decreasing to about 77% at a molecular mass of 3×10^5. Permeate flux generally declined slowly with increase in molecular mass to 5×10^4 and increased at molecular masses above this figure. Attachment of PAA to the the hydrous zirconium membrane occurred only at low pH values and desorption did not occur when the pH was raised. The only other work reported in the literature directly relating to other organic polyelectrolytes used in these dual-layer membranes was published by Spencer, Todd and McClellan in 1984[50]. Their approach was to post-treat an existing hydrous zirconia/ polyacrylic acid (ZOPA) membrane with weak base polyelectrolytes containing amine functionality to form what was termed a "polyblend" membrane. These membranes exhibited a higher fructose rejection than the conventional ZOPA membrane but had no other advantages.

Other single-layer membranes deposited on porous supports are reported by Ozari et al[51] based on poly(acrylic acid), poly(styrene sulphonic acid) and poly(vinyl sulphonic acid) and block copolymers of these materials. No dynamic membrane formation (using CA supports) was reported for the poly(styrene sulphonic acid) and poly(vinyl sulphonic acid) systems.

Igawa et al[52] studied the deposition of dynamic membranes on "Millipore" ultrafiltration membranes of 0,025 μm pore size using poly(acrylic acid), poly(1-methyl-2-vinyl pyridinium iodide) and methyl cellulose. These researchers noted that an increase in molecular mass of PAA was accompanied by a general increase in rejection. Typical figures quoted were (molecular mass/rejection), 2 900/64%, 25 000/60%, 216 000/88%. Unfortunately, no PAA polymers in the molecular mass range 50 000

to 150 000 were studied. The formation of dynamic membranes from feed constituents in pulp mill sulphite wastes has also been reported[53]. Poly(acrylamide) dynamic membranes have also been formed on "Millipore" filters[54].

2.2.3 Dynamic membrane applications

The major advantages of ZOPA dynamic membranes can be summarized briefly as:

(1) Very high fluxes with moderate rejection.
(2) Temperature resistance to 100°C without loss of properties.
(3) Wide pH range with improved properties at high pH (up to pH 10).
(4) Good resistance to organic fouling.
(5) Membranes capable of being stripped and reformed in situ.

A major disadvantage has been the high costs involved in the porous stainless steel support tubes, which makes the process relatively high in fixed cost structure, while running costs are relatively low. Major commercial applications to date lie mainly in the recycling of hot effluents from textile dyehouse dyeing becks[55]; the treatment of laundry wastes[56] and shower and laundry wastes[57]. In the case of dyehouse effluent, savings due to hot water recovery, energy management and dye recovery made for a cost-effective process, and a number of these installations have been commissioned. A study of the use of dynamic ZOPA membranes for the recovery of spacecraft high-temperature wash water has been published[58].

Groves et al[59] have examined the use of ZOPA membranes for the treatment of difficult industrial effluents, including polymer plant discharges, dyehouse effluents and wool scour effluents.

2.3 HOMOPOLYMERS AND COPOLYMERS OF 2,5, FURANDIONE

2.3.1 Introduction

The chemistry of poly(2,5-furandione), known also as poly(maleic anhydride), and its copolymers has been very extensively studied because of the wide commercial use of maleic anhydride in copolymers for the manufacture of unsaturated polyesters and in copolymers and terpolymers for the surface coating industry. This review will therefore include only those polymers and copolymers defined in the objectives section of this thesis.

2.3.2 Homopolymerization

Prior to 1960, it was believed that maleic anhydride (MA) would not form homopolymers under any conditions. However, in 1961 Lang et al[60,61] obtained a copolymer by irradiating molten monomer with gamma radiation. Polymer was also formed in lower yields by irradiation of the monomer in acetic anhydride solution and in dioxane and benzene. This result was confirmed by Heseding and Schneider in 1977[62]. A polymer of average molecular mass 23 000 was reported to be formed under melt irradiation conditions, whereas only oligomeric products were formed in benzene solution.

Polymerization by free-radical means was investigated extensively by Bartlett[63] and Lang[61], who showed that the reaction proceeded slowly and that it yielded only oligomeric products having a degree of polymerization (DP) of about 10 to 30.

Higher molecular masses produced by the incremental addition of free-radical initiators to the molten polymer have been patented[64]; this patent claimed also that the use of benzoyl peroxide in a total amount of 5% of the mass of monomer in 5 additions of 1%, yielded homopolymers of molecular mass 30 000 to 94 000. A further patent[65] described the use of acetyl peroxide

at 2-6% m/m in the melt, to produce polymers of molecular mass 3 500 - 7 500.

The patents disclose that carbon dioxide is liberated during polymerization to yield a partially decarboxylated polymer. Elimination of carbon dioxide is also reported during free-radical polymerization using various solvents and initiators[66,67] to produce a partially decarboxylated polymer. No information on molecular mass is given. Homopolymerization appears to require large quantities of active initiator and high temperature to be successful and this led Gaylord et al[68,69] to advance the concept that, whereas MA will not itself polymerize, excited MA readily polymerizes and propagation is via the monomer or dimer excimer reacting with ground-state monomer. This was confirmed[60] by carrying out peroxide-induced polymerization in the dark in the presence of photosensitizers having 284-355 KJ/mole triplet energies, which increased the yields substantially. When quenchers were added molecular masses were reduced.

Ionic polymerization of MA has been attempted but no satisfactory polymer was obtained.

MA will spontaneously polymerize in the presence of imidazoles[70], poly(1-vinyl-2-methyl imidazole)[70] and poly(4-vinyl pyridine)[71] due to formation of charge-transfer complexes with the pyridine and imidazole moities present in the polymer chain, to produce grafted structures rather than homopolymers.

2.3.3 Alternating copolymers

It is now generally accepted that MA, being electron deficient, can form charge-transfer complexes with electron donor monomers and polymerize to form regular alternating copolymers, whatever the composition of the monomer mixture.

2.3.3.1 Copolymers with vinyl ethers

Both alkyl and aryl vinyl ethers undergo free-radical copolymerization to produce equimolar alternating products[72]. The rather slow spontaneous polymerization is catalyzed by aluminium trialkyls[73]. A commercially useful polymer, equimolar poly(methyl vinyl ether-co-maleic anhydride) ("Gantrez AN"), is prepared in aromatic solvents at 50°-80°C, the ether being slowly added to a refluxing solution of MA with benzoyl peroxide (BPO) as initiator[74].

2.3.3.2 Copolymers with vinyl esters

The only vinyl ester to be studied in any detail is vinyl acetate. Several authors have stated that a charge transfer complex (CTC) is involved in the alternating copolymerization[75-77]. The reaction proceeds easily in bulk or solution at 50°-80°C when BPO is used as initiator. At temperatures above 90°C the CTC is not formed and a random copolymer is produced[78]. Aqueous polymerization to give alternating vinyl acetate/maleic acid copolymers has been reported[79].

2.3.3.3 Copolymers with vinyl ketones

An alternating mechanism has been suggested[80] for the copolymerization of vinyl cyclohexyl ketone with MA. No other ketones appear to have been studied.

2.3.3.4 Acrylic monomers

With acrylic acid, equimolecular alternating polymers are formed when MA is in excess, which could be explained only by assuming the formation of a CTC[81,82]. This is supported by the results of ultraviolet spectral studies. Shantarovich et al[82] asserted that the CTC was intramolecularly hydrogen-bonded and that it yielded a stereoregular polyacid on polymerization.

Acrylamide is reported[83,84,85] to form alternating copolymers with MA and with some derivatives of MA.

2.3.4 Random copolymers

2.3.4.1 Vinyl sulphonic acid

Vinyl sulphonic acid has been shown to copolymerize readily with MA in the presence of free-radical initiators[86]. No information regarding the molecular mass of the product is given in the patent specification.

2.3.4.2 Glycidyl methacrylate

Random copolymers of glycidyl methacrylate with MA have been described in the patent literature[87,88,89]; these are produced by the use of free-radical initiation in aromatic solvents. The copolymers are of a random structure and no information on molecular mass is given.

CHAPTER 3

THEORETICAL INTRODUCTION

3.1 REVERSE OSMOSIS

A detailed discussion of the theories and mechanisms of salt rejection by reverse osmosis (RO) membranes is inappropriate to this thesis. The reader is referred to the excellent review by Dresner and Johnson[90] who make the important point that, unlike ultrafiltration membranes, RO membranes can not separate salts from water by a sieving action but only by affecting the thermodynamic and transport properties of the salts and water by short-range Van de Waals forces or, as in the case of charged membranes, by long-range coulombic forces.

Salt rejection is still considered to be a complex process and no totally satisfactory mathematical models have been developed, largely because the process involves substantially non-equilibrium thermodynamics. Phenomenological analyses by means of mathematical models of rejection behaviour have been developed extensively, however, and the particular case of a single solute (electrolyte) -ion exchange system is described well on page 438 of the abovementioned review[90].

3.2 THE AQUEOUS SOLUTION CHEMISTRY OF ZIRCONIUM

Zirconium is an element of the second transition series (Group IV A) and normally exhibits a valency of 4. Zirconium cations have a maximum coordination number of 8 and show no stereochemical preferences. The high coordination number is due to the high charge density of the Zr^{4+} ion.

There is clear evidence that Zr (IV) species are polymeric in aqueous solution[91]. Evidence of this was obtained by X-ray diffraction studies on zirconyl chloride crystals, which have a

composition $ZrOCl_2.8H_2O$. The zirconyl "ion" in these compounds was shown to be a tetramer $[Zr(OH)_2.4H_2O]_4^{8+}$ consisting of the four zirconium atoms located at the corners of a slightly distorted square, linked by double hydroxyl bridges above and below the plane of the square. The coordination numbers of the zirconium centres are completed by having four water molecules bonded to each. The halide ions are not bonded to the zirconium atoms but are held within the crystal lattice. The aqueous chemistry is more complex and has been reviewed by Clearfield[93]; a short synopsis of the review is given below.

The zirconyl system on dissolution in water forms a strongly acid solution due to hydrolysis, though the tetrameric species remains intact

$$[Zr(OH)_2.4H_2O]_4^{8+} \rightleftharpoons [Zr(OH)_{2+x}\ (4-x)H_2O]_4^{(8-4x)+} + 4xH^+$$

Fig. 3.1 Hydrolysis of zirconyl ion
(the accompanying halide ions have not been shown)

The hydrolysis step may be represented structurally as

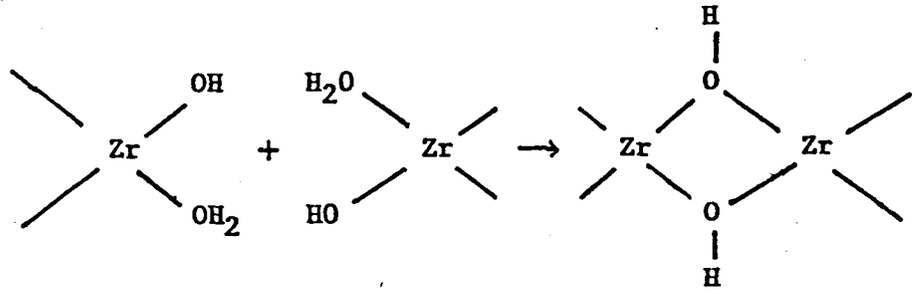

Fig. 3.2 Detail of olation process

(The Zr coordination sphere is made up with H_2O molecules)

Within the tetramer complex there are two sets of di-ol bridges bonded to each zirconium atom lying in planes at right angles to one another. Further condensation can occur between adjacent

tetramers in such a way as to place the new diol bridges at right angles to those already present, allowing for simultaneous polymeric growth in many directions. This would tend to produce a random structure as in Fig. 3.3.

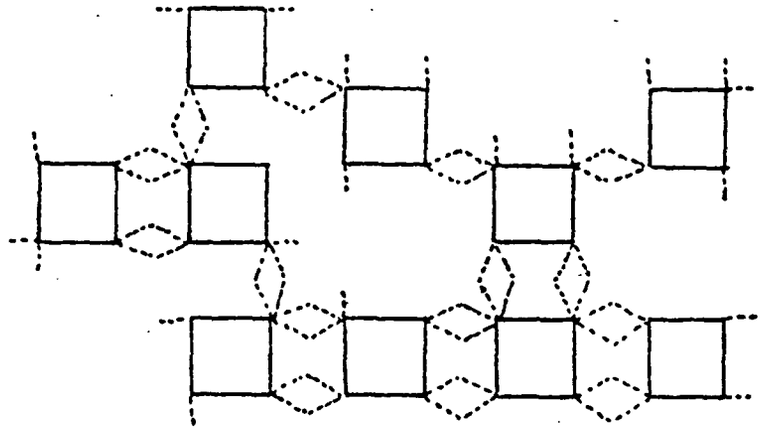

Fig. 3.3 Random hydrous zirconium polymer

This growth habit would be favoured by rapid polymerization brought about by rapid increase in pH.

When polymerization is brought about slowly, the structure obtained is much more orderly and would lead to the formation of polymeric sheets of composition $[Zr(OH)_4]_n$ where the Zr-Zr distance would be 3,56 Angströms.

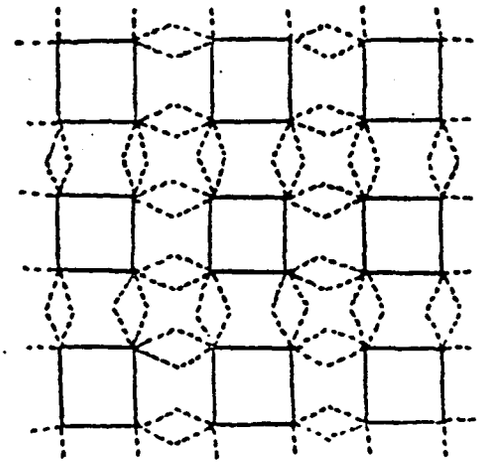

Fig. 3.4 Ordered sheet polymer of hydrous zirconia

Figures 3.3 and 3.4 require further explanation as these are two-dimensional representations. The squares of solid lines represent the original $Zr_4(OH)_8$ tetrameric units. Dashed lines represent -OH groups formed by hydrolysis. A bent dashed line represents a hydroxyl bridge, the diol bridges connecting the orginal tetramer units being visualized as lying both above and below the plane. Further polymeric sheets are laid down and condensation occurs between hydroxyl groups in adjacent layers with the formation of -oxo- bridges.

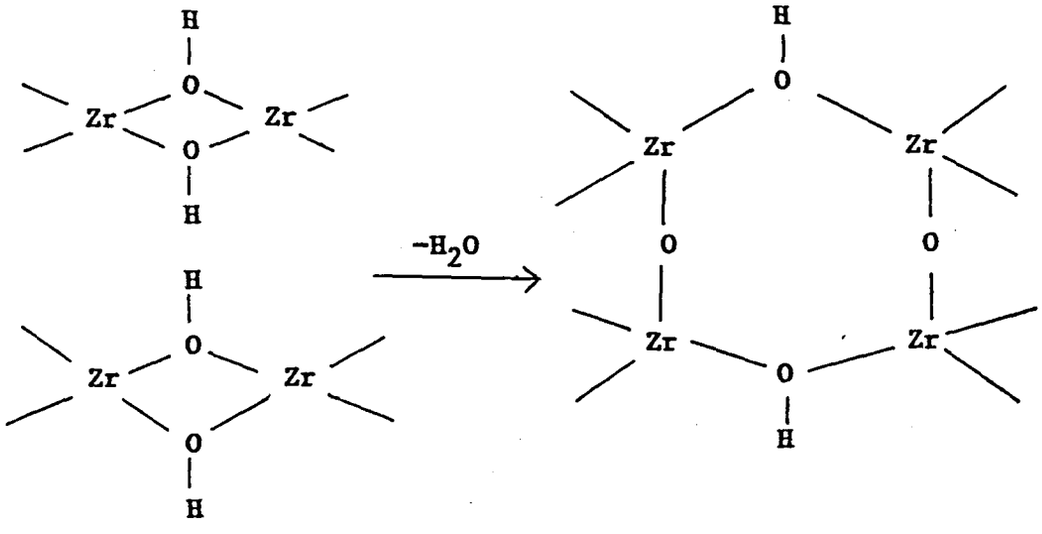

Fig. 3.5 Interlayer oxolation of polymeric hydrous zirconia.

In this way the layers aggregate into a three-dimensional structure having a rather indefinite composition containing:

(a) Zirconium centres linked by -ol and-oxo groups.
(b) Water molecules coordinated to Zr centres.
(c) Reactive hydroxyl groups.
(d) Loosely bound free water and chloride counter-ions.

The polymerization reaction may be induced by boiling a zirconium salt solution or by raising the pH of the aqueous solution of the salt to above 0,3. At pH above 0,7 polymerization is quite rapid[91].

3.3 POLYMERIZATION PROCESSES

3.3.1 FREE-RADICAL INITIATORS

The only initiators which have been used in this st
α,α' -azo bis(isobutyronitrile) and benzoyl peroxi
organic solvents) and potassium persulphate (for
systems).

3.3.1.1 α,α' -azobis(iso butyronitrile) decomposition

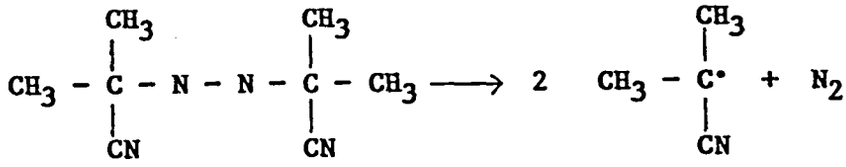

Fig. 3.6 Decomposition of AIBN

3.3.1.2 Benzoyl peroxide radical formation

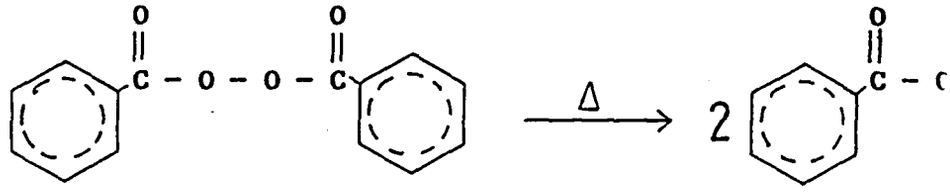

Fig. 3.7 Decomposition of benzoyl peroxide

The radicals formed are highly reactive and are capa
abstraction from most monomers (including maleic anh
form chain radicals.

3.3.1.3 Radical formation from potassium persulphate

$$S_2O_8^{2-} + HSO_3^- \longrightarrow SO_4^{2-} + [SO_4^-]\cdot + [HSO_3]\cdot$$

Fig. 3.8 Sulphate radical formation

This is a persulphate - bisulphite redox system and is effective at low temperatures.

3.3.2 MOLECULAR MASS CONTROL IN FREE-RADICAL POLYMERIZATION

Molecular mass is an important value for determining the performance of polymers in dynamic membrane applications. A number of methods may be adopted for control, including regulators and chain transfer agents, but in this study molecular mass was controlled by varying initiator concentration in relation to monomer concentration.

The equations for steady-state kinetics of free-radical polymerization are well known and will not be derived, but the general expression for the degree of polymerization in such a system is given by

$$1/DP_n = (K_{TC} + K_{TD})/K_p^2\ [M]^2 + C_M + C_I\ [I]/[M] + C_S\ [S]/[M]$$

where K_{Tc} = rate constant for termination by combination
K_{Td} = rate constant for termination by disproportionation
K_p = propagation rate constant
[M] = monomer concentration
[I] = initiator concentration
[S] = solvent concentration
C_M = transfer constant to monomer
C_I = transfer constant to initiator
C_S = transfer constant to solvent

It can be seen that if the system variables are kept constant in terms of solvent type, solvent and monomer concentrations, and temperature (which affects the transfer constants), the ratio [I]/[M] is the controlling term and an increase in the initiator concentration will result in a reduction in the degree of polymerization.

The magnitude of the change with increase in [I] is, of course, determined by the absolute values of the constants in the equation, and the effect of initiator concentration change may be quite small if the transfer constants to monomer and to solvent are high.

3.3.3 FREE-RADICAL HOMOPOLYMERIZATION OF 2,5 FURANDIONE (MALEIC ANHYDRIDE)

Examination by ^{1}H and ^{13}C Fourier transform NMR of peroxide-initiated poly(maleic anhydride) by Regel and Schneider[94] has demonstrated conclusively that such polymers contain the poly(2,5-dioxotetrahydrofuran-3,4-diyl) structure and are therefore predominantly of the structure given in Fig. 3.9

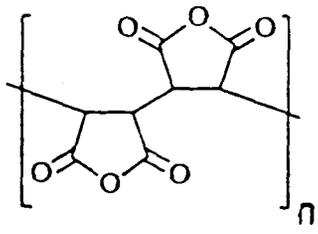

Fig. 3.9 Structure of poly(maleic anhydride)

A small amount of decarboxylated polymer may also be present. Polymerization requires large amounts of initiator (2-10 mole %) and molecular masses have been shown to be only 500 - 1 000 and the yields to be very low, with trapped radicals being detected[95]. Reaction schemes for common free-radical initiators are given below.

3.3.3.1 Homopolymerization using AIBN initiator[95,96]

[AIBN is an abbreviation for α,α' azo bis (isobutyronitrile)]

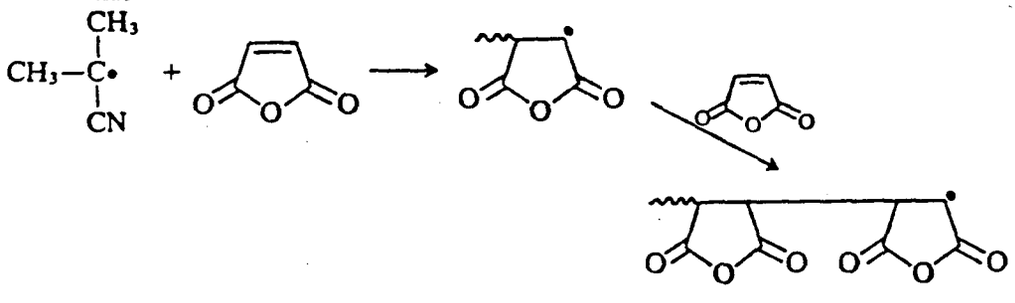

In the presence of high initiator concentration, there is transfer to initiator.

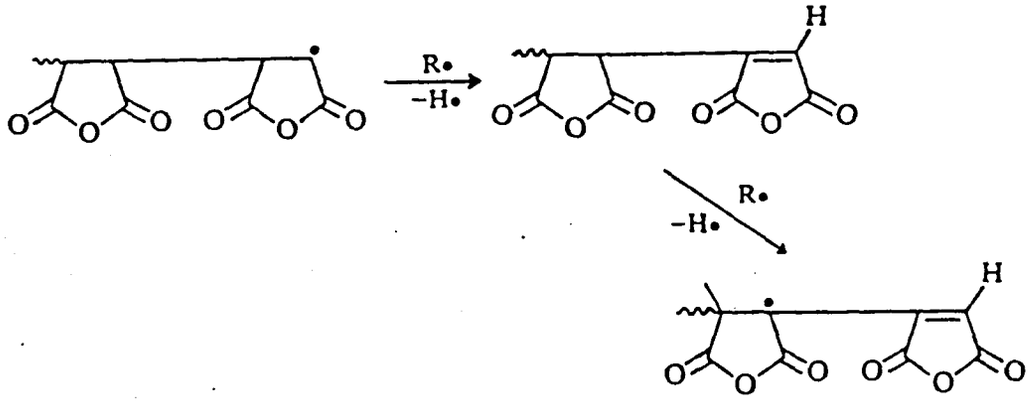

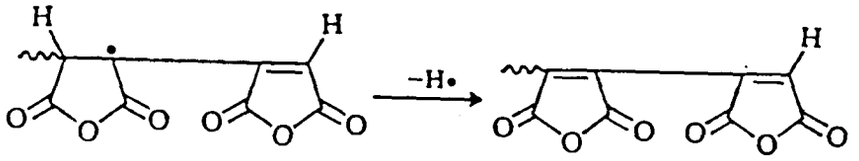

Fig. 3.10 AIBN initiated homopolymerization of maleic anhydride

3.3.3.2 Homopolymerization using benzoyl peroxide initiator

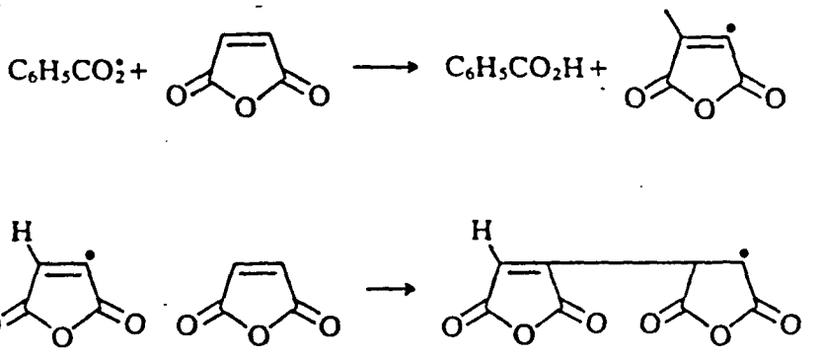

Leading to the formation of a polymer. These radical species can form a conjugated radical due to the influence of unpaired electrons, and carboxyl and maleoyl groups.

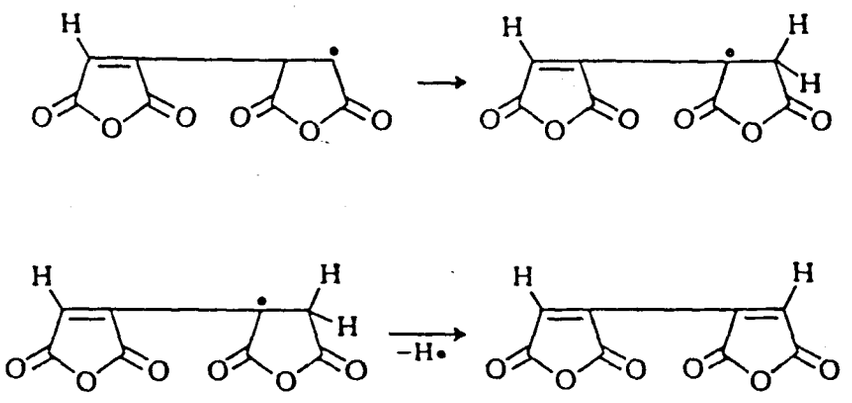

Fig. 3.11 Benzoyl peroxide-initiated homopolymerization of MA

The conjugated polymer systems which result are resistant to polymerization and the predominance of these termination reactions limits the attainable molecular mass to a low figure.

3.3.3.3 Solvent effects in free-radical homopolymerization

Cyclic ethers[95] are effective chain-transfer agents and tetrahydrofuran and dioxane as chain transfer solvents have been observed to increase kinetic rate and yield.

3.3.3.4 Maleic anhydride radicals as cationic initiators

The conjugated radical of maleic anhydride has been shown to be capable[96] of initiating cationically certain olefin oxides via a resonance structure.

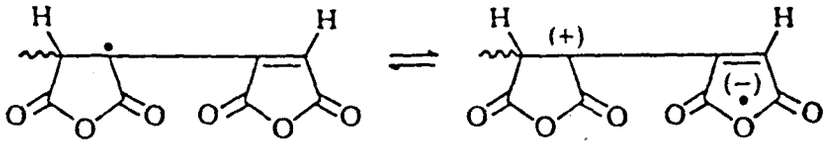

Fig. 3.12 Conjugated MA radical - resonance structure

3.3.4 INTRODUCTION TO COPOLYMERIZATION

Specific copolymer compositions can be designed by use of the copolymer equation[98,99], which is discussed briefly below.

When two monomers M_1 and M_2 copolymerize, the relationship between the polymer composition and the monomer mixture is given by

$$\frac{dm_1}{dm_2} = \frac{M_1(r_1M_1 + M_2)}{M_2(r_2M_2 + M_1)}$$

where M_1 and M_2 are molar concentrations in the monomer mixture, and m_1 and m_2 are molar concentrations entering the polymer; r_1 and r_2 are the reactivity ratios for monomers 1 and 2, respectively.

The free-radical propagation reactions during copolymerization are given as

$$M_1^{\bullet} + M_1 \xrightarrow{k_{11}} M_1M_1^{\bullet}$$

$$M_1^{\bullet} + M_2 \xrightarrow{k_{12}} M_1M_2^{\bullet}$$

$$M_2^{\bullet} + M_2 \xrightarrow{k_{22}} M_2M_2^{\bullet}$$

$$M_2^{\bullet} + M_1 \xrightarrow{k_{21}} M_2M_1^{\bullet}$$

The monomer reactivity ratios r_1 and r_2 for a given monomer pair are defined as

$$r_1 = K_{11}/K_{12}$$

$$r_2 = K_{22}/K_{21}$$

The product r_1r_2 is frequently used as an index to determine the

alternating tendency in binary copolymerization.

The ideal (random) copolymerization case is where $r_1 r_2 = 1$ (r_1 and r_2 being individually close to the value 1).

Where r_1 and r_2 are both small and $r_1 r_2$ tends to zero, an alternating tendency is indicated.

The values of r_1 and r_2 have been determined for many systems, but values are not quoted for some of the copolymers examined or considered in this study. These values can be derived from the Alfrey-Price Q and e values[100] which are quoted for many individual monomer species. Accordingly

$$r_1 = K_{11}/K_{12} = (Q_1/Q_2) \exp [-e_1(e_1-e_2)]$$

$$r_2 = K_{22}/K_{21} = (Q_2/Q_1) \exp [-e_2(e_2-e_1)]$$

This scheme is regarded as being semi-empirical, but may be useful for predicting the type of copolymer that will be formed. In the case of maleic anhydride copolymers, the formation of charge transfer complexes can force alternation when r_1 and r_2 values calculated from Q-e values would not indicate the likelihood of such structures. This technique must therefore be used with circumspection.

3.3.5 ALTERNATING COPOLYMERS

Conventional free-radical copolymerization usually results in the formation of random copolymers. At the same time certain monomer pairs yield regular alternating copolymers whatever the ratios of the monomer feeds. Maleic anhydride, though it does not homopolymerize under normal free-radical conditions, does produce a large number of alternating copolymer structures. This has been attributed to the participation of 1:1 monomer-monomer,

donor-acceptor charge transfer complexes (CTC) as the propagating species. The most common view holds that reaction occurs by preliminary formation of a CTC between the monomers[103-108] or between the propagating radical and the monomer[109,110]. Conventional free-radical kinetics apply in all cases. Characteristics of alternating systems which involve CTCs can be summarized as follows:

(a) Monomer mixtures may undergo spontaneous polymerization.
(b) Copolymers have 1:1 alternating structures over a wide range of monomer feed ratios.
(c) Charge transfer complexes (spectroscopically confirmed) exist in the reaction mixture.
(d) Reaction rates are usually the maximum at equimolar feed ratios.
(e) Copolymerization may be photochemically initiated.
(f) Polymerization stops whenever one monomer has been consumed.

The formation of the CTC may be represented by

$$ED + EA \rightleftharpoons \underbrace{(ED.....EA)}_{\text{non-bonded}} + \underbrace{(ED^{+}EA^{-})}_{\text{dative}}$$

where ED and EA represent a ground-state electron donor and electron acceptor, respectively. The complex is usually of a donor-acceptor type. The equilibrium constant K may be represented simply by

$$K = {}^{[CTC]}/_{[ED][EA]}$$

A full discussion of CTC polymerizations and kinetics is beyond the scope of this thesis and the reader is referred to Chapter 10 of the excellent review of maleic anhydride chemistry by Trivedi and Culbertson[111].

In this study a number of comonomers have been identified as producing copolymers having potentially interesting chelating structures. Those comonomers that have been identified as having

alternating tendencies are discussed below.

3.3.5.1 Maleic anhydride-alt-methyl vinyl ether

The copolymerization has been shown by du Plessis et al to proceed under mild conditions[101], but only polymer of low molecular mass is formed. Polymer of high molecular mass was produced under high-pressure conditions[102] where the methyl vinyl ether was in large excess. The solvent used was methylene chloride at a temperature of 40-60°C and lauroyl peroxide was used as the initiator.

3.3.5.2 Maleic anhydride-alt-vinyl acetate

Alternating copolymers in this system were reported as long ago as 1949. Imoto and Horiuchi[139] studied the system and found maximum polymerization rate at 1:1 mole ratio. If excess anhydride was present no vinyl acetate homopolymer was formed. Caze and Loucheux[75,75] demonstrated that a CTC was present in the reaction system. At temperatures above 90°C no CTC was present and a random copolymer was formed[112].

Commercial polymer is manufactured in solution or in bulk at 60-80°C, being initiated by BPO. Values of r_1(MA) and r_2(VA) are reported as 0,055 and 0,015.

3.3.5.3 Maleic anhydride-alt-acrylic acid

Alternating polymers are formed[81] when MA is in excess, polymerization being in bulk or in solution with BPO initiator.

The reported reactivity ratios are r_1(MA) = 0,007, r_2(AA) = 15,6. Since a 1:1 polymer is formed it is likely that a CTC is present. El Saied[81] et al showed that the ultraviolet spectra of the monomers changed when they were mixed and assigned the structure below to the CTC formed.

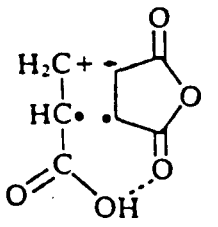

Fig. 3.13 MA/AA charge transfer complex

The internal hydrogen bond gives great stability to the complex. Shantarovich[82] et al proposed a charge transfer complex structure as in Fig. 3.14 and made the observation that the internal H-bonding structure leads to a stereo-regular copolymer.

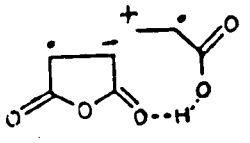

Fig. 3.14 MA/AA CTC giving stereo regular copolymer

3.4 POLYMER CHARACTERIZATION

3.4.1 MOLECULAR MASS DETERMINATION

The polymers synthesized in this work were all strongly acid polyelectrolytes (the first pKa for polymaleic acid is 1,83) and, after purification procedures, were generally available as the partial potassium salts. The only solvent common to all the copolymers was water and it was decided to use aqueous gel permeation chromatography (GPC) as a basic method. GPC is a secondary technique and requires the use of narrow molecular mass polymers as calibration standards. These standards are required to be of a chain structure similar to that of the polymer under study for accurate results.

Molecular mass standards of structure similar to those of the copolymers to be characterized are not available and an

alternative calibration approach is necessary. A solution to the problem is found in the use of so-called "universal calibration" techniques pioneered by Grubisic[113]. A short explanation of the theoretical basis is given below.

3.4.1.1 Universal calibration

GPC methods depend upon measurement of the size of molecules in solution (as discussed in 3.4.1.2 below) and universal calibration techniques depend upon the relationship between intrinsic viscosity, polymer dimensions and molecular mass as expounded by Flory and Fox[114].

$$[\eta] \cdot M_v = \phi_o V_h = \phi (\bar{r}^2)^{3/2} = \phi_o \alpha^3 (\bar{r}_o^2)^{3/2}$$

where $[\eta]$ = intrinsic viscosity
m_v = viscosity average molecular mass of polymer
ϕ_o = a hydrodynamic constant
V_h = hydrodynamic volume
$\bar{r}^2$ = mean square end-to-end distance of the molecule
$\bar{r}_o^2$ = unperturbed mean square end-to-end distance of a molecule
α = an expansion factor

From this basic statement it is clear that the value of $[\eta].M_v$ for a given solvent and temperature is a direct measure of the hydrodynamic volume of the molecule. For GPC evaluation Grubisic[113] determined that

$$\text{Log } [\eta].M_v \propto R_v$$

where R_v is the retention volume for a given column and solvent.

It is therefore possible to determine viscosity average molecular mass if the intrinsic viscosity and GPC retention volumes are

determined.

It is, of course, necessary to calibrate, but polymer standards of widely differing chemistry and structure have been shown to fall on the same calibration line.

This technique is therefore potentially useful in determining molecular masses of the copolymers synthesized, using readily available Dextran standards for calibration. The technique is well established in non-aqueous systems, but little work has been done using aqueous solvents for ionic polyelectrolytes. Particular problems arise in this case since the polyelectrolyte must be undissociated and unassociated in solution. Dissociation of ionic groups leads to a major increase in molecular hydrodynamic volume due to charge repulsion and makes molecular mass values obtained quite meaningless. Spatorico and Beyer[115] demonstrated that the use of sodium sulphate (0,2 - 0,8 mole.dm^{-3}) as an electrolyte allowed the GPC techniques to be used for ionic polyelectrolytes such as sodium polystyrene sulphonate, the electrolyte suppressing ionization of the acid salt.

3.4.1.2 Gel permeation chromatography

Gel permeation chromatography, otherwise known as size-exclusion chromatography, is a well-established technique for separation of molecular mass species by molecular size and will not be discussed in detail. Specific aspects of the technique which relate to polyelectrolytes in aqueous solution will, however, be noted briefly largely by reference to a publication by Rollings et al[116].

The major problems to which the method gives rise, compared with those posed by systems based upon organic solvents are:

(i) Suitable controlled pore-size column packings are difficult to obtain and plate counts are substantially lower than

those of polystyrene-based columns used for organic phase GPC. As an example, based on information given by Waters Associates[117], a typical "ultrastyragel" (polystyrene based) 300 mm column would have a plate count of at least 14 000 whereas the corresponding porous silica-based Micro Bondagel column has a minimum plate count of only 2 500.

(ii) Major problems arise with the hydrodynamic volume of polymers in aqueous solutions. Referring to Section 3.4.1.1 and to Fox and Flory's work [114] it is readily seen that the hydrodynamic volume of a molecule is governed by both the unperturbed mean square end-to-end distance $\bar{r}_o^2$ and the expansion factor α , that is,

$$v_h = \alpha^3 (\bar{r}_o^2)^{3/2}$$

The expansion factor α in the polymer/solvent system is required to be very close to 1 if the hydrodynamic volume function, as determined by GPC universal calibration techniques, is to reflect accurately the actual molecular dimensions and hence the true molecular mass. For polyelectrolytes in polar solvents[116] the conformation of the polymer molecule is significantly expanded from the hypercoiled (α=1) state due to the expansion effect of ionically charged species, since it undergoes hypercoiled to expanded helix conformational changes as charge density increases. A solvent having high ionic strength can repress the changes in conformation and produce an essentially unperturbed molecule.

(iii) Ionic charges in the polymer structure can also cause association with solvent[116], adsorption onto the chromatographic support[118] and excluded ion and included ion effects[119]. These factors seriously affect the use of GPC techniques in this field, causing elution times to be

generally increased with multiple peak effects becoming noticeable[118].

Most of the problems outlined above may be overcome by using a suitable aqueous solvent and Spatorico et al[115] suggested that a suitable ionic strength solvent would be sodium sulphate at concentrations of between 0,2 and 0,8 mole.dm^{-3}. Their studies involved sodium polystyrene sulphonate polymer species, and they demonstrated that reproducible and consistent chromatograms could be produced with this polymer using sodium sulphate solutions for elution. In the present study 0,5 mole.dm^{-3} sodium sulphate was used at a temperature of 50°C as the eluting solvent, since lower temperatures and higher electrolyte concentrations produced unacceptably high back-pressures in the columns used, and increased the probability of column damage. In addition, the use of elevated temperatures is recommended for reducing the problems associated with polymer/solvent interactions with the column packing[120].

3.4.1.3 Dilute solution viscosity

The use of solution viscometry for molecular mass determination is well known in polymer chemistry. The theoretical details will not be reproduced here in full, but a short synopsis of those facets of the topic which are relevant to the present study are given below.

When a polymer is dissolved in a solvent, the solution invariably has a higher viscosity than that of the solvent, the increase being a function of the concentration of the solute and the size of the solute molecules in solution. The relative viscosities of a series of polymer solutions of differing concentrations are determined by measuring their efflux times through a capillary viscometer; the following relationships are determined:

(i) Relative viscosity $\eta_r \approx t/t_0$ *

(ii) Specific viscosity $\eta_{sp} = \eta_r - 1$

(iii) Intrinsic viscosity $[\eta] = \lim_{c \to 0} \left(\eta_{sp}/c \right)$

t = efflux time for solution
t_0 = efflux time for solvent
c = solute concentration in g/100ml

* Note - a correction factor is included in the calculation of η_r from efflux time data. This correction can be ignored for efflux times greater than 200 s. Intrinsic viscosity is determined by calculating values of (η_{sp}/c) at various concentrations (c) and graphically extrapolating to c=0.

It should be noted that for solutes which interact strongly with the solvent system the slope of the above plot is significant. Ideal solvents (non-interacting or theta solvents) have zero slope. In the present study, 0,5M sodium sulphate was used as solvent at 40°C and for most solutes the slopes of the plots were very low, indicating that the solvent was close to the theta condition.

In many cases, intrinsic viscosity values can be used to calculate molecular masses by use of the Flory-Huggins-Sakudara equation. In this case intrinsic viscosity values were used as variables in the universal calibration procedure since the relevant constants were not available.

3.4.2 pH TITRATIONS TO DETERMINE COPOLYMER COMPOSITION

For certain of the copolymers synthesized, it was necessary to determine the composition of the copolymer. All copolymers contained maleic anhydride as a comonomer and the concentration of this comonomer in the polymer was determined by pH titration

of the polyacid with sodium hydroxide to the first end-point of maleic acid at a pH of about 3,6.

3.5 DYNAMIC MEMBRANE FORMATION

3.5.1 ZIRCONIUM DYNAMIC MEMBRANE FORMATION

The formation of hydrous zirconia dynamic membranes on a variety of supports was thoroughly studied by Freilich and Tanny[46] who demonstrated that the formation of such a membrane involved two distinct stages:

(i) A pore-filling or bridging stage where colloidal particles of polymerizing zirconia are captured on the walls of the pores of the support material. This process causes the pores to close after a period of time.

(ii) Formation of a surface filtration "cake" from colloidal particles as commonly occurs in other types of cross-flow filtration systems.

Freilich and Tanny developed mathematical models which correlated well with the observed phenomena and proceeded to examine the effects of varying formation conditions. A summary of their findings is given below.

(i) Support pore size
Pore sizes of 0,025 to 0,45 μm were examined in a number of non-selective support materials. The larger pore size materials required slightly longer to form membranes but this pore size was not important in the overall performance of the membrane.

(ii) pH of formation
As mentioned previously in the discussion of the chemistry of zirconium, the effect of raising pH is to increase the degree of polymerization of the hydrous zirconia particles.

Tanny reported that at pH above 3,5 the larger size of the polymerizing particles formed a membrane of high porosity. At lower pH the zirconia polymer particles became noticeably protonated and electrostatic repulsion effects again resulted in a porous membrane. It was concluded that a pH of formation between 3,2 and 3,8 gave optimum results.

(iii) Feed concentration

If the concentration of zirconium salt in the feed was increased, the time to formation was reduced, but properties were essentially unchanged.

(iv) System pressure

Johnson et al[43] examined the effects of pressure and concluded that high pressures produced membranes of lower flux and higher rejection.

(v) Circulation velocity

Johnson[43] et al determined that membranes formed under high flow rate conditions were invariably thinner, and gave markedly higher fluxes with (typically) higher rejections.

3.5.2 THE FORMATION OF THE POLYELECTROLYTE MEMBRANE

Tanny and Johnson[45] made a specific study of the deposition of polyacrylic acid layers onto hydrous zirconia substrates, and their results, although not conclusive, indicated that the PAA component filled the pores of the sublayer rather than forming a gel layer on the surface. It was suggested that at low pH values the PAA molecules are hypercoiled and easily able to penetrate the zirconia substrate and react with the substrate in some way at this pH. As the pH is raised the PAA molecules ionize and expand to block the pores, causing a rapid flux decline and an increase in rejection.

This model would also explain, and in turn be supported by, the observations made by Johnson, et al[43] on the effect of molecular

mass of PAA. Johnson reported that there is an optimum molecular mass in the range of 50 000 - 150 000 for the PAA polymer if maximum rejection properties are to be demonstrated. Using the pore-filling model it could be postulated that molecules of high molecular mass would be unable to penetrate the pore structure in sufficient concentration to fill the pores. Lower molecular mass material could enter the pores but would be insufficiently swollen at the operating pH to bridge the pore sufficiently to exert the maximum influence on flux and rejection.

3.5.2.1 Formation conditions and performance

(i) System pressure
High system pressures during formation of membranes result in higher rejection and lower flux.

(ii) Circulation velocity
With the polyacrylate layer, high circulation velocity was found to cause a marginal improvement in rejection properties with no effect on flux. Thomas and Mixon[121] recommended circulation velocities greater than $6 ms^{-1}$.

(iii) pH control
Addition of PAA at pH 2, followed by stepwise adjustment of pH of 1 pH unit per 30 minutes was recommended by Johnson[43] and Thomas[121].

(iv) Polyacrylic acid concentration
Tanny and Johnson[45] found little effect on final rejection properties when the initial PAA concentration was varied between 25 ppm and 200 ppm, though the higher concentrations caused a faster initial flux decline.

(v) Polyacrylic acid molecular mass
Johnson's results[43] have previously been quoted in Section 3.5.2.

(vii) Sublayer rejection properties

Tanny[47] demonstrated that an optimum pore size and hence optimum rejection, for a hydrous zirconia sublayer was a prerequisite for good final membrane performance. A rejection of 40 - 50% (of 0.05M NaCl solution) by the hydrous zirconia layer yields the best results in the final composite membrane. This was attributed to optimum "fitting" of polymer size to the sublayer pore size.

3.5.2.2. Chemical interactions

The chemistry of interaction between the hydrous zirconia membrane and PAA membrane has not been studied although some authors have speculated on the possible interaction mechanism. Tanny and Johnson[45] suggested that, as interaction occurs only at low pH, some interaction could occur between the polycarboxylate groups and the cationic zirconium centres. Why such an interaction is not reversible as pH approaches neutrality is not explained, and the authors themselves consider this an unsatisfactory argument. Johnson et al[43] postulated ionic group interactions related to the "complex coacervation" effect between oppositely charged colloids, but no evidence is offered to support this view. It has also been suggested that covalent bonding[122] may be involved in the linkage between the PAA acid groups and free hydroxyls present in the sub-layer structure, but no convincing mechanism is presented.

It is apparent that the structure and chemistry of dynamic membranes are extremely complex and difficult, if not impossible, to evaluate under the non-equilibrium conditions of formation. The work of Hock[123] is therefore particularly helpful in this area since he used model compounds, studying their interactions with zirconium centres in zirconyl tetramers. With di-acids he showed convincing evidence of chelation between the bidendate acid ligand and the zirconium atom, with water molecules being displaced from the co-ordination sphere of the zirconium. This work is fundamental to an understanding of the interaction

processes between hydrous zirconia and organic polyelectrolytes, and the major features of Hock's publication are therefore discussed briefly below. Hock's investigations were centred upon oxidic organic compounds and his conclusions may be summarized thus:

(i) Compounds with single hydroxyl groups will not co-ordinate.

(ii) Polyols (glycols, glycerol and sugars) do show a degree of co-ordination leading to soluble polyol-zirconia complexes at high pH values (10 - 12).

(iii) Monocarboxylic and dicarboxylic acids co-ordinate.

(iv) Hydroxy carboxylic acids with -COOH and -OH groups on adjacent carbon atoms can form very stable structures with both groups involved in the co-ordination.

(v) Ether groups will not co-ordinate.

(vi) β - diketones co-ordinate strongly.

Hock observed that in this system bi- and multidendate ligands complexed much more strongly than monodendate ligands, to produce chelate structures. The stability of the chelate complexes are affected by a number of structural factors:

(i) With metals of the transition series, chelate complexes having 5- or 6-membered rings are particularly stable, since there is minimum bond angle distortion. This is particularly important in stiff chain ligands in which the chelation "bite" is required to be tailored to the co-ordination geometry of the metal.

(ii) Chelation normally spans cis-positions on the metal centre, and this puts a further restraint on the ligand geometry.

(iii) Co-ordination of a flexible long-chain ligand results in a reduction in the overall entropy of the reaction system due to chain immobilization. This would tend to be unfavourable to the formation of complexes, but as chelation involves the displacement of bound water molecules and consequent increase in entropy, complex stability can in fact be enhanced by entropy effects.

(iv) When one ligand group has co-ordinated, the likelihood of formation of a stable multidendate ligand complex is directly related to the density of ligand groups in the vicinity of the co-ordination sphere.

This question of formation of stable complexes must be taken into account when suitable polymers and copolymers for dynamic membrane use are being considered. Strong complex-formation abilities will lead to membrane structures which would be expected to be resistant to degradation and to function over a long period of time without significant loss of properties. The acrylic acid ligand has been used extensively and apparently forms sufficiently stable complexes.

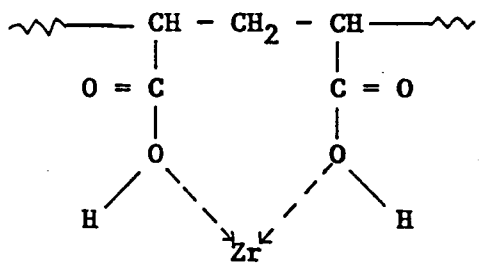

Fig. 3.15 Polyacrylic acid chelation

The maleic acid moiety, incorporated into a polymer chain, could be regarded as having a more favourable "bite", since it forms a smaller chelate ring and induces higher local ligand density.

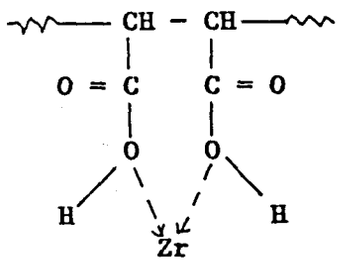

Fig. 3.16 Chelation by maleic acid grouping

Other possible maleic acid copolymer structures having possibly better chelation properties than that of acrylic acid are given below.

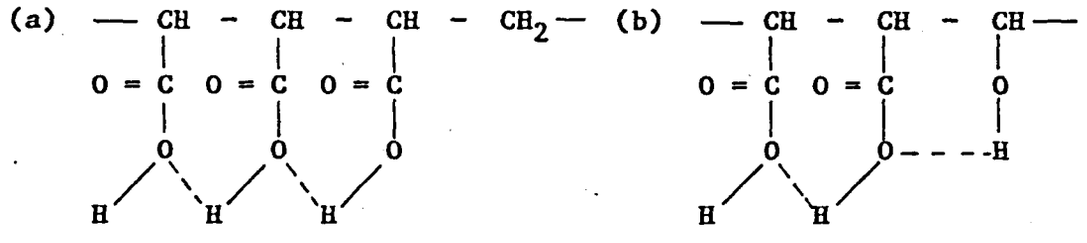

poly(maleic acid-alt-acrylic acid)

Poly(maleic acid-alt-vinyl alcohol)

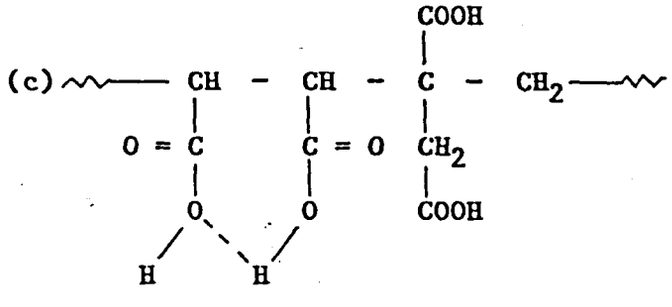

Poly(maleic acid-alt-methylene succinic acid)

Fig. 3.17 Maleic acid copolymers expected to have good chelating properties.

According to Hock's rules, the above copolymers would be expected to have good chelating properties for the following reasons:

(a) Poly(maleic acid-alt-acrylic acid)
A higher local ligand density is present and a number of alternative chelate "bites" are available.

(b) Poly(maleic acid-alt-vinyl alcohol)
In this case an α-hydroxy carboxylic acid group, which was shown to be strongly chelating, is present.

(v) Poly(maleic acid-alt-methylene succinic acid)
This alternating copolymer has a high ligand density with a wide range of possible ligand "bites".

Consideration must also be given to other factors in the choice of suitable copolymers for use as dynamic membranes but the above copolymers have been incorporated in this study specifically because of their chelation potential.

3.5.2.3 Stereochemistry of maleic acid polymers and copolymers

The importance of the maleic acid moiety as the principal chelating group in maleic acid copolymers has been discussed in Section 3.5.2.2. For this chelation to occur effectively the carboxylate functionalities are required to be in a cis-configuration. This is attained in the maleic acid molecule itself by the presence of the double bond, but in the polymer and copolymers it could be expected that free rotation would occur and this arrangement lost. In fact, the alkaline hydrolysis of maleic anhydride polymers and copolymers yields polyacids in which the cis-configuration is maintained by hydrogen bonding forces.

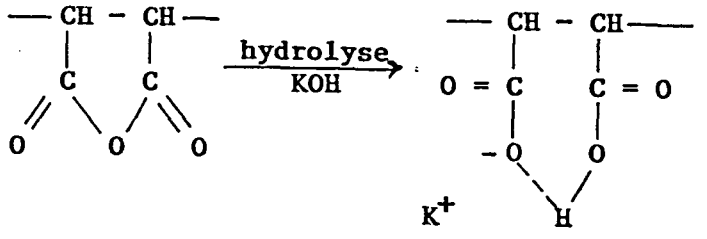

Fig. 3.18 Hydrogen bonding in hydrolyzed poly (maleic anhydride).

This hydrogen bonding is so strong that the second acid group is not titratable under normal conditions and poly (maleic acid) behaves as a monoprotic acid.

Addition of a simple electrolyte at sufficient concentration to repress the first ionization enables the second acid group to be titrated normally. Normal titration behaviour is observed with bases having divalent cations as would be expected.

Polymers and copolymers of hydrolyzed maleic anhydride are therefore shown to have a suitable configuration for the chelation process. In the specific case of poly (maleic anhydride-alt-acrylic acid), Shantarovich[82] et al have demonstrated that a stereo-regular isotactic polymer is formed due to hydrogen bonding effects and this would be expected to form a hydrogen bonded polyacid in much the same way.

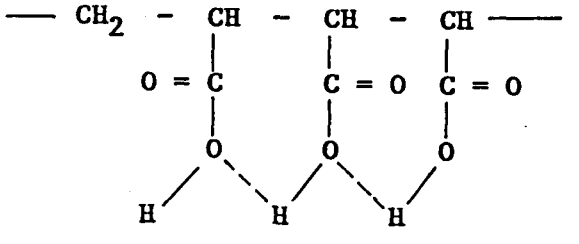

Fig. 3.19 Hydrogen bonding in hydrolyzed poly(maleic anhydride-alt-acrylic acid).

3.6 DYNAMIC MEMBRANE EVALUATION

3.6.1 REJECTION AND CONCENTRATION POLARIZATION

If one considers a reverse osmosis desalination situation in which saline water is being circulated under pressure across the face of a partially rejecting membrane, the observed rejection of the membrane (Robs) can be represented by:

$$R_{obs} = 1 - C_p/C_f \qquad [1]$$

where C_p is the salt concentration in the permeate
C_f is the salt concentration in the feed

The observed rejection will, in practical situations, always be less than the potential rejection of which the membrane is capable. At finite rates of flow, rejected solute builds up in a layer close to the membrane surface. Dynamic membranes demonstrate ion exchange effects which result in a noticeable deterioration of rejection performance at higher feed concentrations. The solute-rich surface layer thereby reduces the rejection performance of the membrane.

This phenomenon has been studied extensively and a review by Shor[124] relating to dynamic membrane systems is recommended for those requiring a detailed analysis. Only the results of the treatment will be presented here.

$$\ell n \left[\frac{1-R_{obs}}{R_{obs}}\right] = k\left[\frac{v}{u^{0,75}}\right]\left[\left(\frac{d}{\eta_k}\right)^{0,25}\left(\frac{\eta_k}{D_2}\right)^{0,67}\right] + \ell n \left[\frac{1-R}{R}\right]$$

R_{obs}	observed rejection of membrane
R	intrinsic rejection of membrane
K	Colbourn factor, (empirical constant)
v	linear permeate flow rate through membrane
u	linear velocity of circulating feed
d	inside diameter of the tubular membrane
ηk	kinematic viscosity of circulating solution
D_2	coefficient of diffusion of the solute

In practice, rejection is monitored at a series of circulation velocities. A plot of

$$(j) \qquad \ell n \left[\frac{1-R_{obs}}{R_{obs}}\right] \alpha \left(v/_u\, 0,75\right)$$

is linear, and extrapolation to infinite circulation velocity [i.e. $(v/_u\, 0,75) = 0$] will enable the intrinsic rejection of the membrane to be determined.

In the present study, which is basically a comparison of membrane properties with those of a control membrane, only observed rejection values are recorded and it must be noted that intrinsic rejections will always be higher. The cross-flow techniques used in rejection measurements are specifically designed such that u (circulation velocity) is high and d (channel diameter) is small. In this way concentration polarization effects are minimized. Certain high flux membranes (where v is increased) would be expected to show rather higher concentration polarization effects. In addition, the rejection properties of ion exchange

membranes show a sensitivity to feed salt concentration and as membranes are evaluated at various feed concentrations, comparison of membranes by their observed rejection values is clearly not entirely satisfactory.

3.6.2 MEMBRANE FIGURE OF MERIT

In an attempt to overcome the problems of membrane comparison associated with concentration and concentration polarization variances and to introduce a consideration of membrane flux, Lonsdale[125] proposed a comparison by means of a "figure of merit" (FOM) determination. Lonsdale proposed that membranes should be evaluated in terms of a figure of merit.

$$FOM = A^2/_B$$

where A is a membrane constant for water permeability
B is a membrane constant for salt permeability

A and B may be defined in terms of fluxes

$$\text{Water flux } F_w = A(\Delta P - \Delta\pi) \qquad [1]$$

where ΔP is the pressure difference across the membrane

and $\Delta\pi$ is the osmotic pressure difference across the membrane

$$\text{salt Flux } F_s = B\Delta C \qquad [2]$$

where Δc is the salt concentration difference across the membrane

As previously discussed in 3.6.1, concentration polarization effects must be considered. The concentration polarization (C_p) is defined as the ratio of salt concentration at the membrane wall (C_w) divided by the concentration in the bulk solution (C_b)

i.e. $$C_p = C_w/C_b \qquad [3]$$

Rosenfelt and Loeb[126] developed an expression for concentration polarization in tubular membranes as follows

$$C_p = C_w/C_b = 1/D_r + \left(1 - 1/D_r\right) \exp \left[F_1 \frac{\eta_k}{D} \Big/ uK\right]^{0,67} \qquad [4]$$

where D_r = ratio of salt concentration in feed/salt concentration in permeate
F_1 = permeate flux
η_k = feed kinematic viscosity
D = diffusion coefficient
u = feed linear velocity
K = Chilton-Colbourn mass transfer factor (an empirical constant)

note $K = 0,023\ N_{re}^{0,17}$
where N_{re} is the Reynolds number for the flow system.

The basic transport equations [1] and [2] can be expanded and simplified:

$$F_1 = A\left[\Delta p - \pi_b \left(C_w/C_b\right) + \left(\pi_b/D_r\right)\right] \qquad [5]$$

$$F_2 = B\, C_b \left[C_w/C_r - 1/D_r\right] \qquad [6]$$

The concentration polarization equation can be expanded fully to

$$C_p = \left(C_w/C_b\right) = 1/D_r + \left(1 - 1/D_r\right) \exp\left[F_1 \eta_k^{0,5} d^{0,17} / 0,023\, u^{0,83}\right] \quad [7]$$

Applying equation [7] to a particular RO situation, it is possible to calculate C_p at a given tube diameter (d) and linear flow velocity (u) for a given solution at a standard temperature and for which the kinematic viscosity (η_k) is known.

The value of C_p (= C_w/c_b), when substituted in equations [5] and [6] enable values of A and B to be determined and therefore of A^2/B. This treatment refers only to tubular membranes. In this particular experimental work a flow channel of semicircular cross-section was used and this equation does not strictly apply. In order to use this treatment the value of (d) in the above equation was taken as the diameter of a circular cross-section having the same area as that of the semicircular channel used. The error introduced is regarded as being small and does not affect the comparison of FOM values for membranes. The data reduction for the large number of measurements was performed by means of a computer programme supplied by Mr A van Reenen[127].

3.6.3 SALT CONCENTRATION AND MEMBRANE PROPERTIES

The polyelectrolyte membranes which are the subject of this study are ion exchange types and their rejection and flux properties are a function of the concentration and type of salt present in the feed. If we are to compare such membranes realistically, we must take these factors into account. The membranes formed and reported in this study were evaluated at various salt concentrations in the feed and some form of normalizing procedure is necessary.

3.6.3.1 Normalization of membrane performance data

A rather simple empirical relationship exists between solute flux (s) and feed concentration (m) in an ion exchange membrane, as outlined by Dresner and Johnson.

$$\log s = E \log m + H$$

where s is the apparent solute passage through the membrane
(s = 1 - R where R is the observed rejection)
m is the molality of the electrolyte in the feed
E and H are empirical constants depending on both electrolyte and membrane type.

For a particular membrane and electrolyte it is therefore possible to determine E and H by measurement of rejection values at varying salt concentration and thereby fully define the relationship between solute passage and concentration and thereby calculate a rejection value at a particular concentration.

Membrane fluxes have a weak inverse relationship to salt concentration and may also be normalized to a given concentration figure. Combining these normalized results into "figures of merit" at a given concentration for a number of different membranes allows assessment of the comparative performance of these membranes in a realistic manner.

3.6.3.2 Fixed charge density and homogeneity index

The empirical constants E and H determined by the procedure outlined in 3.6.3.1 have been shown to have real meaning in terms of membrane structure and charge density by Spencer[146].

Spencer[146] developed an electrolyte exclusion model for RO of electrolytes by charged gel membranes, which included hydrous

zirconia/polyelectrolyte types. The derivation will not be repeated here, but the final form of the derived relationship is given as

$$\log S = \left(\frac{nb}{y} - 1\right) \log m + \log B - \frac{a}{y} \log (\bar{M}/ay)$$

where
- s = apparent solute passage
- m = molality of salt in the feed
- a = counter-ion subscript in the electrolyte A_aY_y (=1 in the case of $NaNO_3$)
- y = co-ion subscript in the electrolyte A_aY_y (=1 in the case of $NaNO_3$)
- n = a + y
- b = micro heterogeneity parameter
- $\bar{M}$ = molality of free fixed charges in the active membrane layer
- B = coupling constant for solute and solvent in the membrane

In the case of the 1:1 electrolyte sodium nitrate, this equation reduces to

$$\log S = (2b - 1) \log m + (\log B - \log \bar{M})$$

It can readily be seen that a plot of log s against log m will have:

$$\text{slope} = (2b-1)$$
$$\text{intercept} = \log B - \log M$$

The value of (b) determined from the slope is termed an "index of membrane fixed-charge homogeneity".

Fixed-charge density ($\bar{M}$) can be determined from the intercept of the plot if a value for (B), the coupling coefficient, is assigned.

There have been two approaches

(a) Estimate B from the limiting diffusion coefficients of the counter-ion D_A^o and co-ion D_y^o using the relationship

$$B = 1 + a\,(D_y^o / D_a^o)$$ which is good approximation for dilute solutions

(b) Assign B=1

This approach will only enable comparisons to be made and a meaningful estimate of the membrane fixed-harge density (M) will not be obtained. Arbitary use of B=1 will not change the relative values of (M) for different membranes, however.

The mathematical model outlined here does allow for prediction of membrane properties given a knowledge of membrane charge density. It does, however, appear that the model has shortcomings in respect of predictions of rejection properties of membranes in electrolytes of other types such as A_2Y and AY_2 salts. This may be due to H^+ and OH^- transport effects in membranes which affect the results.

3.6.4 MEMBRANE CHARGE DENSITY

The membranes under consideration are of the ion exchange type and a knowledge of the effective charge density in the membrane is an important means for characterizing membrane properties. When two electrolyte solutions of different concentrations are separated by a membrane containing fixed charges, a steady electromotive force arises between the solutions. This EMF, known as the membrane potential, has been the subject of many theoretical studies. The earliest work published was by

Toerell[128] and by Meyer and Sievers[129]. The joint approach is known usually as the TMS theory. The theoretical derivations were based upon completely selective membranes, which are not attainable in practice. A mathematical model for membrane potential, based upon the thermodynamics of irreversible processes, was propounded by Kobatake et al[130]. A good fit to experimental data was obtained by this approach. Kobatake extended this work later[131,132] to include effective fixed-charge density determinations. A critical review of the TMS approach and of the various treatments by Kobatake and co-workers was made by Beg et al[133] who used these various techniques to evaluate hydrodynamically effective fixed-charge densities in inorganic membranes. These workers succeeded in forming Kobatake's various approaches into a workable and easily used form.

By making the assumptions that small ions do not behave ideally in a charged membrane and that the contribution to potential by mass movement is negligible, Kamo et al[132] derived the following equation for membrane potential E_m.

$$(t) \qquad E_m = \frac{RT}{F}\left[\ell n\, {}^{c_2}/_{c_1} + (2\alpha - 1)\,\ell n \frac{(4c_2^2 + \phi^2 X^2)^{0,5} + (2\alpha-1)\,\phi X}{(4c_1^2 + \phi^2 X^2)^{0,5} + (2\alpha-1)\,\phi X} - \ell n \frac{(4c_2^2 + \phi^2 X^2)^{0,5} + \phi X)}{(4c_1^2 + \phi^2 X^2)^{0,5} + \phi X}\right] \qquad [1]$$

where C_1 and C_2 are salt concentrations either side of the membrane,

$\alpha = {}^{u}/_{u+v}$ u and v are cation and anion mobilities, respectively, in the bulk phase,

ϕ is a characteristic value of the

membrane/electrolyte pair

$\emptyset X$ is the thermodynamically effective fixed-charge density of the membrane

(Note, in TMS theory $\emptyset X=1$ and equation [1] reverts to the TMS form).

In order to evaluate $\emptyset X$ Kobatake and Kamo[134] proposed to use the modified Nernst equation for the diffusive contribution to the EMF of a cell with transport

$$E_m = -\frac{RT}{F}(1 - 2\,T_{app})\,\ell n\,{}^{c_2}/_{c_1} \qquad [2]$$

where T_{app} is the apparent transference number of co-ions in the membrane.

Comparison of equations [1] and [2] gives

$$(w) \qquad T_{app} = \left(\frac{1-2\alpha}{\alpha}\right) \frac{\ell n \left[\dfrac{(4E_2^2 + 1)^{0,5} + (2\alpha-1)}{(4E_1^2 + 1)^{0,5} + (2\alpha-1)}\right]}{\ell n\,\gamma} + \frac{\ell n \left[\dfrac{(4E_2^2 + 1)^{0,5} + 1}{(4E_1^2 + 1)^{0,5} + 1}\right]}{2\,\ell n\,\gamma} \qquad [3]$$

where $E_i = c_i/\phi X$

$\gamma = c_2/c_1$

When the external salt concentration is much greater than the effective charge density, that is $C_i/\emptyset X \gg 1$ equation [3] reduces to

$$1/T_{app} = \left(1/1-\alpha\right) + \left(\gamma-1/\gamma \ell n\gamma\right)\left(\alpha/1-\alpha\right)\left[\phi X/c_1\right] \qquad [4]$$

If now $\gamma = c_2/c_1$ is kept constant, but C_1 and hence C_2 are changed then a plot of $1/Tapp$ against $1/c_1$ will have a slope

$$\left(\gamma-1/\gamma \ell n\gamma\right) \cdot \left(\alpha/1-\alpha\right)\left(\phi X/c_1\right)$$

and intercept $\left(\alpha/1-\alpha\right)$

(The value of T_{app} at any concentration is determined from membrane potential using equation [3]).

Hence, from the plot of $1/T_{app}$ against $1/C_1$, α can be obtained from the intercept and $\emptyset X$ from the slope.

Siddiqi and Beg[133] found in a large series of trials that the

value of T_{app} determined by this technique was very close to the actual co-ion transference number T_- determined by other means (differences of less than 2% were found). It was therefore considered that the values of ØX obtained by this technique were representative of the true thermodynamic fixed-charge density at an electrolyte concentration of $C = (C_1 + C_2)/_2$.

The membranes produced in the present work programme were evaluated for ØX using this method using a cell of similar design to that used by Kobatake et al[130].

CHAPTER 4

EQUIPMENT AND EXPERIMENTAL METHODS

4.1 MONOMER PURIFICATION

4.1.1 2,5-FURANDIONE (MALEIC ANHYDRIDE)

This monomer was a puriss.grade obtained from Fluka, stored in a desiccator and freshly vacuum-sublimed/distilled before use, following the technique of Mason[135]. No degradation occurs in air at temperatures below 350°C[136].

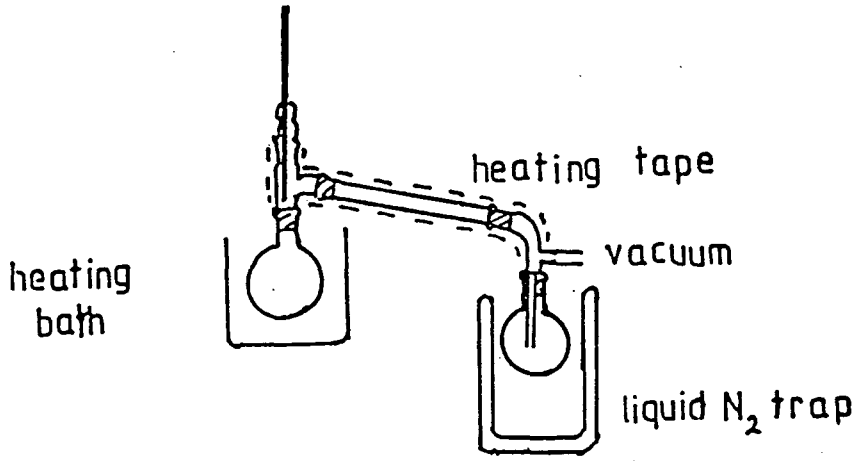

Fig. 4.1 Vacuum sublimation equipment

The monomer is a solid, melting at 52°C and boiling at 200°C under ambient pressure conditions. The flask containing the molten monomer was maintained at 100°C under 2mm Hg vacuum and the distillate/sublimate collected at liquid-nitrogen temperatures to prevent contamination of the vacuum system. Purity was checked by melting point determined by differential scanning calorimetry techniques; this was peak 52,4 - 52,6°C, literature 52,8°C[137].

4.1.2 OTHER MONOMERS

The co-monomers used in this work were all liquid at ambient temperature and were purified immediately before use by vacuum distillation.

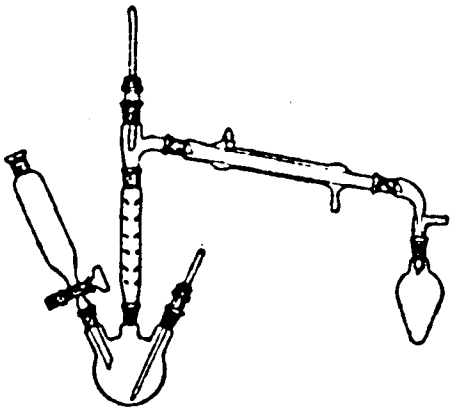

Fig. 4.2 Vacuum distillation equipment

A dry argon bleed through a fine capillary tube was used to prevent "bumping" effects and carry-over of stabilizers present in the monomer. The following monomers were purified in this way (common names in brackets): 2-propenoic acid - Fluka A.R. grade (acrylic acid); methylene butanedioic acid - Fluka A.R. grade (itaconic acid); ethenyl acetate - Fluka A.R. grade (vinyl acetate); 2,3 - epoxy propyl methacrylate - Fluka A.R. grade (glycidyl methacrylate); Ethene sulphonic acid (Na^+ salt) - 30% solution in water was used as received (sodium vinyl sulphonate).

4.2 POLYMERIZATION TECHNIQUES

4.2.1 EQUIPMENT

Polymerizations were carried out in sealed 250 ml ampoules under inert gas, after vacuum freeze/thaw techniques had been used for the removal of air from the ampoule contents. A diagram of the vacuum line is given in Fig. 4.3 below. A photograph of the complete line appears in Appendix E1.

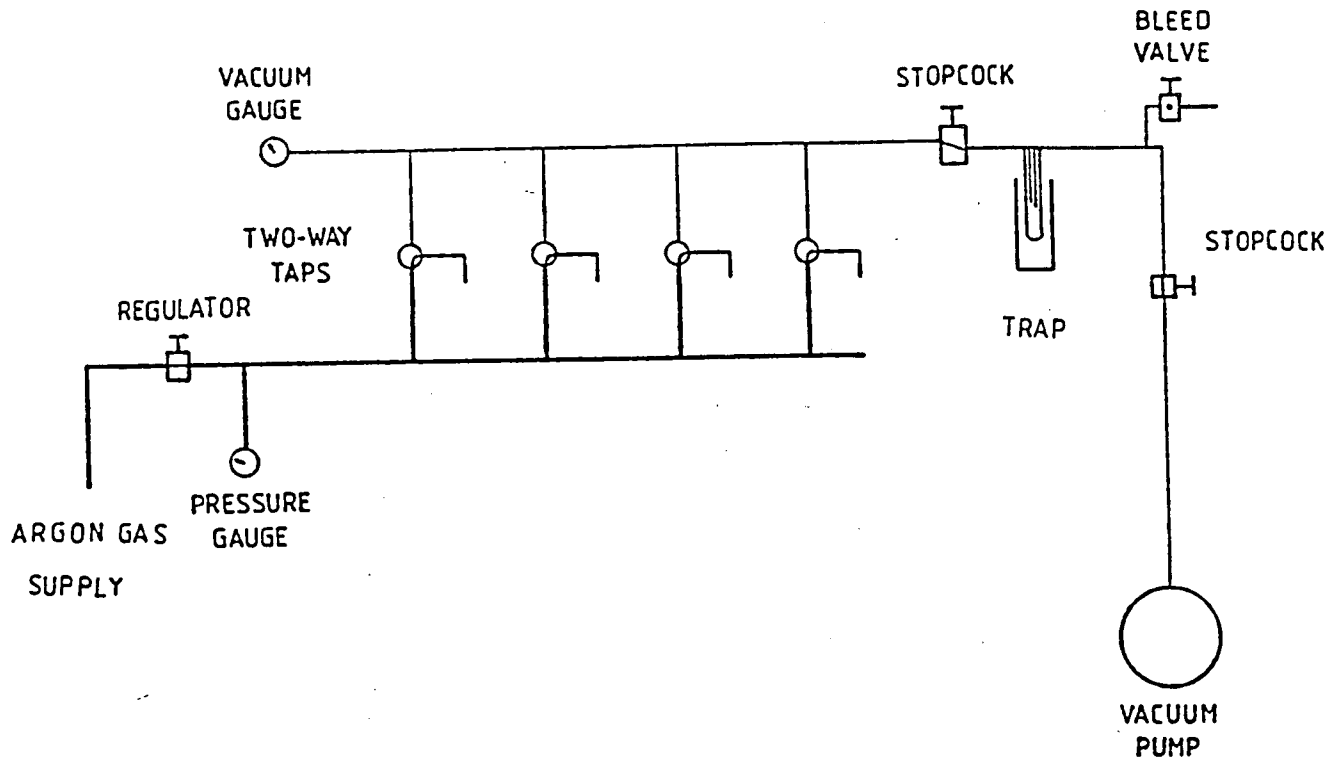

Fig. 4.3 Vacuum line

Details of the gas/vacuum changeover valving are given in Fig. 4.4 and ampoule description in Fig. 4.5.

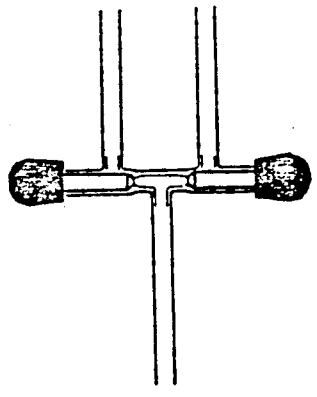

Fig. 4.4 Change-over detail

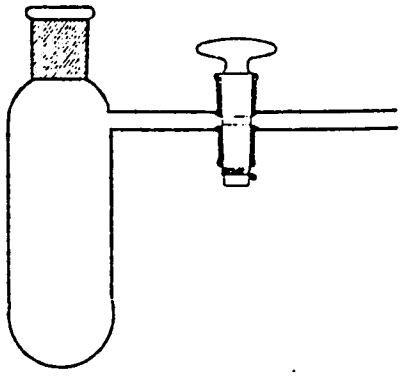

Fig. 4.5 Ampoule

Photographs appear in Appendix E1.

4.2.2 EXPERIMENTAL TECHNIQUES

For consistent and reproducible results in most free-radical systems it is important that oxygen is excluded from the polymerization system. For the purposes of this study a vacuum

freeze/thaw technique was used in conjunction with an inert gas blanket. This technique has the advantage of requiring only a modest vacuum (about 2 mm Hg pressure) and results in a low level of residual oxygen being present in the system.[138]

The general procedure was as follows:

(a) Thoroughly clean the reaction ampoule with chromic acid mixture, rinse thoroughly and dry at 90°C, cool in a desiccator.

(b) Weigh out monomers and solvent directly into an ampoule, add a PTFE-coated magnetic follower and seal with a rubber septum.

(c) Enclose the ampoule in a stainless-steel gauze sleeve (in case of vacuum implosion), connect gas/vacuum line to the side arm via thick-walled vacuum tubing. Cool the ampoule in an iso-propanol/liquid nitrogen mixture until the monomer and solvent freeze. Add initiator dissolved in a known volume of solvent via the septum cap.

(d) Allow the bath temperature to rise until the mixture just begins to thaw and, while maintaining this temperature, apply vacuum to the ampoule while stirring the mixture.

(e) When evolution of gas has ceased, close the vacuum tap and open the gas tap to allow argon to fill the ampoule from the gas line (previously flushed to remove air). Allow the argon gas to saturate the monomer/solvent mixture; this takes about 15 min.

(f) Repeat the alternate application of vacuum and gas flush for a further five cycles, pressurize the ampoule with argon and close off the gas line and the ampoule side-arm tap.

(g) Remove the ampoule and contents from the freezing mixture, place in a stirred, thermostatically controlled, liquid bath at the required temperature for a sufficient time for polymerization to be completed.

For homopolymerization of 2,5-furandione slight modifications to the equipment and techniques were required, as follows:

(h) Bulk homopolymerization required the top half of the ampoule to be heated with an electrical heating tape to a temperature of 60°C to prevent accumulation of sublimed solid monomer.

(i) Solution homopolymerization of 2,5-furandione frequently required successive additions of initiator. This was accomplished by the transfer, via the rubber caps, of a previously degassed stock solution of initiator, stored at 4°C, into the polymerization system. Where high-boiling-point solvents were used, a water-cooled reflux condenser was fitted to the ampoule with the rubber septum cap fitted to the top of the condenser.

All solvents used in the polymerizations were of A.R. grade and were freshly redistilled before use. Solvents for precipitation were of A.R. grade, and were used without further purification.

4.2.3 EXPERIMENTAL DETAILS

4.2.3.1 Homopolymerization of 2,5-furandione (maleic anhydride)

Monomer

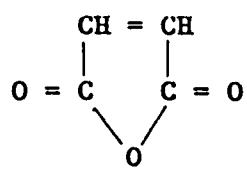

(i) Method A - solution polymerization[141]

The reaction mixture consisted of 2,5-furandione (41,51 g; 0,423 mole); chlorobenzene (150 ml) in ampoule 1. AIBN (3,34 g; 2,03 x 10^{-2} mole); chlorobenzene (50 ml) in ampoule 2.

Both ampoules were vacuum degassed as described in Section 4.2.2. Ampoule 1 was equipped with a reflux condenser and was heated to 381°K± 1°K in a silicone oil bath. While the contents were being stirred 10 ml of the initiator solution in ampoule 2 was transferred to ampoule 1 by means of a long cannula, by piercing the rubber septum of each ampoule and applying a partial vacuum to ampoule 1 while the inert gas pressure in ampoule 2 was maintained. The flow of initiator solution was stopped when required by equalizing the pressures. The remaining 40 ml of initiator solution was added in four 10 ml aliquots at 30-min intervals. The polymerization was terminated after 4 hours by cooling the reaction machine to ambient temperature. The tarry brown polymer formed was separated, washed with hot chlorobenzene and dried under vacuum. The polymer was purified by dissolving it in an excess of 2N potassium hydroxide and then precipitating it in methanol. The polymer salt was dissolved in water, re-precipitated in methanol and dried to constant mass at 333°K under a vacuum of 2 mm Hg.

Yield 2,93 g (3,96%) of brown waxy polymer. Polymer reference MA-1.

An attempt was made to determine the molecular mass by GPC techniques. The GPC chromatogram showed no peaks other than that assigned to the solvent and it was concluded that the molecular mass of this polymer was below the resolution limit of the column set in use (i.e. less than 2 000).

(ii) Method B - bulk polymerization[142,143]

The reaction mixture consisted of 2,5 furandione (10,86 g; 0,11

mole)and benzoyl peroxide (0,56 g; 2,3 x 10^{-3} mole). The 2,5-furandione was placed in an ampoule and heated to melting point (approximately 325°K) in an oil bath, and degassed as described in Section 4.2.2. The benzoyl peroxide was dried under vacuum and held in a separate container. Approximately 20% (0,118 g; 0,49 x 10^{-3} mole) of the benzoyl peroxide was added to the ampoule and the temperature was raised to 363°K ± 1°K with stirring. Four further additions of benzoyl peroxide were made at 30-minute intervals as follows:

Addition (2) 0,099 g; 0,41 x 10^{-3} mole
Addition (3) 0,115 g; 0,48 x 10^{-3} mole
Addition (4) 0,114 g; 0,47 x 10^{-3} mole
Addition (5) 0,114 g; 0,47 x 10^{-3} mole

The polymerization was terminated after five hours by cooling the reaction mixture and pouring it into 100 ml of methyl benzene. The dark tarry residue was washed with five x 20 ml portions of hot methyl benzene and dried under vacuum at 333°K. The product was purified by dissolving it in 1M potassium hydroxide and precipitating in methanol as previously described. The re-precipitation was repeated once.

Yield - 0,41 g (2,7%) of a dark brown semi-solid. Polymer reference MA-2.

An attempt was made to determine molecular mass by GPC techniques. No peaks were observed other than those assigned to the solvent and it was concluded that the polymer molecular mass was therefore less than 2 000.

(iii) Various homopolymerization methods

Further attempts, based on melt and solution techniques, were made to homopolymerize 2,5-furandione; brief details are given below:

(a) 2,5-furandione; 47,89 g (0,488 mole)
Acetic anhydride; 0,5 ml
1,4 dioxane; 100 ml
AIBN; 2,54 g ($1,55 \times 10^{-2}$ mole)

The AIBN was added in five increments at 30-minute intervals. Solution temperature was 363°K ± 1°K; polymerization time was 5,25 h;

Yield - 0,9 g (1,9%) dark brown waxy polymer. Polymer Reference MA-3.

(b) 2,5-furandione; 48,95 (0,50 mole)
Benzoyl peroxide; 2,533 g ($1,05 \times 10^{-2}$ mole)

Benzoyl peroxide was added in five equal increments at 30-minute intervals. Melt temperature was 398°K ± 1°K, polymerization time was 4 h.

Yield - Trace only.

Polymer MA - 3 proved to have a molecular mass below 2 000 as determined by GPC techniques.

4.2.3.2 Alternating copolymerization of 2,5-furandione and ethenyl acetate[75,76] (Maleic anhydride/vinyl acetate).

monomers 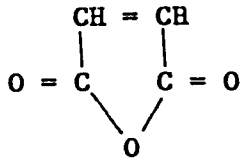 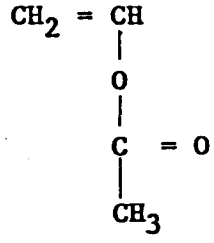

Four reaction mixtures were made up as follows:

(1) Polymer reference MA/VA-1

2,5-furandione (29,51 g; 0,300 mole); ethenyl acetate (26,39 g; 0,300 mole); AIBN (0,571 g; $3,5 \times 10^{-3}$ mole); 1,4-dioxane (100 ml). [Initiator concentration 1,17 mole %]

(2) Polymer reference MA/VA-2

2,5-furandione (15,38 g; 0,156 mole); ethenyl acetate (13,3 g; 0,136 mole); AIBN (0,14 g; $0,85 \times 10^{-3}$ mole); 1,4-dioxane (50 ml). [Initiator concentration 0,625 mole %]

(3) Polymer reference MA/VA-3

2,5-furandione (15,5 g; 0,158 mole); ethenyl acetate (13,25 g; 0,153 mole); AIBN (0,081 g; $0,49 \times 10^{-3}$ mole); 1,4-dioxane (50 ml). [Initiator concentration 0,320 mole %]

(4) 2,5-furandione (15,6 g; 0,159 mole); ethenyl acetate (13,1 g; 0,152 mole); AIBN (0,031 g; $0,19 \times 10^{-3}$ mole). [Initiator concentration 0,125 mole %]

[Note: Initiator concentrations are expressed as mole percentages of the effective monomer concentration.]

The reaction mixtures were placed in ampoules and degassed as described in Section 4.2.2. The ampoules were heated to 333°K $\pm$ 1°K with stirring and maintained at this temperature for 24 h.

Mixtures (1) and (2) showed evidence of exothermal behaviour in the first 15 min of reaction and the ampoules were cooled to try to control the temperature of the contents. Polymer became visible in the mixture as a gelatinous precipitate within 15 min and after successively longer times in the other mixtures. The

polymerizations were terminated after 24 h by pouring the reaction mixtures into methyl benzene to precipitate the polymers. The polymers were washed three times with hot methyl benzene and dried to constant weight at 333°K under a vacuum of 2 mm Hg. The polymers were purified by dissolving them in an excess of cold 2N KOH and precipitating them in methanol. The precipitated polymers were filtered, washed with methanol and dried. The polymers were then dissolved in water and precipitated in methanol; this last step was repeated once:

The polymers were finally dried to constant weight at 333°K under a vacuum of 2mm Hg.

Yield (1) MA/VA-1 62,6 g or 93,9%
(2) MA/VA-2 27,8 g or 92,0%
(3) MA/VA-3 29,2 g or 85,4%
(4) MA/VA-4 28,4 g or 84,1%

The polymers were characterized using GPC with universal calibration techniques; the results are given in Chapter 5.

5-g samples of each MA/VA copolymer were hydrolyzed to the corresponding alcohols. The reaction mixtures were as follows:

Copolymer (5,0 g; 0,027 mole), potassium hydroxide A.R. (5,6 g; 0,100 mole) de-ionized water (40 ml).

The potassium hydroxide was dissolved carefully in the water and the copolymers added with stirring. The mixtures were stirred and heated to reflux temperatures under a water-cooled condenser, the flask and condenser being purged slowly with pure nitrogen to reduce oxidative degradation. After 12 h under reflux the mixtures were cooled and the polymers precipitated in methanol, filtered, washed and dried. The polymers were purified by dissolving them in water and reprecipitating in methanol; this procedure was repeated once. The polymers were dried at 333°K under a vacuum of 2 mm Hg.

Yield (typical figure) 4,3 g (73,0%)

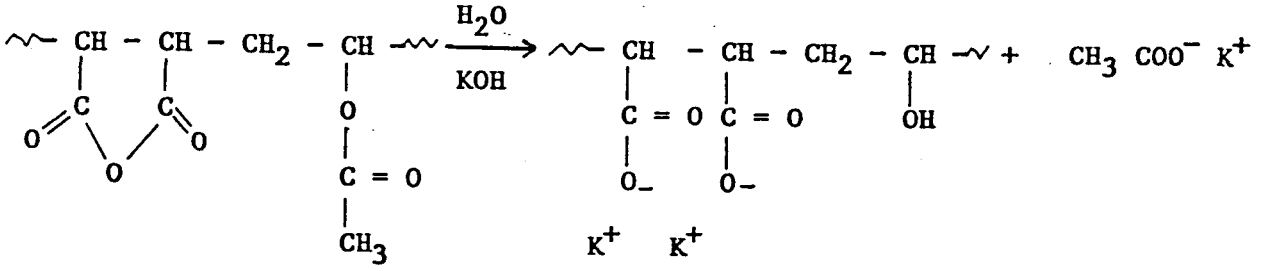

Polymer reference: From MA/VA-1 is produced MA/VOH-1
From MA/VA-2 is produced MA/VOH-2
From MA/VA-3 is produced MA/VOH-3
From MA/VA-4 is produced MA/VOH-4

4.2.3.3 Alternating copolymerization of 2,5-furandione and 2-propenoic acid. (Maleic anhydride/acrylic acid)

monomers

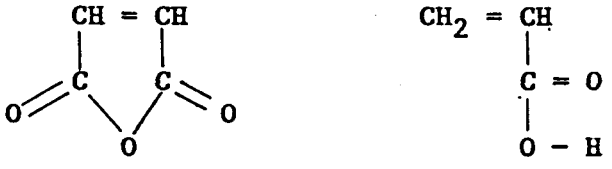

METHOD A

Two reaction mixtures were made up as follows:

(1) Polymer reference MA/AA-1

2,5-Furandione (22,07 g; 0,225 mole); 2-propenoic acid (16,05 g; 0,223 mole), benzoyl peroxide (0,206 g; $0,85 \times 10^{-3}$ mole), 1,4 dioxane (100 ml). [Initiator concentration 0,38 mole % with respect to monomer]

(2) Polymer reference MA/AA-2

2,5-furandione (30,27 g; 0,307 mole), 2-propenoic acid (14,71 g;

0,204 mole), benzoyl peroxide (0,25 g; 1,03 x 10^{-3} mole), 1,4-dioxane (100 ml). [Initiator concentration 0,51 mole % with respect to monomer]

The reaction mixtures were placed in ampoules, degassed as described in Section 4.2.2, and heated to 323°K±1°K with stirring. Exotherms were noted in the first 15 min and the ampoules were cooled vigorously to maintain the set temperature. The solution viscosity increased rapidly during this first period. The polymerization was terminated after a total of 18 h by cooling the reaction mixture and pouring it into methyl benzene. The precipitated polymers were filtered and repeatedly washed with hot methyl benzene and dried to constant weight at 333°K under a vacuum of 2 mm Hg.

Yield	(1)	MA/AA-1	73,5 g or 96,0%
	(2)	MA/AA-2	33,5 g or 97,5%

The polymers were further purified by dissolving them in excess 2M KOH and precipitating in methanol. The precipitated polymers were dissolved in de-ionized water and precipitated in methanol twice more and were then dried to constant mass at 333°K under a vacuum of 2 mm Hg. The molecular masses of the polymers were determined by the GPC method with universal calibration; results are reported in Chapter 5.

METHOD B

Two reaction mixtures were made up as follows:

(3) Polymer reference MA/AA-3

2,5-Furandione (10,3 g; 0,105 mole), 2-propenoic acid (7,4 g; 0,103 mole); benzoyl peroxide (0,036 g; 0,149 x 10^{-3} mole); 1,4-dioxane (25 ml). [Initiator concentration 0,144 mole % with respect to monomer]

(4) Polymer reference MA/AA-4

2,5-Furandione (10,3 g; 0,105 mole), 2-propenoic acid (7,4 g; 0,103 mole); benzoyl peroxide (0,018 g., 0,743 x 10^{-4}); 1,4-dioxane (25 ml). [Initiator concentration 0,072 mole % with respect to monomer]

The reaction mixtures were placed in ampoules and degassed as described in Section 4.2.2. The mixtures were then heated to 323°K $\pm$1°K with stirring and maintained at this temperature for 48 h. The polymerizations were terminated by cooling and pouring the mixtures into methyl benzene. The polymers precipitated and were filtered off, washed repeatedly with hot methyl benzene and dried to constant mass at 333°K under a vacuum of 2 mm Hg.

Yield	(3)	MA/AA-3	5,2 g or 29,7%
	(4)	MA/AA-4	6,5 g or 37,1%

The polymers were further purified by neutralization with an excess of 2N potassium hydroxide, precipitation in methanol and filtration. The precipitates were then dissolved in de-ionized water and re-precipitated in methanol; this last procedure was done twice. The polymer was dried to constant mass at 333°K under a vacuum of 2 mm Hg. The molecular masses of the polymers were determined by GPC techniques using universal calibration; the results are reported in Chapter 5.

4.2.3.4 Copolymerization of 2,5-furandione and methylene butanedioic acid (maleic anhydride/itaconic acid)

monomers

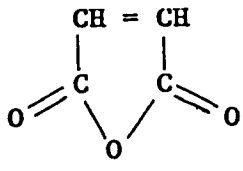

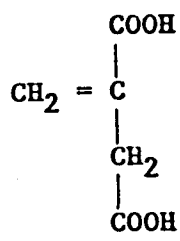

METHOD A

Two reaction mixtures were made up as follows:

(1) Polymer reference MA/IA-1

2,5-furandione (9,96 g; 0,102 mole); methylene butanedioic acid (13,26 g; 0,102 mole); potassium persulphate (0,115 g; $4,25 \times 10^{-4}$ mole); potassium hydrogen sulphite (0,046 g; $4,42 \times 10^{-4}$ mole); de-ionized water (50 ml). [Initiator concentration 0,417 mole % with respect to monomer]

(2) Polymer reference MA/IA-3

2,5-Furandione (14,80 g; 0,151 mole); methylene butanedioic acid (13,26 g; 0,102 mole); potassium persulphate (0,092 5; $3,40 \times 10^{-4}$ mole); potassium hydrogen sulphite (0,040 g; $3,84 \times 10^{-4}$ mole); de-ionized water (50 ml). [Initiator concentration 0,333 mole % with respect to monomer]

The reaction mixtures were placed in an ampoule and degassed as described in Section 4.2.2. The ampoules were heated to 323°K $\pm$ 1°K and maintained at this temperature, with stirring, for 24 h. The polymerizations were terminated by cooling and the polymers were converted to the partial potassium salts by neutralization with an excess of cold 5N KOH. The polymer salts were then precipitated in an excess of methanol, filtered, washed thoroughly with cold methanol and dried. The polymers were further purified by dissolving them in water and precipitating them in methanol; this procedure was repeated once. The polymers were then dried to constant mass at 333°K under a vacuum of 2 mm Hg.

Yield (1) MA/IA-1 36,1 g or 90,7% (As K+ salt)
(2) MA/IA-3 32,5 g or 80,0% (As K+ salt)

The molecular masses of the polymers were determined by the GPC method using universal calibration; the results are reported in Chapter 5.

METHOD B

A reaction mixture was made up as follows:

(3) Polymer reference MA/IA-2

2,5-furandione (11,60 g; 0,118 mole); methylene butanedioic acid (13,03 g; 0,100 mole); benzoyl peroxide (0,13 g., 5,37 x 10^{-4} mole); 1,4-dioxane (50 ml).

The reaction mixture was placed in an ampoule, degassed as described in Section 4.2.2, and heated to, and maintained at, 333°K $\pm$ 1°K with stirring. The polymerization was terminated after 46 h by cooling the mixture and pouring it into an excess of methyl benzene. The polymer precipitated out and was filtered and washed thoroughly with hot methyl benzene. The polymer was dried to constant mass at 333°K under a vacuum of 2 mm Hg.

Yield (3) MA/IA-2 9,72 g or 42,6%

The polymer was further purified by neutralization with an excess of cold 5N KOH and precipitation in methanol. The polymer was thoroughly washed with methanol and dried. The precipitated polymer was dissolved in de-ionized water and re-precipitated in methanol, this last procedure being repeated once. The polymer was then dried to constant mass at 333°K under a vacuum of 2 mm Hg. The molecular mass of the polymer was determined by the GPC method using universal calibration and the results are reported in chapter 5.

METHOD C

Reaction mixtures were made up as follows:

(4) Polymer reference MA/IA-4

2,5-furandione (15,2 g; 0,155 mole); methylene butanedioic acid (19,6 g; 0,151 mole); potassium persulphate (0,070 g; $2,59 \times 10^{-4}$ mole); potassium hydrogen sulphite (0,028 g; $2,69 \times 10^{-4}$ mole); de-ionized water (150 ml). [Initiator concentration 0,178 mole%]

(5) Polymer reference MA/IA-5

2,5-furandione (15,3 g; 0,156 mole); methylene butanedioic acid (19,5 g; 0,150 mole); potassium persulphate (0,040 g; $1,48 \times 10^{-4}$ mole); potassium hydrogen sulphite (0,014 g; $1,00 \times 10^{-4}$ mole); de-ionized water (150 ml). [Initiator concentration 0,099 mole%]

The reaction mixtures were placed in ampoules and degassed as described in Section 4.2.2. The ampoules were heated to 303°K $\pm$ 1°K and maintained at this temperature.

The polymerizations were terminated after 72 h. The polymers were neutralized by addition of excess 5N KOH and precipitated in methanol. The precipitated polymers were filtered, washed thoroughly with methanol and dried. The polymers were further purified by being dissolved in de-ionized water and precipitated in methanol; this last procedure was repeated once. The polymers were then dried to constant mass at 333°K under a vacuum of 2 mm Hg.

Yield (4)	MA/IA-4	29,4 g or 54,1%
(5)	MA/IA-5	42,5 g or 78,7%

The polymers were sparingly water-soluble, but were not soluble at the 1% level in aqueous 0,5 M Na sodium sulphate solution and therefore viscometry and GPC measurements could not be performed.

4.2.3.5 Copolymerization of 2,5-furandione and ethene sulphonic acid (sodium salt)

monomers 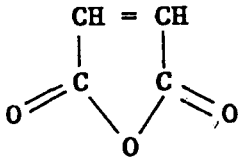 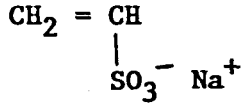

The ethene sulphonic acid (Na^+ salt) was supplied unstabilized as a 30% m/m solution in water and was used as supplied.

METHOD A

(1) Polymer reference MA/VSA-1

A reaction mixture was made up as follows:

2,5 furandione (10,76 g; 0,110 mole); sodium ethene sulphonate (7,143 g; 0,055 mole); potassium persulphate (0,27 g; $1,00 \times 10^{-3}$ mole). [Initiator concentration 1,82% with respect to monomer]

The reaction mixture was placed in an ampoule and degassed as described in Section 4.2.2. The ampoule was heated to 333°K $\pm$ 1°K with stirring and maintained at this temperature for 60 h. The reaction mixture was then cooled, neutralized with 2N sodium hydroxide and the polymer precipitated in acetone. The precipitated polymer, which was an oily liquid, was filtered, washed thoroughly with acetone and dried. It was then purified

by being dissolved in water and precipitated in acetone; this procedure was repeated once. The polymer was finally dried to constant mass at 333°K under a vacuum of 2 mm Hg.

Yield (1) MA/VSA-1 12,5 g or 90,6%

Measurement of molecular mass by GPC methods was attempted but no response was noted. This would indicate a low molecular mass, below the minimum column resolution of 2 000.

METHOD B

Two reaction mixtures were made up as follows:

(2) Polymer reference MA/VSA-2

2,5-furandione (10,150 g; 0,104 mole); sodium ethene sulphonate (6,912 g; 0,053 mole); potassium persulphate (0,083 g; 0,307 x 10^{-3} mole). [Initiator concentration 0,58% with respect to monomer]

(3) Polymer reference MA/VSA-3

2,5-furandione (14,78 g; 0,151 mole); sodium ethene sulphonate (14,30 g; 0,110 mole); potassium persulphate (0,050 g; 0,185 x 10^{-3} mole). [Initiator concentration 0,17% with respect to monomer]

The reaction mixtures were placed in ampoules and degassed as described in Section 4.2.2. The ampoules were then heated, with stirring, to 323°K $\pm$ 1°K and maintained at this temperature for 24 h. The reaction mixtures were neutralized with 2N sodium hydroxide and the polymers precipitated in acetone. The precipitates were filtered, washed thoroughly with acetone and dried. The polymers were then dissolved in de-ionized water and re-precipitated in acetone; this procedure was repeated once. The polymers were dried to constant mass at 333°K under a vacuum

mm Hg.

Yields (2) MA/VSA-2 2,57 g or 19,3%
(3) MA/VSA-3 6,80 g or 24,6%

Molecular mass determinations were done by GPC methods using universal calibration. No detector response was identifiable for MA/VSA-2, indicating a molecular mass below 2 000; the results for MA/VSA-3 are reported in Chapter 5.

4.2.3.6 Alternating copolymerization of 2,5-furandione and 2,3-epoxy propyl methacrylate[144] (Maleic anhydride/glycidyl methacrylate)

monomers

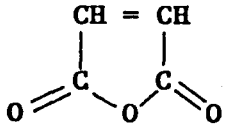

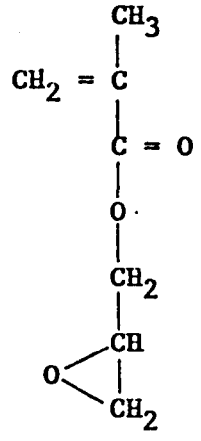

A reaction mixture was made up as follows:

(1) Polymer reference MA/GMA-1

2,5-furandione (10,01 g; 0,102 mole); 2,3-epoxy propyl methacrylate (14,31 g; 0,100 mole); AIBN (0,140 g; 0,853 x 10^{-3} mole); 1,4-dioxane (150 ml).

The reaction mixture was placed in an ampoule and degassed as

described in Section 4.2.2. The ampoule was heated, with stirring, to 333°K ± 1°K and maintained at this temperature for 64 h. The polymer, in the form of a swollen gel, was transferred to a beaker containing a large volume of methyl benzene and the mass broken up, filtered and washed thoroughly with copious amounts of hot methyl benzene. The polymer mass was dried at 333°K under a vacuum of 2 mm Hg. The hard, glassy polymer was insoluble in common solvents, including water and aqueous potassium hydroxide solution, producing a swollen gel after long periods of immersion in such solvents.

A number of repeated polymerizations also yielded insoluble polymers despite rigorous attempts to keep the reaction system absolutely dry, and it is presumed that the copolymer crosslinked during polymerization to give an insoluble product. This aspect is discussed in Chapter 5.

Yield of insoluble product 17,24 g or 71,8%.

4.3 POLYMER CHARACTERIZATION

4.3.1 DILUTE SOLUTION VISCOMETRY

The intrinsic viscosities of all copolymers were determined by solution viscometry in the same solvent (0,5 mole.dm^{-3} sodium sulphate) as that used for the GPC work, so that the universal calibration technique could be used. A brief description of this method is given below, the background theory having been covered in Section 3.4.1.3. The solvent used for viscometry and GPC work was taken from a 2 l stock solution made up by dissolving 142,040 ± 0,001 g of anhydrous sodium sulphate (A.R. Fluka) in de-ionized water and making up to 2 l. The solution was then filtered twice through "Millipore" aqueous ultrafilters (0,45 micrometer pore size) to remove particulate contaminants.

Pure dry polymer samples of about 0,2500 g mass were weighed out to a precision of ± 0,000 1 g. directly into clean dry 25 ml

volumetric flasks. The polymers were then dissolved in about 15 ml of stock 0,5 M sodium sulphate solution with ultrasonic agitation. The flasks were then made up to the mark with 0,5 M sodium sulphate solution. The solutions were again filtered through a semi-micro sintered glass filter (porosity 1) with vacuum assistance. Exactly 20 ml of the filtered polymer solutions were transferred by pipette, in each case, to a clean dry Ubbelohde dilution viscometer maintained at 313°K $\pm$ 0,1°K in a water bath.

After suitable temperature equilibration the efflux time of the solution was determined repeatedly, until three consecutive timings agreed to within 0,1%. The polymer solution was then precisely diluted with temperature-equilibrated solvent, by means of a pipette. After the solvent had been mixed thoroughly the new efflux time was determined as previously. The procedure of dilution and efflux time determination was repeated until values had been obtained at four or five dilutions.

The viscometer was then drained, thoroughly rinsed with solvent and replaced in the constant-temperature bath. The efflux time for pure solvent was then determined, after sufficient time had been allowed for temperature equilibration. The viscometer was then drained and washed repeatedly with hot de-ionized water and then oven-dried. The intrinsic viscosities of the polymers were calculated as explained in the theory section (see Section 3.4.3).

4.3.2 GEL PERMEATION CHROMATOGRAPHY

4.3.2.2 Equipment

The equipment used was a Waters model 150c gel permeation chromatograph using 0,5 M sodium sulphate as the mobile phase. The columns used were Waters 300 mm micro Bondagel type using a silica gel packing with a coating having an ether functionality. In the initial stages two columns were used, an E-linear column

(resolution range of 2 000 to 2 000 000 molecular mass) in series with an E500 column (resolution range of 5 000 to 500 000 molecular mass). During the course of the series of determinations the E-linear column became defective and only one E500 column was used for the remaining determinations. The column and injector compartments were maintained at a temperature of 323°K and a pump flow rate of 1 ml/min was maintained. Injection volumes were 100 µl and three determinations of retention volume were performed for each sample, with the mean value being reported. The detector used was the E401 refractive index detector.

4.3.2.1 Calibration

A number of polymer water-soluble standards were evaluated and rejected for various reasons during initial screening. Poly(ethylene oxide) standards were tried but they proved to have a high affinity for the column packing material (also coated with a polyether). As a result these standards failed completely to elute off the column. Narrow molecular-mass distribution poly(styrene sulphonic acid) standards also exhibited undesirable effects with multiple peaks being observed, probably due to ion inclusion/exclusion effects associated with partial ionization of the strong sulphonic acid groups on the polymer. The standard polymers used finally were a series of dextrans, supplied by "V-labs" and available over a molecular mass range of $12,5 \times 10^3$ to 151×10^3. In addition, a polyacrylic acid sample of molecular mass 148×10^3 was used. The polyacrylic acid sample had been previously characterized by viscometric measurements in dioxane. The dextrans used were carefully characterized materials having a polydispersity of about 1,5.

The standards were made up to about 1% solutions in 0,5 M sodium sulphate and viscometry data obtained as described in Section 4.3.1. About 2 ml of the solutions were drawn from the volumetric flasks, diluted with a further 2 ml of 0,5 M sodium

sulphate solution and filtered, using a syringe filter and 0,22 micrometre ultrafilter, into the vials supplied with the GPC equipment. The vials were sealed with PTFE septa and caps, placed in a carousel (holding up to 16 samples) and loaded into the instrument. After a period to allow temperature equilibrium to be achieved the instrument processed the samples automatically according to pre-programmed variables. These variables which were vital to the method were (1) flow rate (1,0 ml/minute), (2) column temperature (323°K) (3) injection volume (100 µl.) and were consistently maintained for all standards and samples. The instrument detector output was processed and plotted by a "Waters" model 730 integrator/plotter running in "GPC calibrate" mode, since no integration data were required. The graphic output was a plot of detector response against time (see Fig. 4.6).

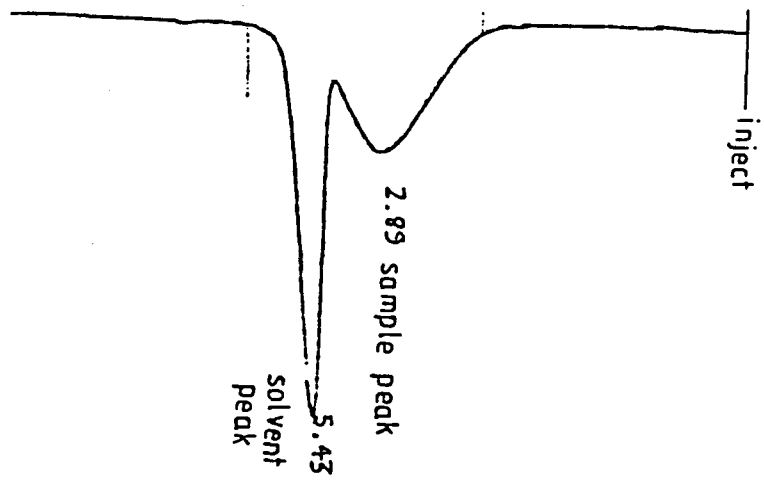

Fig. 4.6 Typical GPC plot

The GPC plot has two marked peaks, the earlier one being a response to the polymer and the later peak a so-called "solvent" peak. The solvent peak is explained by considering the composition of the sample injected. Each sample consists of both solute (polymer) and solvent (0,5 M sodium sulphate solution) and the presence of the solute reduces the local concentration of the solvent in the injected sample. The solvent in this case, being a concentrated electrolyte, shows a marked charge in refractive index with concentration and the sample of solvent used to dissolve the polymer standard is readily distinguished as a

separate peak. This solvent peak is of considerable importance as the elution time to the solvent should be unvarying, and variation of solvent peak elution time indicates a malfunction in the pumping system.

In practice, minor variations of the order of a few percent do occur in pump delivery rate and, for standards and samples, the given retention times were corrected to a common solvent elution time to correct for these minor variations. Each standard was run three times and a mean value of retention time calculated. The corrected retention times for the standards were converted to elution volumes; in all cases the flow rate was set at 1,0 ml/min and elution times and volumes were numerically equal.

As a first stage in the analysis of the standards, a plot of log M_w against retention volume (R_v) was made. Within a series of dextran standards this should be linear if the column set is correct for the molecular mass range. It was found that, in some circumstances, only the centre portion of the plot was linear, and results at either end of the molecular mass spectrum were then excluded from further analysis.

The retention volumes of the acceptable standards were then used to make universal calibration plots of log (Mw.[η]) plotted against R_v. The relevant plots for the standards used are given in Chapter 5.

4.3.2.3 Sample molecular mass determination:

Copolymer samples were prepared and run through the GPC in precisely the same way as that described for standards in the previous section. Three runs were done for each sample and a mean (corrected) value for Rv obtained. By reference to the universal calibration plot (or the regression equation thereof) the values of log (Mw.[η]) corresponding to these Rvs were determined. Insertion of the previously obtained values for intrinsic viscosity [η] enabled Mw to be calculated.

Some comment is necessary regarding the precision of the GPC method in molecular mass determination. This value is not easily determined, but the general opinion is that figures so obtained are subject to an error of, usually, not less than about 5%. In the present case the probable error is somewhat greater as universal calibration procedure also involves intrinsic viscosity determinations, which are also liable to error. In addition, some error is probable due to the use of calibration standards which were not monodisperse.

4.3.3 pH TITRATION

4.3.3.1 Equipment

Titrations of pH were carried out using a Metrohm E415 "Dosimat" titrator, pH values being read visually and recorded manually using a Beckman model 71 digital pH meter.

4.3.3.2 Method

The copolymers to be evaluated were in the acid form and were pure and dry. Sufficient polymer was accurately weighed out to make 25 ml of about 0,1 N solution (with respect to the first ionization of the maleic acid group). The polymer was weighed directly into a 25 ml volumetric flask, dissolved in about 15 ml deionized water and made up to the mark. Five millilitres of this solution were placed in a small stirred titration vessel, 0,030 g of sodium chloride (A.R. grade, Fluka) added and the contents titrated with 0,1 N sodium hydroxide past the first end point to about pH 4. Sodium hydroxide was added in 0,1 ml increments and the pH of the solution recorded at each addition.

4.3.3.3 Calculation

The end-points of the titrations were determined by calculation

only using the method of Hahn and Weiler[145]. By this means, the normality of the maleic acid group in the copolymers could be determined, and hence the copolymer composition.

4.4 MEMBRANE FORMATION

The procedures used for the formation of both zirconia and polyelectrolyte membranes are based upon the recommendations of Johnson et al[3] with some minor modifications. The conditions of formation were rigorously standardized to enable reliable comparisons to be made. No optimization was attempted.

4.4.1 EQUIPMENT

A schematic diagram of the membrane formation/test equipment is given in Fig. 4.7.

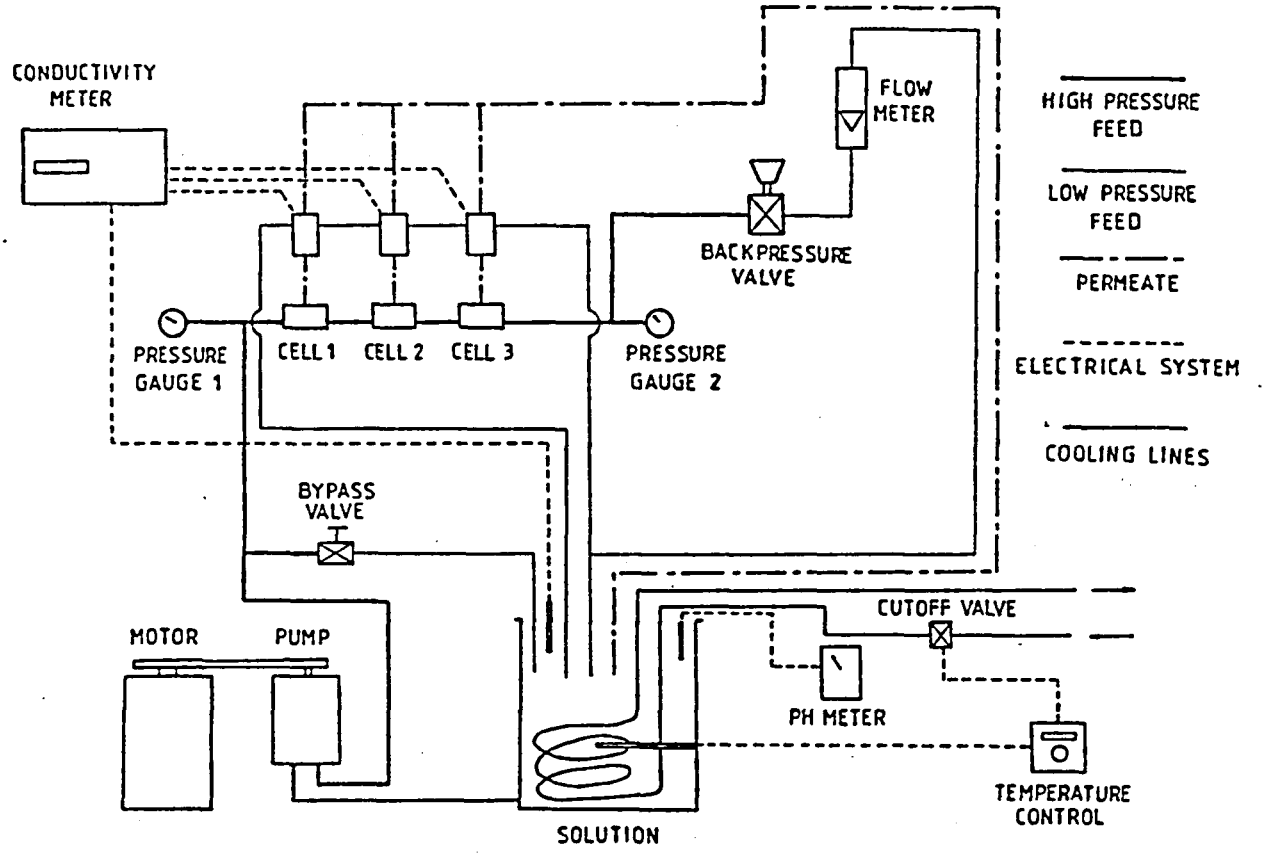

Fig. 4.7 Schematic diagram of membrane formation and evaluation equipment.

Photographs of various aspects of the equipment are given in Appendix E2.

The equipment was constructed from only non-corroding and non-contaminating materials, principally stainless steel (pumps, valves and piping), high-density polyethylene (feed tank) and acrylic plastics (rotameter and cell turbulence promoters). A feed tank of 40-litre capacity, equipped with a cooling coil for thermostatic control of feed temperature, supplied feed solution to the high-pressure pump. This pump was a diaphragm pump (using fluoroelastomer diaphragms) of the "Hydrocell" design, driven at 1 000 rpm and capable of supplying 15 l/min at pressures of 6 MPa. The flow from the pump was split at a high-pressure bypass valve, allowing control of volumetric flow to the formation/test cells. Three cells were used, connected in series, and the pressure applied to the cells was controlled by a precision back-pressure valve. Volume flow was monitored by a flowmeter on the low-pressure side of the back-pressure valve. In evaluation mode, permeate passing through the membrane was monitored by three individual conductivity flow cells and the permeate flux could be determined by measuring the volume of liquid leaving the individual cells. Permeate was finally collected by a manifold and returned to the feed tank so that feed concentration remained constant.

The cell design featured a tortuous flow path, designed to promote turbulent flow; the flow path is shown in Fig. 4.8 below. Photographs of the cell construction are also given in the Appendix.

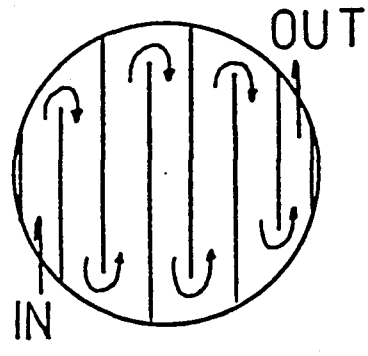

Fig. 4.8 Cell flow path

The dimensions of the flow channels were such that a flow rate of 3,67 l/min developed a linear flow rate of 6 m/s (inducing fully developed turbulent flow), which is necessary for both formation and for evaluation of membranes.

4.4.2 SYSTEM CLEANING

Thorough cleaning of the system was essential if reproducibility was to be obtained. The following procedure was used between membrane formation runs:

(1) Remove membranes, manually clean cells and replace membranes with impermeable discs cut from low-density polyethylene sheet; re-assemble cells.

(2) Drain conductivity cells, clean with nitric acid at pH 1 and rinse with reverse osmosis permeate water (RO permeate).

(3) Wash main system, with RO permeate adjusted to pH 1 with concentrated nitric acid, for 2 h at 50°C. A flow rate of about 2 l/min at a pressure of about 1 MPA was sufficient.

(4) Drain system and rinse with RO permeate for 15 min.

(5) Drain rinse solution, refill with RO permeate and adjust to pH 11 with concentrated aqueous NaOH. Circulate for 2 h at 50°C under previous pressure and flow conditions.

(6) Drain and rinse repeatedly with RO permeate.

(7) Check feed tank for the presence of Fe^{++} ions, using prussian blue.

4.4.3 FORMATION OF HYDROUS ZIRCONIA MEMBRANE

The dynamic membranes were formed on "Millipore" type HA (0,45 µm) ultrafiltration membranes. The membranes were placed in the cell with the active face towards the feed. Cellulose filter papers (grade 0) were placed behind the membranes for support and backed up with stainless steel mesh discs. The cells were then tightened up with the bolts provided to seal the membranes against the cell "O" ring.

The feed tank was filled with 40 litres of RO permeate and 80 g of sodium nitrate (Fluka AR) were added to give a concentration of 2 g/l. The pump was started and the solution circulated at 3,67 l/min with 2 MPa pressure and the system was checked for leaks. The pH of the feed was adjusted to 4,0 by addition of nitric acid (Fluka A.R. grade). Zirconium nitrate (1,7 g Fluka A.R. grade) was dissolved in water (50 ml) and added to the feed tank to give a zirconium nitrate concentration of 1×10^{-4} M. Addition of zirconium nitrate caused a drop in pH and the pH was adjusted to 3,8 $\pm$ 0,1 by addition of 10% m/v aqueous sodium hydroxide.

The back-pressure valve was adjusted to increase the cell inlet pressure by 1 MPa at 5 min intervals until a final pressure of 6 MPa was reached.

Cell flux and rejections were then monitored continuously until the fluxes dropped to 500-800 $l/m^2/hr$ and rejections of 40-60% were obtained. At this stage, pH was adjusted to 2,0 with nitric acid, the pump was switched off and the tank drained. The tank was refilled with RO permeate adjusted to pH 2 with nitric acid and the pump restarted at low pressure (2 MPa) to flush the system. The pump was stopped again and the system drained and refilled with RO permeate adjusted to pH 2 with nitric acid. The pump was restarted, pressure was adjusted to 6 MPa and flow rate to 3,67 l/min.

4.4.4 FORMATION OF POLYELECTROLYTE MEMBRANE

Immediately following formation of the zirconia membrane formation, the polyelectrolyte layer was applied as follows:

The feed was adjusted to pH 2,0 $\pm$ 0,05 and 80 g sodium nitrate was added.

The flow rate was adjusted to 3,67 l/min and the cell inlet pressure to 6MPa. Two grams of the polyelectrolyte, dissolved in water, was added to the feed tank, giving approximately 50 ppm polyelectrolyte concentration. At 30-min intervals, the pH was adjusted upwards by 0,5 unit by addition of 10% m/v sodium hydroxide solution until pH 7,0 was reached.

At each pH during formation, the flux and rejection of the membranes were monitored and recorded.

After a 30-minute period of equilibration at pH 7 the system was dynamically flushed of remaining polyelectrolyte by slowly draining the tank while continuously adding RO permeate. A flushing volume of about 120 l of RO permeate was used (three tank volumes). 80 gm of sodium nitrate were then added to the feed tank to return the concentration to 2g/l and the membranes were allowed to equilibrate for 20 hours at a pressure of 4 MPa and a flow rate of 3,67 l/min. At the end of this period the pressure was raised to 6 MPa, the system was allowed to equilibrate for 1 h and values of rejection and flux again determined.

The pH of the system was then raised successively to pH 8 and then to pH 9 and flux and rejection determined after 45 min at each pH. The pump was then stopped and the membranes removed for charge density determinations. The system was then cleaned as described in Section 4.4.2.

4.5 MEMBRANE EVALUATION

4.5.1 FLUX, REJECTION AND FIGURE OF MERIT DETERMINATION

Flux and rejection figures were determined both during formation and after formation of membranes as follows:

4.5.1.1 Evaluation during formation

Figures obtained during formation are of minor interest since they represent conditions during transient phases of membrane formation, but have been recorded to illustrate the stages of polyelectrolyte membrane growth. The membrane-formation equipment was equipped with two conductivity meters (Radiometer model CDM 83), one of which was used to monitor the feed conductivity, whilst the second was switched between the three flow conductivity cells monitoring the permeate from the three membrane cells.

For the purpose of this evaluation observed rejection was calculated as

$$Robs = (1 - {}^{K_p}/_{K_f}) \times 100\%$$

where Kp is conductivity of permeate
Kf is conductivity of feed

This relationship is not precisely correct but is sufficiently accurate for this phase of the evaluation.

Membrane flux was determined for each cell by measuring the time (to the nearest 0,1 sec) for permeate to fill a 10-ml measuring cylinder and converting this figure to a cell flux in ml/min. Multiplication of this figure by a constant factor of 906,0 enabled the flux in $l/m^2/day$ to be determined. (Note: This factor includes a correction for the exposed area of the membrane).

4.5.1.2 Membrane evaluation after formation

Flux and observed rejection figures were determined for membranes immediately after formation (when pH had been adjusted to 7,0) and 20 h later. This was done to evaluate the membrane permanence.

Flux figures were determined as in Section 4.5.1.1 but in this case conductivity figures were determined off-line by means of an identical conductivity bridge (Radiometer model CDM 83) and a single flow cell which was equilibrated at 30°C. The flow cell/conductivity bridge combination was carefully calibrated using a series of five known concentrations of sodium nitrate, and the calibration was checked before each membrane evaluation by a single point check. For this cell the relationship between concentration and conductivity is given by

$$C = 0,009\ 31\ K - 0,002\ 22$$

where C = concentration of sodium nitrate in $mole.dm^{-3}$
K = conductivity of solution in ms (millisiemens)

The correlation coefficient for this relationship was established as 0,998).

Hence, values for observed rejection for the equilibrium membrane determinations are given by

$$Robs = (1 - {}^{Cp}/_{Cf}) \times 100\%$$

where Cp = calculated value of permeate concentration ($mole.dm^{-3}$)
Cf = calculated value of feed concentration ($mole.dm^{-3}$)

Values are reported in Chapter 5.

In addition, values of flux and rejection were determined at pH 8

and pH 9 for certain membranes, using an identical method. Figure of merit values were calculated by a computer program, and are given in Chapter 5.

4.5.2 CONCENTRATION EFFECTS ON MEMBRANE PROPERTIES

Section 4.5.1 outlines the procedures for assessment of the properties of polyelectrolytes in the form of dynamic membranes. These results were, however, obtained at various concentrations of feed solution and are not directly comparable. The polyelectrolytes in each copolymer group which exhibited the best overall performance were then re-assessed by forming new membranes and examining their rejection and flux properties at a range of concentrations up to about 0,1 mole.dm^{-3}. For each polymer the constants in the equation

$$\text{Log } S = E \log M + H$$

were established, and rejection figures and "figures of merit" were determined at a common concentration of 2 000 ppm (0,0235 mole.dm^{-3}). The results are given in Chapter 5. Membrane fixed charge index ($\bar{M}$) and fixed charge homogeneity index (b) were determined for each membrane of this series using the method outlined in Section 3.6.3. These results are also given in Chapter 5.

4.5.3 CHARGE DENSITY DETERMINATION

Selected composite dynamic membranes were evaluated for membrane charge density as discussed in Section 3.6.3.

4.5.3.1 Equipment

The electrolytic cell used in charge-density determinations was designed, built and evaluated in conjunction with Mr. A. van Reenen of this University, following a design by Kobatake[134]. The cell is illustrated in Fig. 4.9 and a photograph is given in

Appendix E.3.

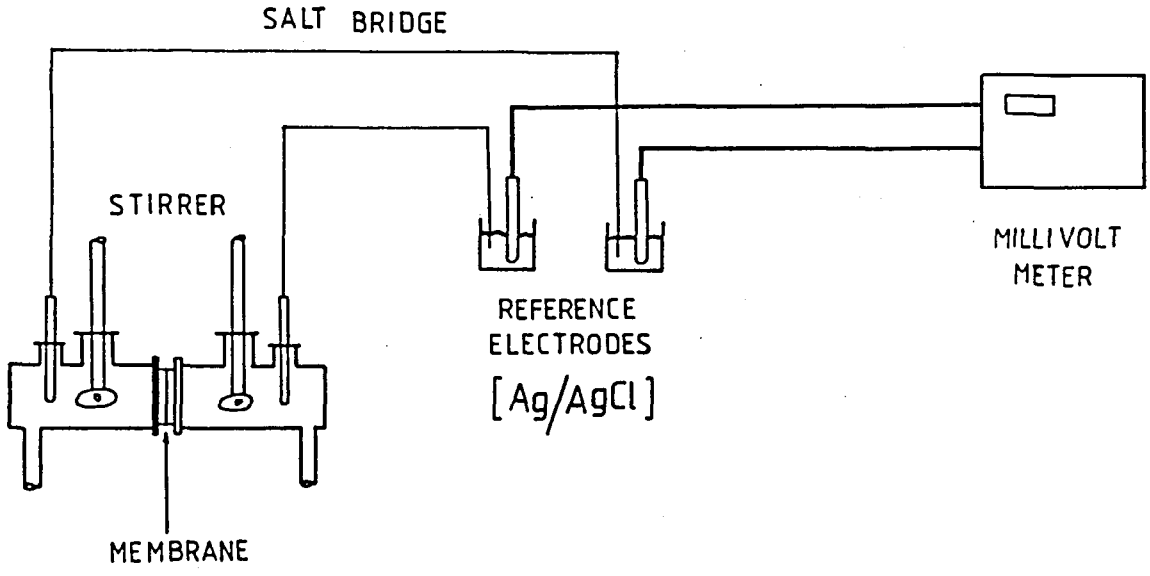

Fig. 4.9 Electrolytic cell

The cell was equipped with coupled stirrers and salt bridge junctions and had flexible drain tubes for rapid solution interchange. The cell potential was measured using a Beckman model 71 pH/MV meter in absolute EMF mode, capable of reading cell potential to 0,1 mV. with a quoted reproducibility of $\pm$ 0,1 mV.

The cell and reference electrode compartment were immersed in a water bath controlled to 298°K $\pm$ 0,1°K by a thermostatically controlled circulator.

Examination of the dynamic membranes, prior to installation in the cell, revealed that certain areas of the membrane had been damaged against the turbulence-promoting acrylic insert in the membrane cell during formation. In order to nullify the effects of these damaged areas "masks" were machined from 3 mm acrylic sheet and the membrane sandwiched between these masks. In this way the damaged areas were blanked off. Mask details are given in Fig. 4.10. Photographs of the masks are given in Appendix E2.

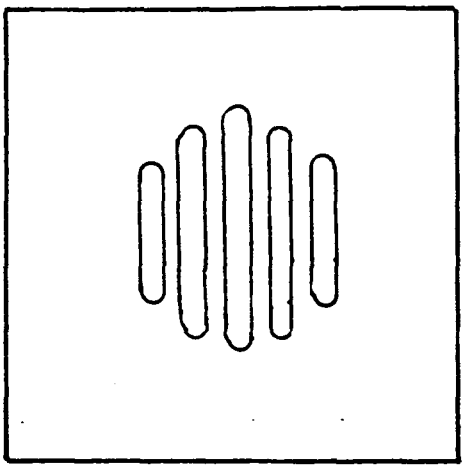

Fig. 4.10 Cell mask details

4.5.3.2 Method

The principal difficulty with the cell measurements was in ensuring that equilibrium conditions had been attained. Some experimentation in respect of stirring speed and equilibration time was necessary, with the work of Kobatake et al[134] being used as a guide. The following standard conditions and procedures were established and used throughout the determinations:

(1) Each membrane was checked before use for gross defects (pinholes, etc.) and rejected if such defects were apparent.

(2) The membrane was clamped between the well-greased faces of the two masks, in the correct orientation and correctly centred.

(3) The clamped membrane was now assembled between the cell halves and the apparatus secured with stainless steel clips, the "active" side of the membrane being carefully identified and marked.

(4) Pairs of solutions of sodium nitrate of the following concentrations were made up.
   (a) 1,0 mole.dm^{-3} and 0,1 mole.dm^{-3}
   (b) 0,5 mole.dm^{-3} and 0,05 mole.dm^{-3}
   (c) 0,1 mole.dm^{-3} and 0,01 mole.dm^{-3}
   (d) 0,05 mole.dm^{-3} and 0,005 mole.dm^{-3}

Solution pair (a) were initially placed in the cell, with the least concentrated solution of the pair being placed in the cell half facing the "active" side of the membrane.

(5) The solutions were vigorously stirred with PTFE paddle stirrers at 300 rpm for a period of 12 h.

(6) The cell halves were emptied and refilled with the same solution pairs. Stirring was resumed.

(7) After a further 12-hour period the potential across the membrane was read to the nearest 0,1 mv by means of the Beckman millivolt meter.

(8) This procedure was repeated for the other three pairs of solvents in turn, the cell being rinsed with deionized water and drained thoroughly between solutions.

The results obtained were evaluated as outlined in Section 3.6.3. Results are reported in Chapter 5 as values of thermodynamically effective fixed charge density ØX and the plots of 1/Tapp against $1/C_1$ are shown in Appendix D2.

CHAPTER 5

RESULTS AND DISCUSSION

5.1 POLYMER CHARACTERIZATION

5.1.1 MOLECULAR MASS DETERMINATION

5.1.1.1 Results

The intrinsic viscosities of all polymers which had been synthesized were determined by viscometry in 0,5 M sodium sulphate solution. The data from these determinations are presented in Appendix A.1 as plots of reduced viscosity vs concentrations. The intercepts of these plots (at c = 0) give the values of intrinsic viscosity $[\eta]$ which are tabulated, with other data, in Table 5.1.2. These data were insufficient for determination of molecular mass as the Mark-Houwink-Sakudara constants were not available for the polymers concerned. The technique of gel permeation chromatography (GPC) using universal calibration was therefore employed in an attempt to determine values for weight average molecular mass (Mw). (See Section 3.4 for the theoretical background and Section 4.3.2 for practical details.)

The standards used for the universal calibration curve were dextrans (Mw 17 700, 40 000, 70 300) and poly(acrylic acid) (Mw 148 000). The universal calibration plot is shown in Fig. 5.1.

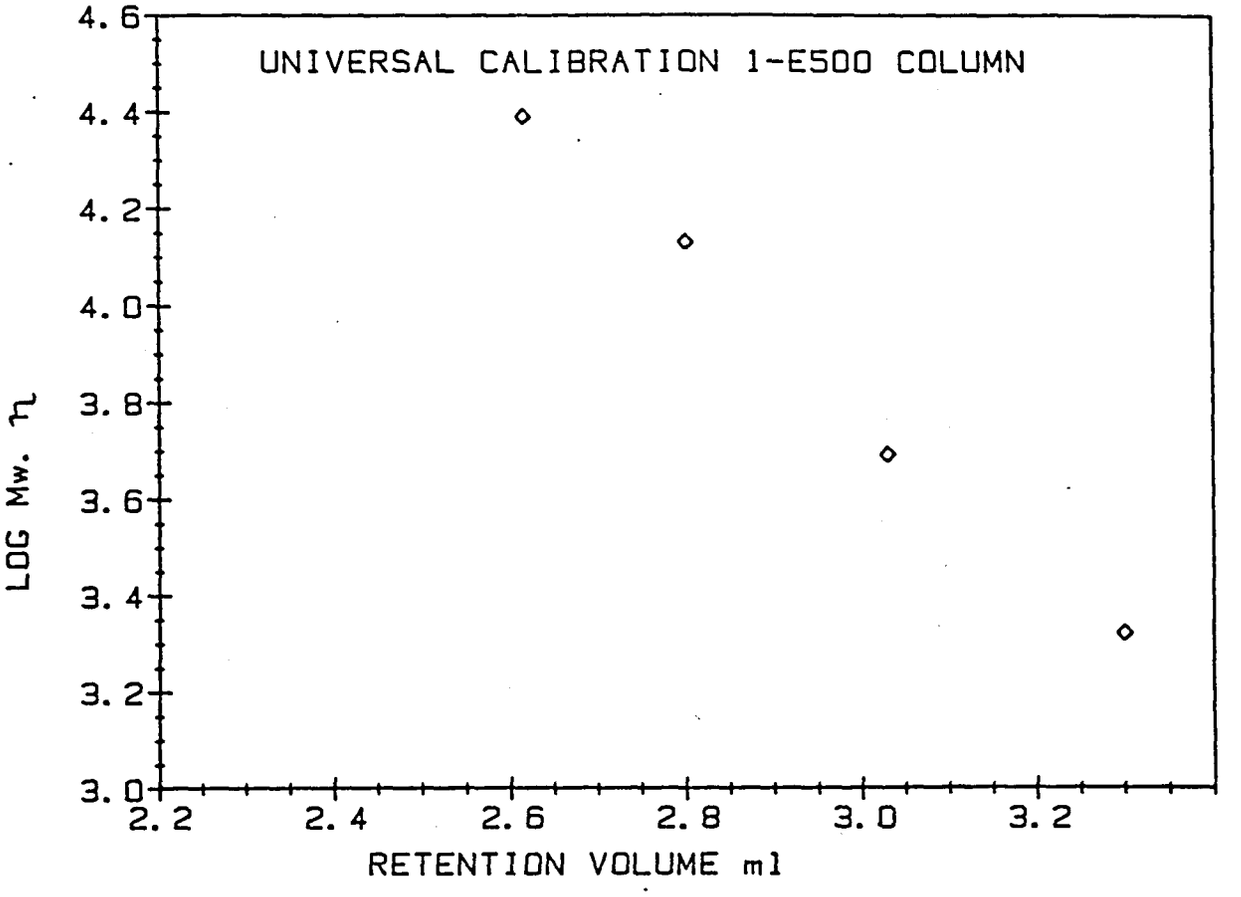

Fig. 5.1 Universal calibration curve

The equation of the regression line is

$$\log M_w.[\eta] = -1,5985\ R_v + 8,5773 \qquad [1]$$

(coefficient of correlation 0,998)

Table 5.1 Molecular Mass Information

POLYMER	[I]	[n]	Rv	log M_w[n]	M.Mass (x 10^{-3})
MA/VA-1	1,17	0,058	3,36	3,200	55,2
-2	0,63	0,103	2,94	3,880	73,7
-3	0,32	0,156	3,01	3,766	37,4
-4	0,13	0,191	3,00	3,782	31,7
MA/AA-1	0,38	0,308	*[1]	*[1]	*[1]
-2	0,51	0,221	3,00	3,780	27,3
-3	0,14	0,771	2,264	4,958	117,8
-4	0,07	0,946	2,396	4,747	59,1
MA/VOH-1		0,212	3,36	3,200	7,5
-2		0,290	2,94	3,880	26,2
-3		0,145	3,26	3,360	15,8
-4		0,139	3,27	3,340	15,7
MA/IA-1	0,42	0,142	3,19	3,480	21,3
-2	0,54	0,111	3,17	3,510	29,2
-3	0,33	0,152	3,06	3,680	31,5
-4	0,18	*[2]	*[2]	*[2]	*[2]
-5	0,10	*[2]	*[2]	*[2]	*[2]
MA/VSA-1	1,82	0,056	*[3]	*[3]	*[3]
-2	0,58	0,018	*[3]	*[3]	*[3]
-3	0,17	0,011	3,00	3,766	(530)

Key to Table [I] initiator concentration in mole%
[n] intrinsic viscosity in $dl.g^{-1}$
R_v GPC retention volume in ml
Polymer references as described in Section 4.2.3

i.e. MA/VA Poly(Maleic anhydride-alt-vinyl acetate)
MA/AA Poly(Maleic anhydride-alt-acrylic acid)
MA/VOH Poly(Maleic anhydride-alt-vinyl alcohol)
MA/IA Poly(Maleic anhydride-co-itaconic acid)
MA/VSA Poly(Maleic anhydride-co-vinyl sulphonic acid)

Notes: *1 unreliable results due to very broad distribution
*2 polymers insoluble in 0,5M sodium sulphate
*3 no observed detector response in GPC determination

5.1.1.2 Discussion

MA/VA co-polymers

The trend in the values of intrinsic viscosity [η] was consistent with the levels of initiator used in the copolymerization, but the retention volumes (R_v) and derived molecular mass values did not follow the expected pattern.

MA/AA co-polymers

These copolymers had intrinsic viscosity (I V) values which were in the expected order considering initiator concentrations, with R_v values showing a similar trend. When these values were combined, however, the molecular mass values calculated showed no correlation with intrinsic viscosities.

MA/VOH co-polymers

These polymers were made by alkaline hydrolysis of the parent MA/VA copolymers. High-molecular mass, high-conversion polymers containing vinyl acetate residues have a tendency to branch by radical attack at the methyl group of the acetate moiety. A branched polymer of this nature suffers a major reduction in molecular mass during hydrolysis and this partly explains the lower values of I.V. for MA/VOH-3 and MA/VOH-4. It is probable

that all of these copolymers suffered some degradation of molecular mass during hydrolysis, but these higher molecular mass polymers would be expected to show the greatest effect. The R_vs observed were not consistent with the intrinsic viscosities and there was no apparent pattern in molecular mass values.

MA/IA co-polymers

Intrinsic viscosities were consistent with respect to initiator concentrations, but values of molecular mass were not. Copolymers prepared with smaller amounts of initiator, which would be expected to have higher molecular masses, were found to be insoluble (or only partially soluble) in the electrolyte solution used for viscometry and GPC, and could not be characterized.

MA/VSA co-polymers

These copolymers had extremely low intrinsic viscosities. The trend observed was opposite to that expected and all results for this copolymer are suspect as efflux times were very close to that of the solvent.

It is generally accepted that, in a series of copolymers of constant structure, an increase in molecular mass is accompanied by an increase in intrinsic viscosity. This relationship would appear to have occurred with the regular alternating copolymers under discussion (MA/VA, MA/AA) and also with the random copolymer MA/IA. The fact that calculated values of molecular mass did not follow the same trend strongly suggested that the aqueous GPC technique used is not applicable to this series of polymers and that the universal calibration curve does not apply. It is probable that the strong hydrogen bonding and chelation properties and low pK_a' of the maleic acid moiety was responsible for the discrepancies. The GPC column packing was a porous silica, coated with a polyether, and it is possible that the copolymers were partially ionized in the electrolyte used,

leading to hydrogen-bonding interactions between the copolymers and the column packing. This interaction could have occurred with either the silanol groups in the silica surface or to the ether oxygen in the polyether coating on the column packing and resulted in longer retention times being observed. In addition, ionization of the maleic acid group could result in intermolecular hydrogen bonding (polymer aggregation) and would certainly cause swelling of the molecule, both of which could result in retention times being substantially reduced. Ion-exclusion effects, as discussed in Section 3.4.1.2 could also have had some effect. The result of above factors was to render the aqueous GPC technique used here impractical for determining molecular mass.

5.1.2 COMPOSITION ANALYSIS

5.1.2.1 Results

A considerable body of evidence exists to confirm that MA/VA copolymers and MA/AA copolymers form strictly alternating 1:1 structures under the polymerization conditions used. It was therefore not considered necessary to analyze these polymers fully for composition (one MA/VA and one MA/AA copolymer was analyzed).

MA/IA-1 and MA/IA-2 and MA/VSA-3 were analyzed by pH titration. The itaconic acid copolymers were titrated with base to the first maleic acid end-point while the vinyl sulphonic acid copolymer was converted to the sodium salt and titrated with acid to the end-point corresponding to the second maleic acid-end point at about pH 6,5. This was done to avoid the overlapping of end-point of the poly(vinyl sulphonic acid)(pKa = 3,00) and the first end-point of poly(maleic acid)(pKa, about 3,5). Results are given in Table 5.2.

Table 5.2 Composition analysis

POLYMER	MOLE% MALEIC ACID	
	Feed	Polymer
MA/VA-3	50	52
MA/IA-1	50	55
MA/IA-2	54	28
MA/AA-4	50	51
MA/VSA-3	67	27

5.1.2.2 Discussion

It is noteworthy that the mole percentage of maleic acid entering the copolymer was substantially higher in the case of MA/IA-1 than in the case of MA/IA-2. MA/IA-1 was copolymerized in water solution with free maleic acid present, whilst in MA/IA-2, maleic anhydride was copolymerized in dioxane solution. It would appear that the maleic acid moiety was more amenable to polymerization than the anhydride. The compositions of these polymers differed very substantially and it was expected that the properties of the series MA/IA-1, -3, -4, -5, which were copolymerized in water solution, would differ noticeably from those of MA/IA-2 which had a lower maleic acid concentration in the copolymer. It was confirmed that the composition of the MA/VA and MA/AA polymers were close to 50:50 mole% (i.e. alternating) within the limits of error of the determinations.

5.2 MEMBRANE FORMATION AND EVALUATION

5.2.1 INTRODUCTION

Copolymers which had been synthesized and characterized as described previously were used to form composite hydrous zirconia/polyelectrolyte membranes, using the procedure described in Chapter 4. Performance characteristics (flux and rejection) of the composite membranes were monitored during formation at pH 7, 30 minutes after completion of formation, and after 20 hours of operation. In addition, most membranes were evaluated for performance at pH values of 8, 9 and 10 after the 20 hour stabilization period. The figures obtained are recorded in full in Appendix B.1., together with details of the performance of the zirconia membrane alone, figure of merit values and concentration conditions. This information was used to select a copolymer of optimum molecular mass in each group for further study. The selected copolymers were used to form a second series of membranes which were more rigorously evaluated, the results being normalized to a feed concentration of 2 000 ppm sodium nitrate to enable meaningful comparisons of performance to be made.

5.2.2 DYNAMIC MEMBRANE FORMATION

The formation of a polyelectrolyte membrane as a composite layer is characterized by three major phenomena:

(a) Interaction of the anionic polyelectrolyte with the cationic zirconia membrane at low pH causes a rapid initial drop in rejection due to charge neutralization.

(b) An anionic polyelectrolyte membrane shows an increase in rejection with an increase in pH as a result of increasing anionic charge density. A zirconia membrane alone is cationic and rejection is reduced as pH rises.

(c) A polyelectrolyte membrane swells, due to charge repulsion

effects, as the pH rises, resulting in a reduction in the membrane flux due to occlusion of the pores of the zirconia membrane.

If all three of the above effects can be demonstrated, then the presence of a composite membrane is confirmed. Table 5.3 gives relevant information extracted from the results in Appendix B.1. These results are flux and rejection figures for the zirconia membrane at the formation pH 4, together with results at pH 2 and pH 7 for the composite membrane.

Table 5.3 Composite membrane formation

	Zirconia membrane pH 4		Composite membrane pH 2		Composite membrane pH 7	
POLYMER	Flux	R_{obs}	Flux	R_{obs}	Flux	R_{obs}
PAA-5(c).2	20,7	45,1	4,2	22,8	2,0	92,4
MA/VA-1.1	23,2	41,8	7,0	26,9	2,2	90,2
MA/VA-2.1	13,1	36,0	9,5	17,7	6,5	76,5
MA/VA-3.1	42,0	37,6	9,1	29,4	7,5	83,5
MA/VA-3.2	29,6	51,3	8,7	14,8	5,8	87,0
MA/VA-4.1	15,7	54,3	6,8	23,4	5,5	81,3
MA/VOH-1.1	38,5	52,0	14,9	16,9	3,6	91,3
MA/VOH-3.1	35,5	43,1	16,2	2,3	2,4	93,1
MA/VOH-4,1	17,7	29,9	15,1	12,6	2,7	95,4
MA/VOH-4.2	29,2	53,3	6,5	8,3	4,7	86,2
MA/AA-1.1	15,8	57,7	7,9	33,6	6,2	72,7
MA/AA-2.1	24,5	29,3	3,3	28,6	12,0	85,4
MA/AA-3.1	33,5	39,0	14,7	27,2	8,5	77,6
MA/AA-4.1	21,5	40,4	10,9	16,3	4,6	84,8
MA/AA-4.2	34,4	52,5	20,1	22,2	9,5	77,9
MA/IA-1.1	35,1	51,3	15,2	24,9	12,4	71,8
MA/IA-1.2	32,9	47,8	18,8	4,8	8,3	73,1
MA/IA-2.1	19,3	41,4	6,9	26,6	6,7	77,3
MA/IA-3.1	28,5	56,6	16,7	5,6	10,9	75,8
MA/IA-4.1	14,7	37,4	8,8	19,3	9,5	45,1
MA/IA-5.1	22,0	48,7	16,1	32,0	11,9	47,7
MA/VSA-3.1	21,1	52,7	19,0	27,8	12,4	52,7

Note: References have the following meaning

MA/VA-1.1

refers to polymer MA/VA-1, first trial. This trial consists of the mean values of results from three cells in the first evaluation of this material as a membrane. One molecular mass copolymer in each group was selected for further evaluation in a second trial (excluding MA/VSA copolymers).

From these membrane results (other than for MA/VSA-3) it can readily be seen that in all cases

(1) Rejection at pH 2 after polyelectrolyte addition was substantially lower than that of the zirconia membrane at pH 4, indicating interaction of the polyelectrolyte with the zirconia membrane.

(2) Composite membrane rejection increased with increase in pH indicating that the effective membrane was anionic.

(3) A substantial drop in flux occurs after addition of polyelectrolyte indicating that "pore-filling" is taking place.

(4) The flux at pH 7 was invariably lower than at pH 2 due to swelling of the anionic polyelectrolyte membrane.

The magnitude of these changes is sufficient to prove that a composite membrane was formed.

In the case of copolymer MA/VSA-3.1, the above changes do take place, but the magnitudes are much smaller. It is likely that a composite membrane was formed in this case, but the performance is poor.

5.2.3 MEMBRANE PROPERTY DEVELOPMENT DURING FORMATION

5.2.3.1 Introduction

Major property changes take place during the process of applying a polyelectrolyte to a preformed zirconia dynamic membrane. These changes are due to neutralization of the poly-carboxylic acid groups on the polymer backbone as pH rises, causing polymer swelling and increases in ion exchange capacity. As the polymer swells, the pores in the zirconia substrate become increasingly occluded causing a rapid reduction in flux. At the same time, the higher charge density and the more homogeneous distribution of charge lead to improvement in rejection. The pH at which the most marked change of properties occurs is expected to be in the area of the pK_as of the acid groups in the polymer structure. In most of the polymers synthesized, other than MA/VSA, the major effect would therefore be expected at the first pK of poly(maleic acid) as this is the carboxylic acid group common to all copolymers and has the lowest pK of all groups present.

The value of the first pK differs from that of the parent unsaturated acid (pK_a = 1,83) due to free-rotation effects and the presence of co-monomers. Dubin and Strauss[148] have shown that, for a series of alternating copolymers of maleic acid and vinyl ethers, the first maleic acid pK is 3,5. It would be expected that this value for pK would apply to the alternating copolymers MA/VA and MA/VOH. The first pK of the MA/AA copolymer would be expected to be lower due to the presence of the neighbouring acrylic acid group. The alternating MA/AA copolymer has a regular repeat structure.

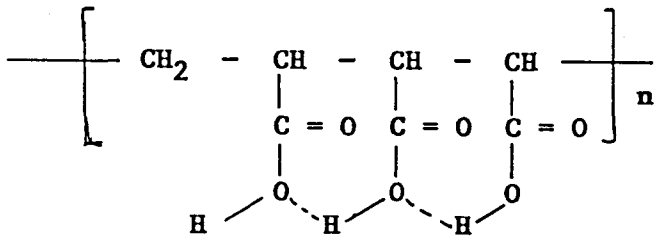

(1) (2) (3)

Fig. 5.2 Structure of poly(maleic acid-alt-acrylic acid)

Poly(maleic acid-alt-acrylic acid) has two equivalent carboxylic acid groups (1) and (3), with expected pK's between about 2 and 3,5, the normal pK of the acrylic acid at 4,25 being depressed by hydrogen bonding effects. At this point, the two equivalent groups would ionize with a rather sudden change in properties expected.

The random copolymer of MA/IA, with itaconic acid having pK's at about 3,8 and 5,5 would be expected to have a broad ionization range reflected by a rather gradual change in membrane properties. The MA/VOH polymers were the only copolymers in which the second maleic acid ionization (pK_a = 6,5) would be expected, since this was the only copolymer in which both maleic acid carboxylic acid groups were neutralized. The alkaline hydrolysis to form these copolymers from the MA/VA parent copolymers resulted in full neutralization of the maleic acid group, whereas the second carboxylic acid will not titrate normally, due to strong hydrogen bonding effects with the neighbouring carboxylic acid anion. Neutralization of the second maleic acid carboxylate group can occur at pH above 6,5, but only in the presence of a high concentration of added simple electrolyte, which functions by partially suppressing the first ionization. Dubin and Strauss[148] used 0,2 M lithium chloride for

this purpose. It is unlikely that any major ionization of this second carboxylic acid group occurred in the other copolymers under the conditions of formation and use. The ionization of the vinyl sulphonic acid group in the MA/VSA polymer occurs at the pK of about 3,0, close to the first pK of the maleic acid residue and a single marked property change would be expected in the pH range 2,5 - 4.

5.2.3.2 Rejection and flux as a function of pH during formation

The data for this comparison are contained in Appendix B.1 and selected information from this source is presented in graphical form in Figures 5.3 to 5.8. The plotting symbols used are consistent throughout the series and the key is given below. The plotted values for flux and observed rejection are mean figures for the three cells in each trial, eliminating results from cells with damaged membranes.

Table 5.4 Key to graphical plots

Polymer	Symbol	Polymer	Symbol
MA/XX-1.1	✣	MA/XX-1.2	+
-2.1	×	-2.2	×
-3.1	◇	-3.2	◈
-4.1	□	-4.2	▣
-5.1	○	-5.2	◎

where MA/XX-1.1 indicates polymer MA/XX-1, first trial
MA/XX-1.2 indicates polymer MA/XX-1, second trial
etc.

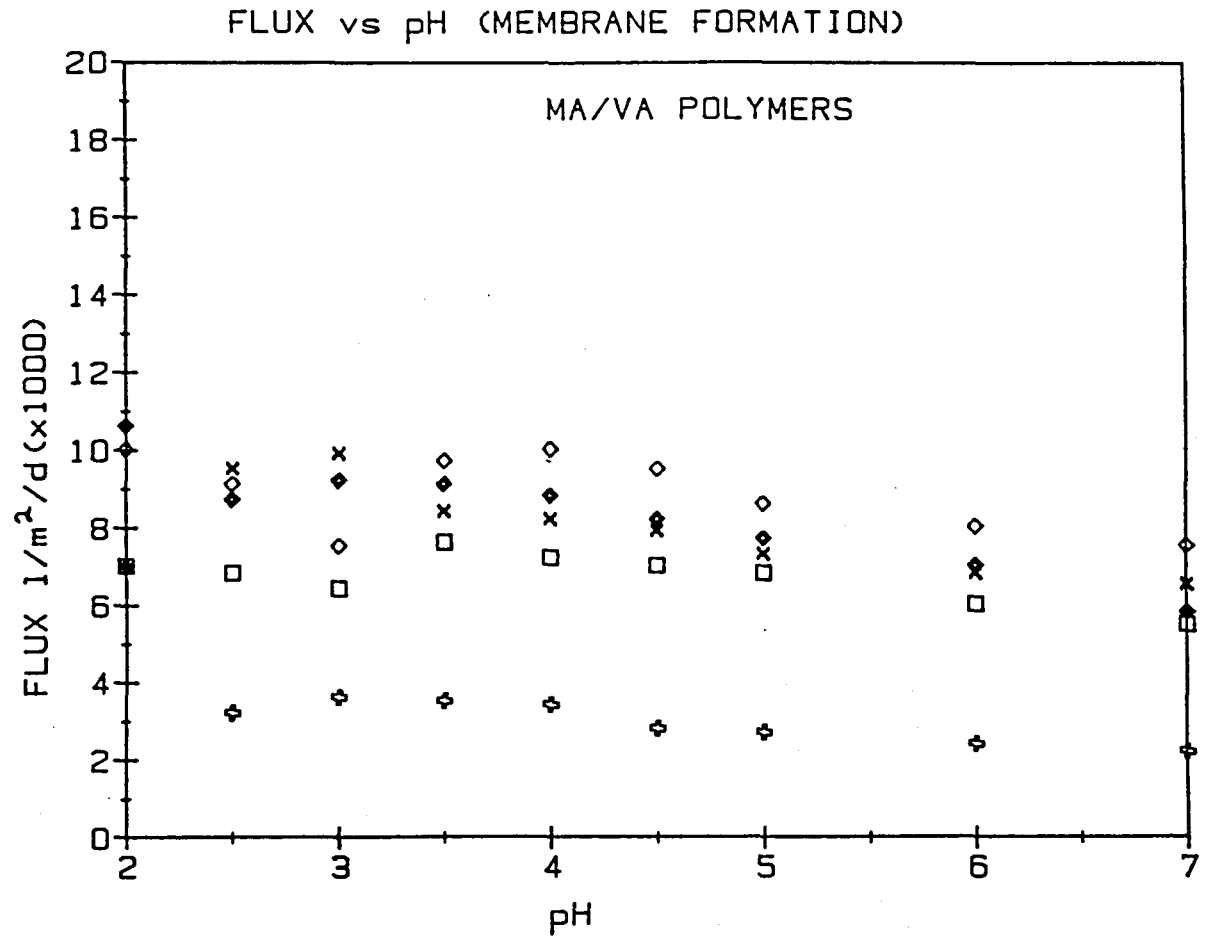

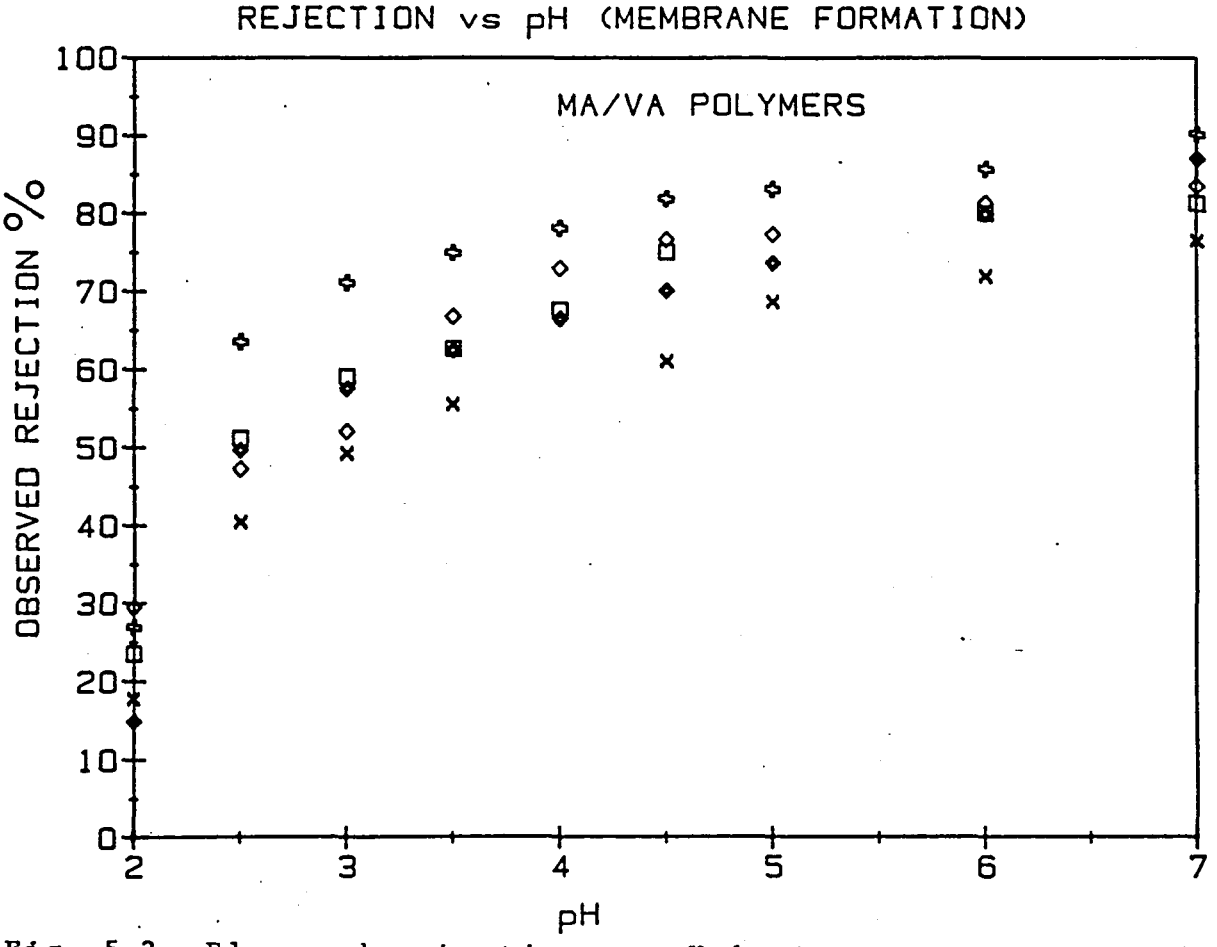

Fig. 5.3 Flux and rejection vs pH during formation - MA/VA polymers

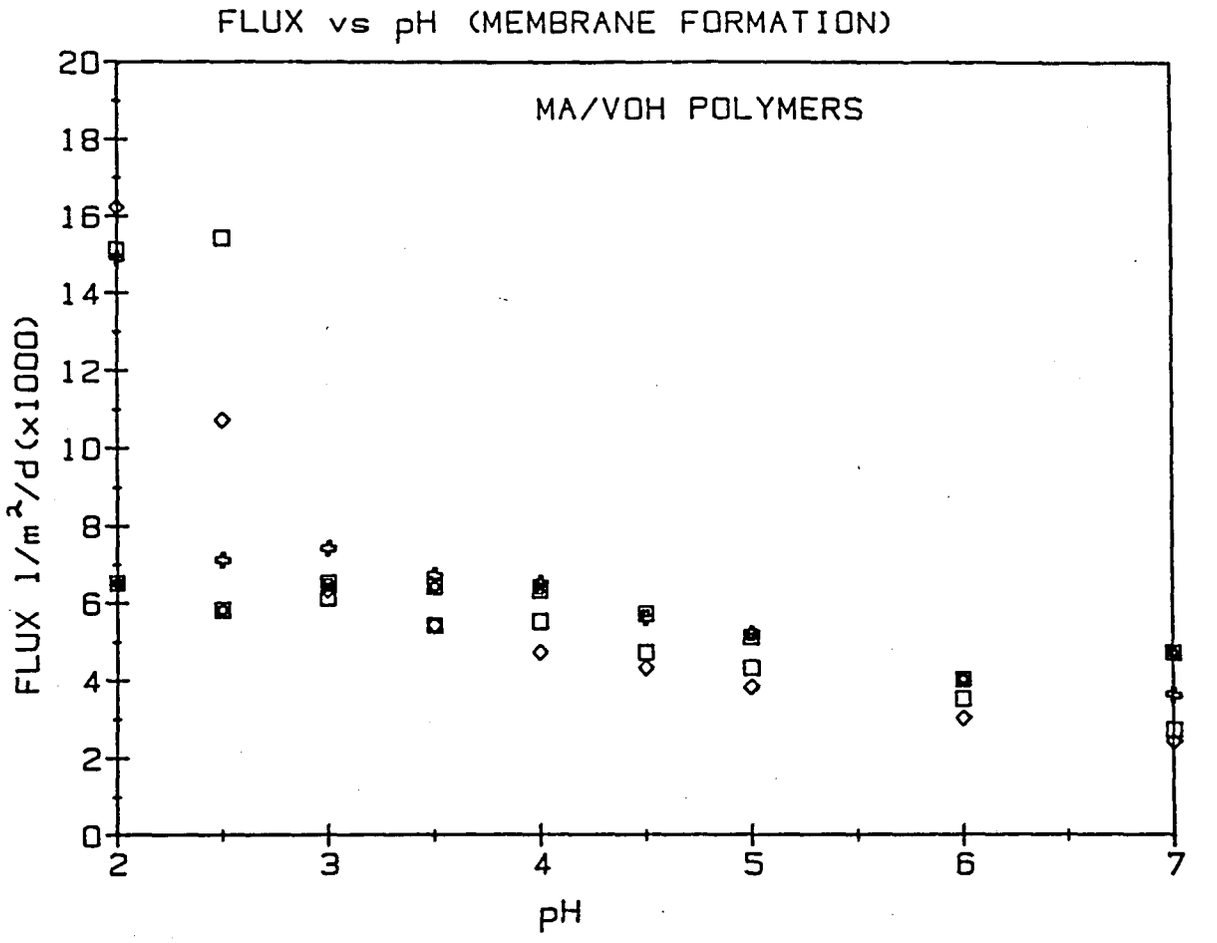

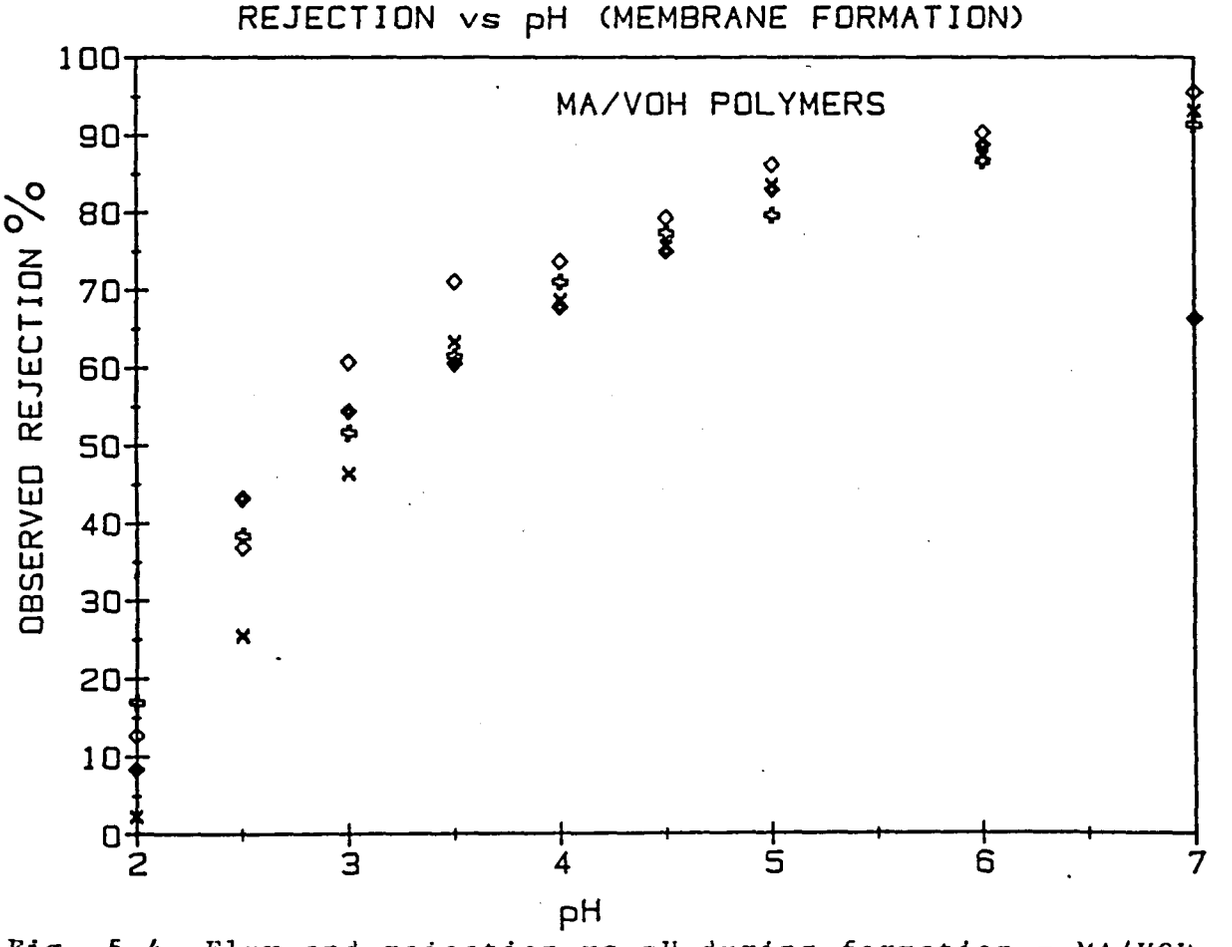

Fig. 5.4 Flux and rejection vs pH during formation - MA/VOH polymers

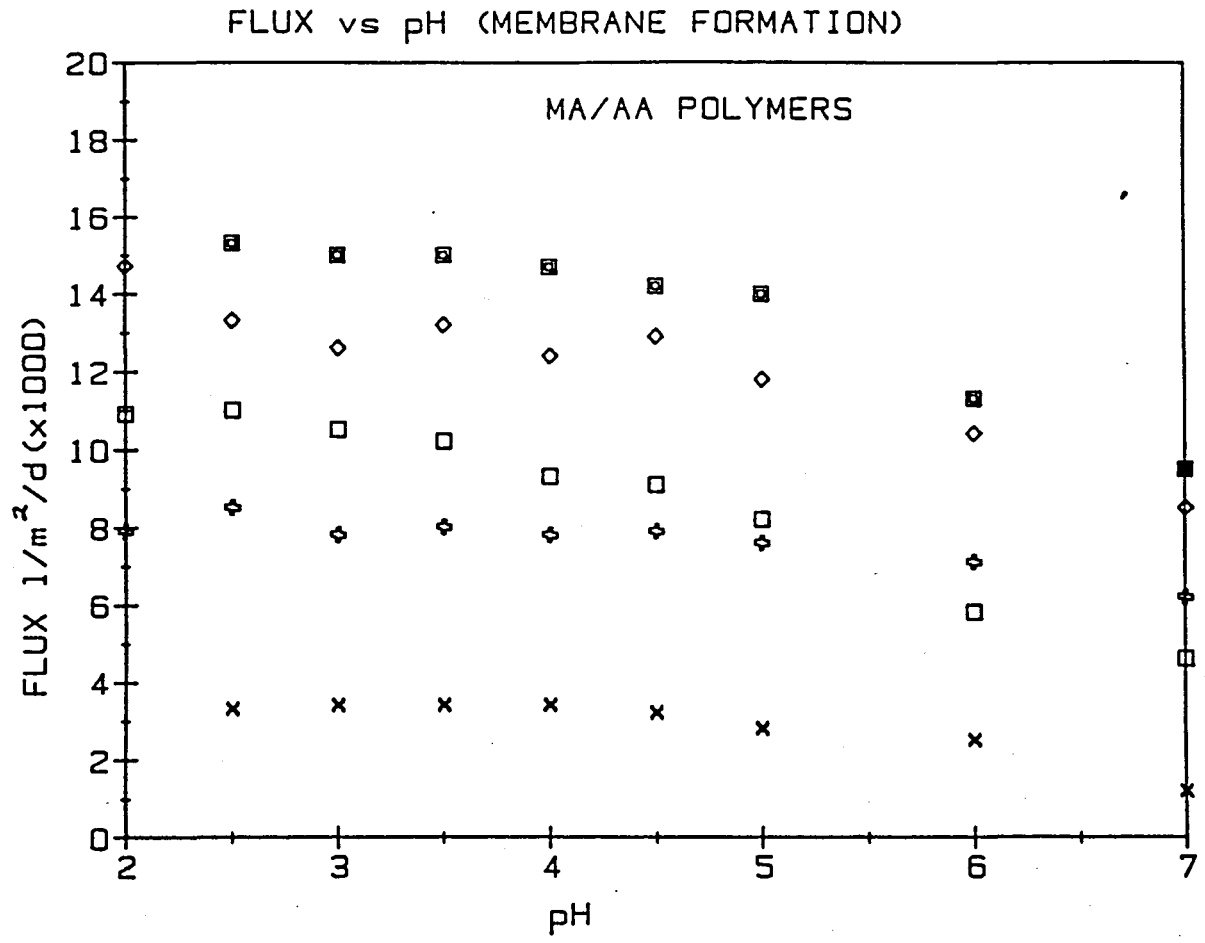

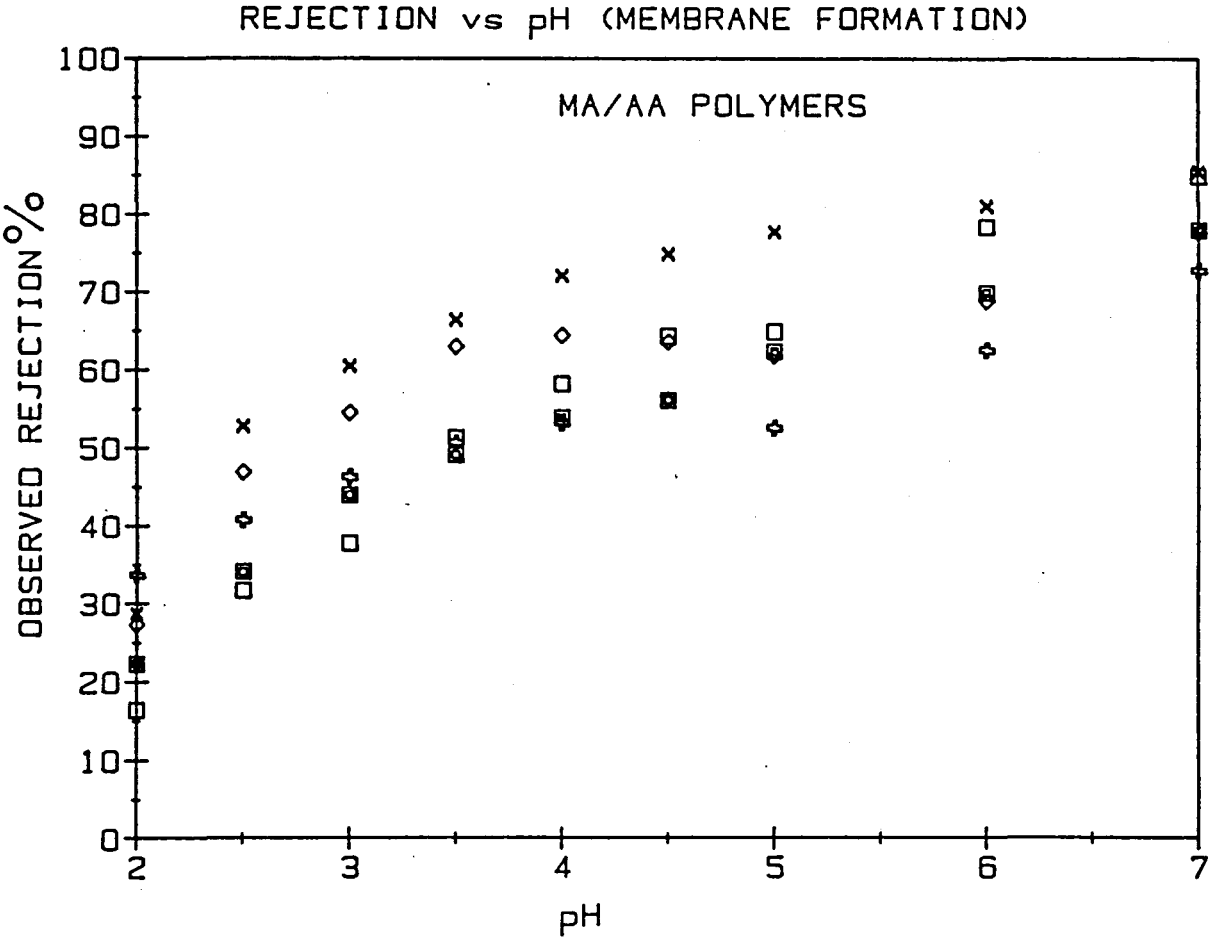

Fig. 5.5 Flux and rejection vs pH during formation - MA/AA polymers

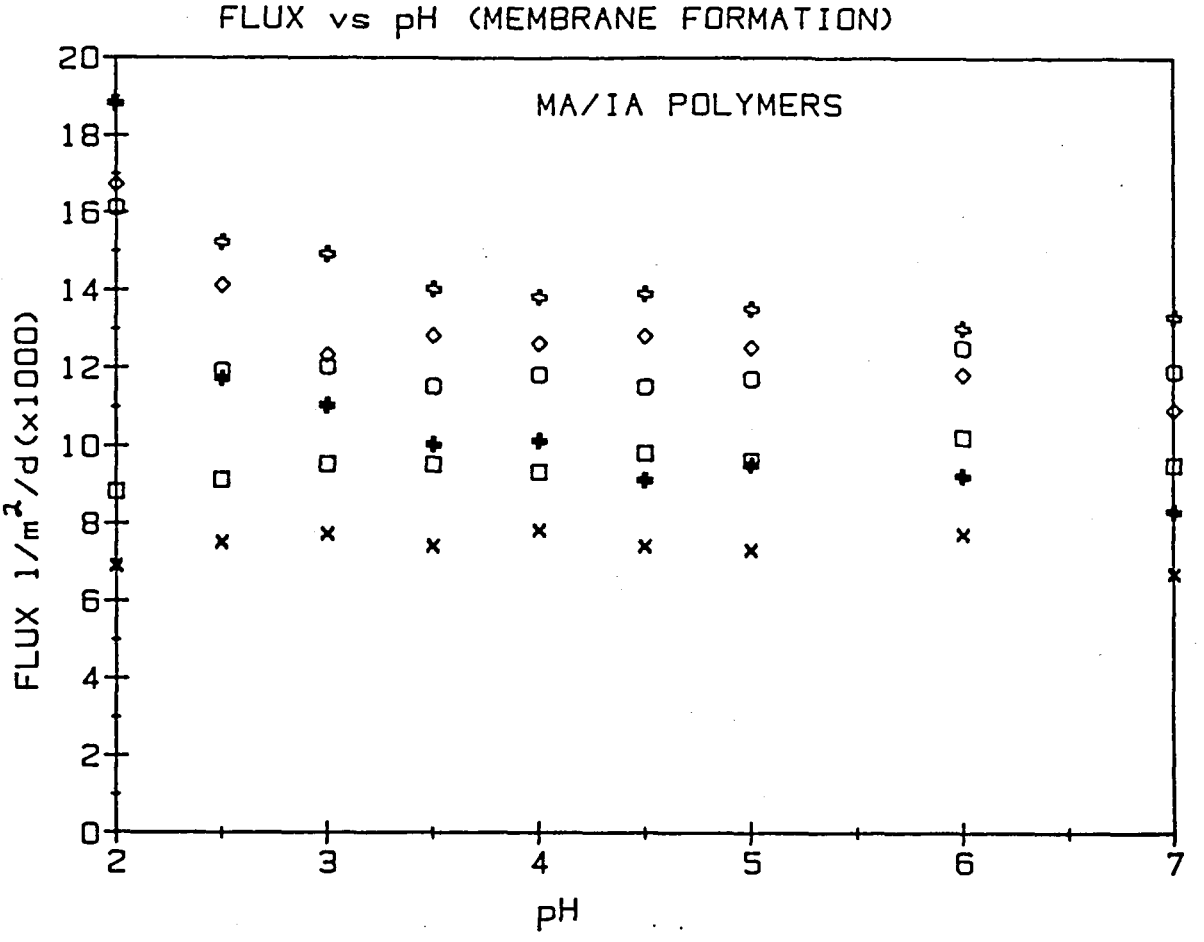

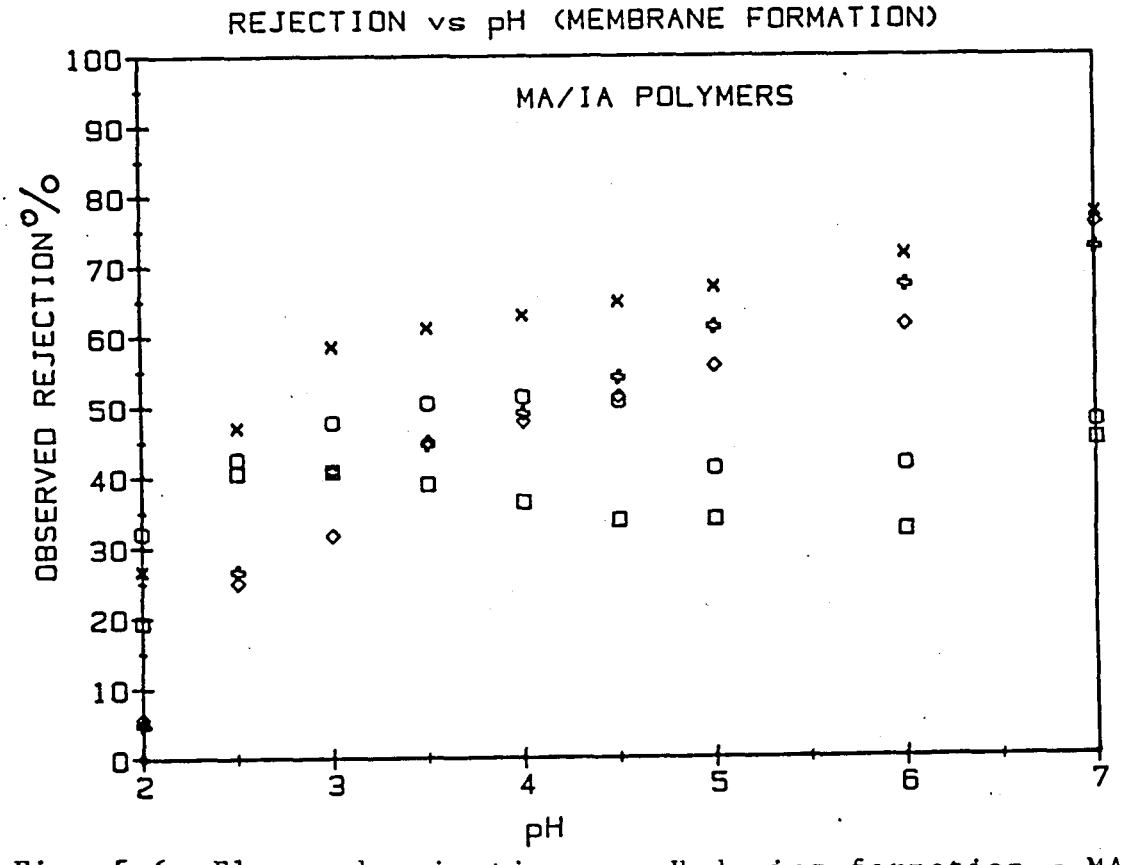

Fig. 5.6 Flux and rejection vs pH during formation - MA/IA polymers

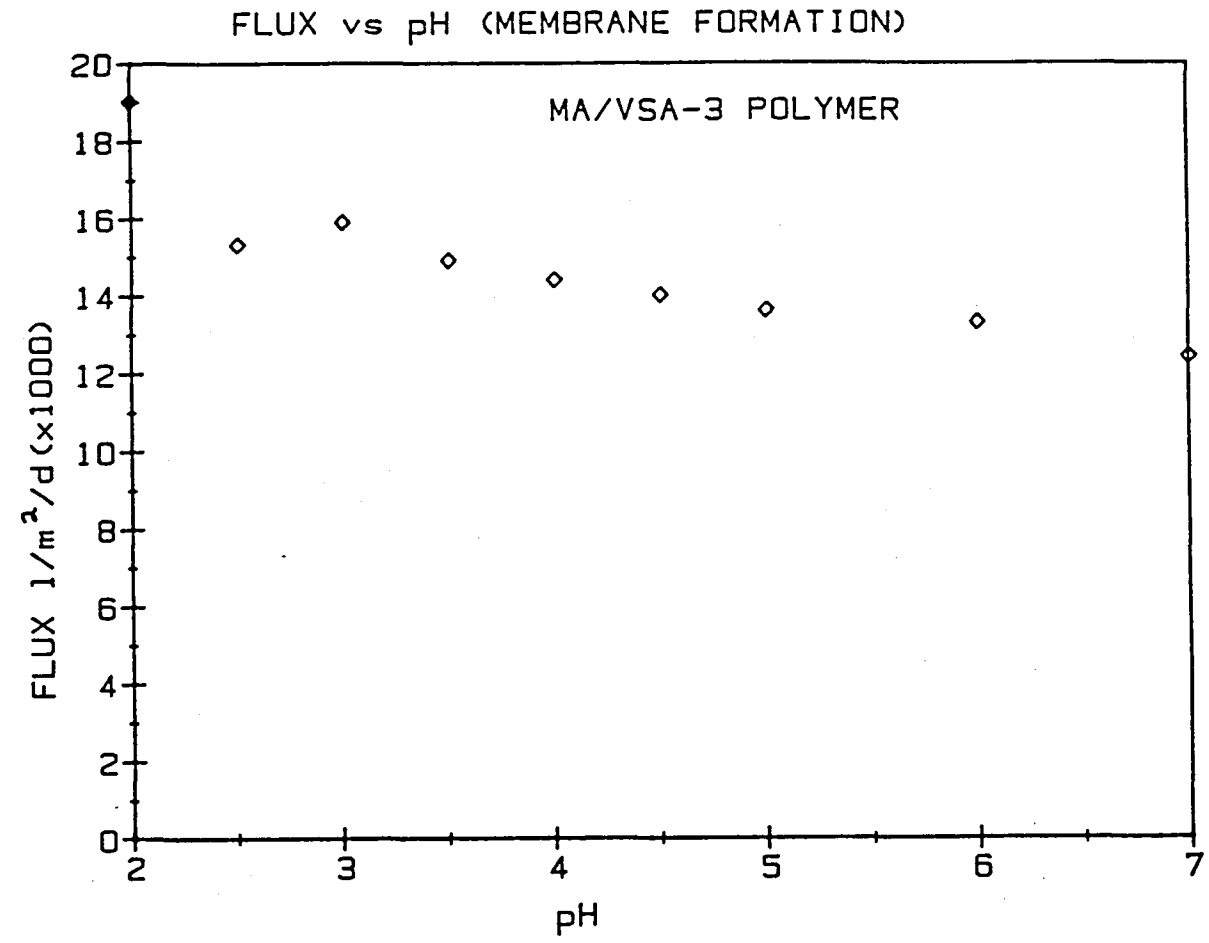

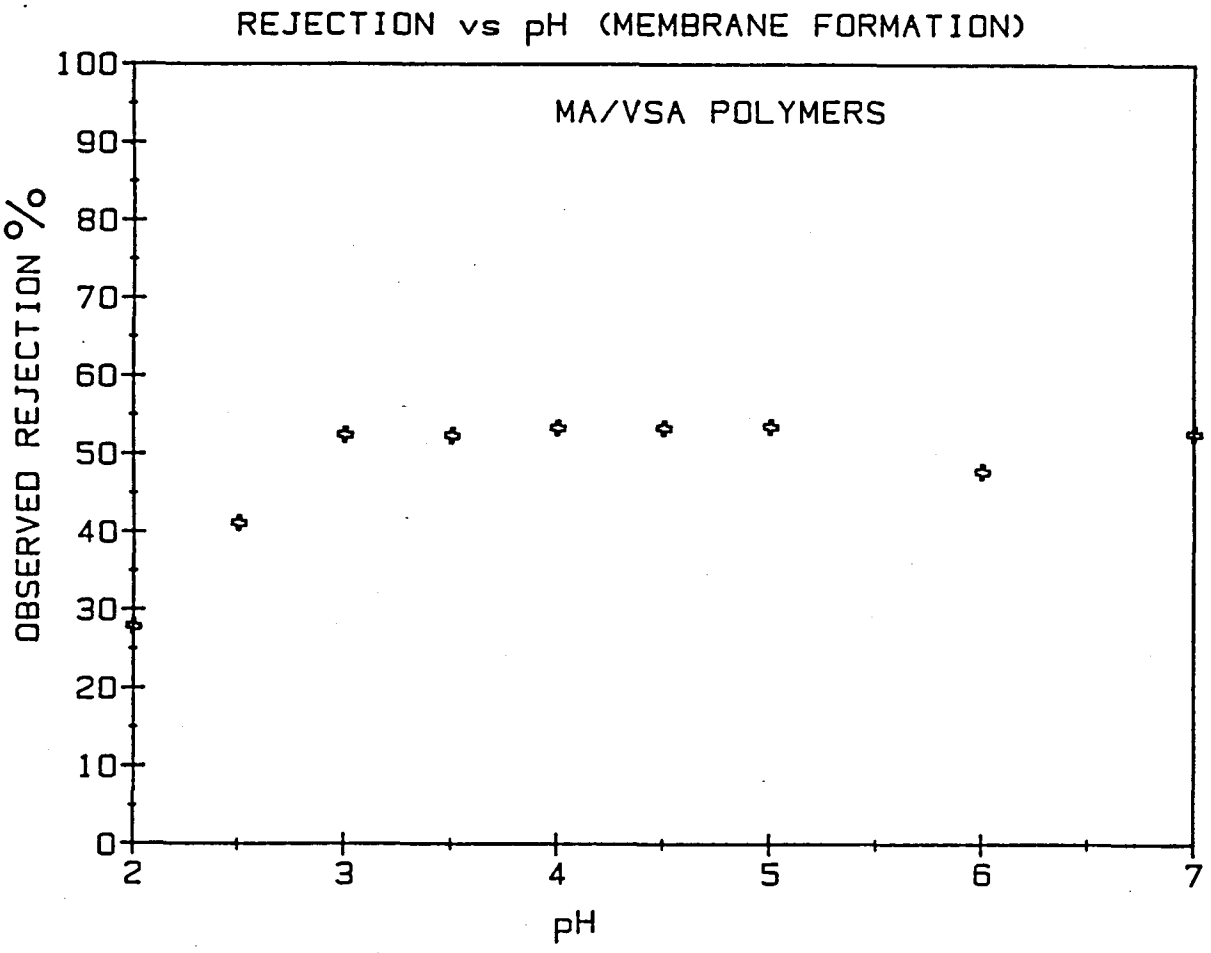

Fig. 5.7 Flux and rejection vs pH during formation - MA/VSA polymers

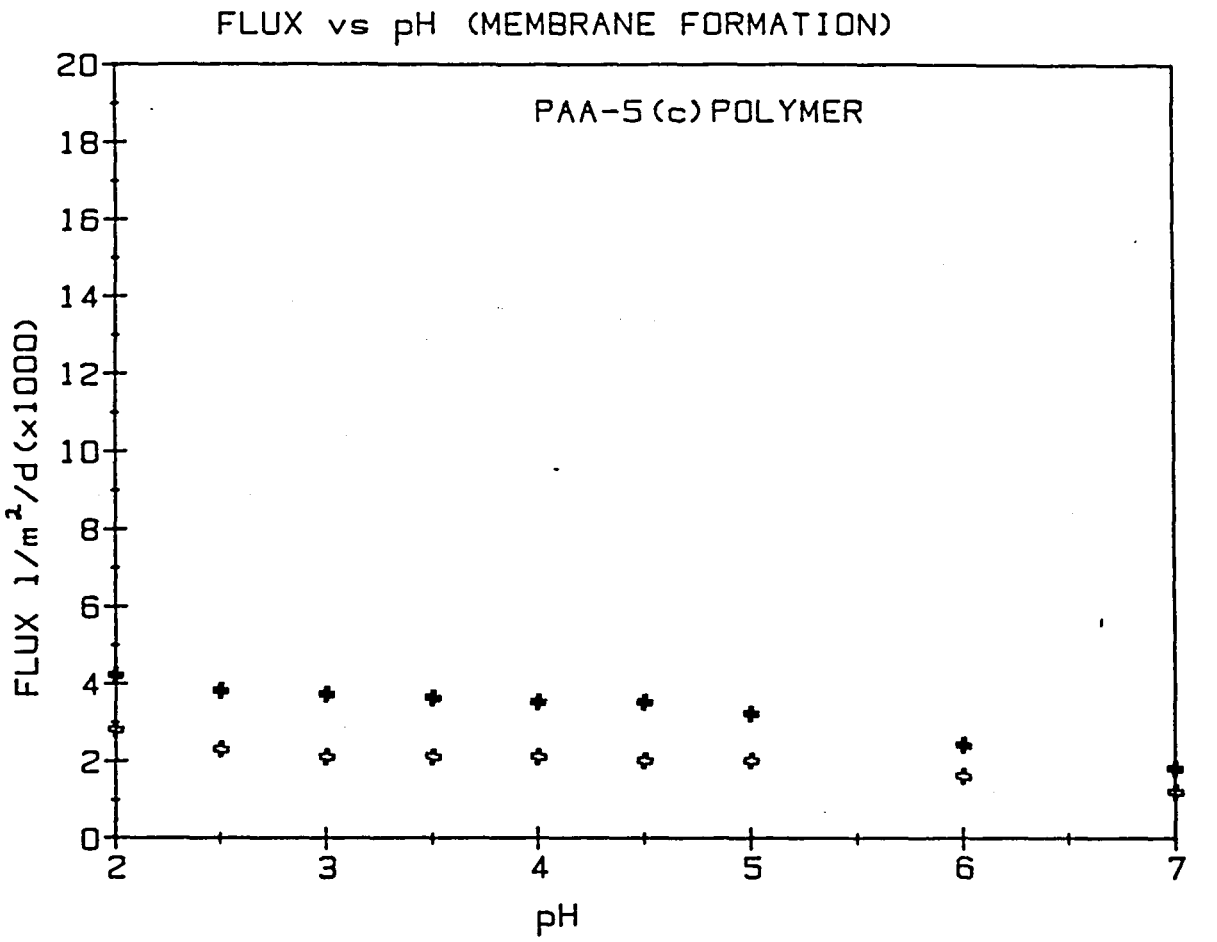

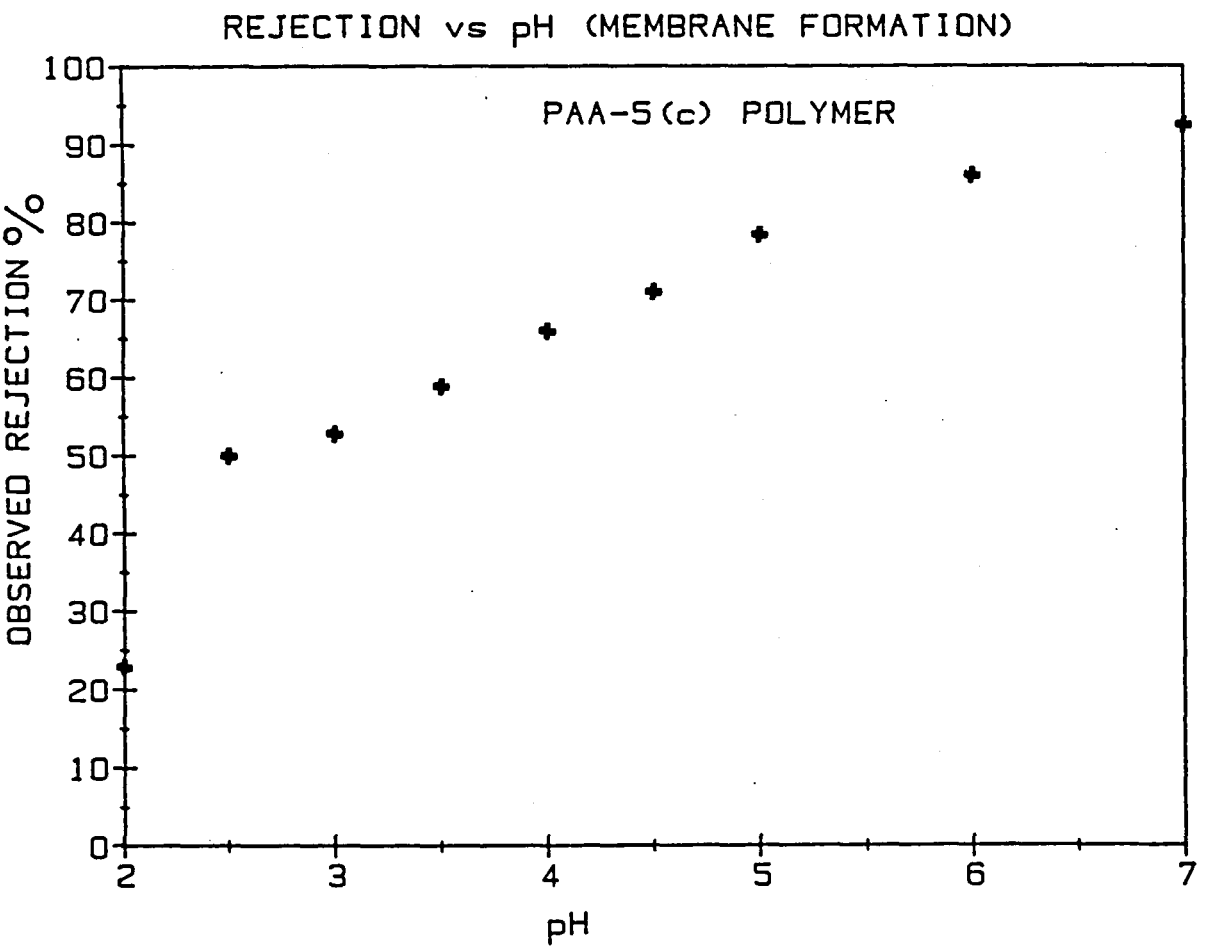

Fig. 5.8 Flux and rejection vs pH during formation - PAA-5(c) polymers

5.2.3.3 Discussion

The membranes to be discussed were all ion exchange types, the rejection properties varying markedly with ion exchange capacity. The ion exchange capacity is a function of the charge density and hence of the degree of ionization of the various acid groups present in the polymer. The change in degree of ionization is most rapid in the area of the pK of the acid group but the change is not as sharp as that observed with monomeric acids because of electrostatic interactions between the fixed acid groups.

The increase in charge density associated with the acid pK's also has the effect of causing swelling of the polymer, due to electrostatic repulsion and to binding of solvent to the anionic sites. The polymer is present primarily in the pore structure of the zirconia base membrane and the swelling of the polymer occludes the pores, producing a "tighter" membrane having higher rejection and lower flux.

The observed characteristics of membrane performance at various pH values can be explained broadly in terms of the effects mentioned above, but it should be pointed out that these observed effects are transient in nature and not amenable to detailed analysis.

(1) MA/VA membranes

These membranes showed a very rapid initial increase in rejection at pH values from 2 to 3,5 associated with ionization of the first maleic acid carboxylic acid group (pK_a^1 about 3,5). A drop in flux also occurred in this range, associated with the pore occlusion phenomenon. It is interesting to note that the most noticeable changes in flux and rejection occurred for the lowest molecular mass polymer MA/VA-1. It is suggested that the low-molecular mass polymer did not "pore-fill" effectively at low pH because of the small molecular hydrodynamic volume in relation to the pore size of the zirconia membrane. As a result membrane

flux was high and rejection low. Ionization of the polymer as pH rose resulted in a large increase in molecular dimensions and a very marked improvement in membrane properties. Above pH 4 only minor changes occurred, probably associated with improved pore filling and membrane compaction effects.

(2) MA/VOH membranes

These membranes exhibited a rapid increase in rejection at pH 2 to 4 associated with the first maleic acid ionization. A small inflexion occurred at about pH 4 - pH 4,5 followed by a further rejection increase at pH 4,5 to pH 7. The polymer from which these membranes were formed was a fully neutralized material which did exhibit partial second ionization in this range of pH (pK_a^2 6,5). The membrane flux results followed a similar pattern.

(3) MA/AA membranes

These membranes gave results which showed very wide scatter, particularly in the area of flux measurements, making interpretation rather difficult. The MA/AA copolymers have two acid groups ionizing in the pH range 2,5 to 4,5 (pK_a^1 maleic acid = 3,5; pK_a acrylic acid = 4,25) which was reflected in a rapid increase in rejection in this range. A plateau, or a slight dip in rejection is apparent at pH 4,5 to pH 5,5, followed by a further rise in rejection at pH 6 to pH 7. The second increase in rejection be explained by partial ionization of the second maleic acid group (pK_a^2 = 6,5).

Flux values were very widely scattered and showed a significant decline only at pH 5. It is apparent that a highly swollen membrane was formed at low pH, where ionization of the polymer was minimal. The polymers from which these membranes were produced had a high carboxylic acid content and were consequently very hydrophilic, forming swollen gels without ionization being present. A membrane of this type will have a high water content and give relatively high fluxes, as was observed in this case.

The reduction in flux later in the formation process was probably due to mechanical consolidation effects.

The very wide scatter of flux results, bearing no relation to molecular mass, can not be explained at this stage.

(4) MA/IA membranes

These polymer membranes were also extremely hydrophilic with an average of four possible ionizable groups in each copolymer repeat unit. As with the MA/AA membranes, this resulted in relatively loose, high-flux membranes with little decrease in flux as a result of polymer ionization. The rejection results can be examined in two distinct groups based on polymer molecular mass (as determined by intrinsic viscosity measurements)

(a) Lower molecular mass polymers MA/IA-1, 2, 3.

Membranes formed from these polymers exhibited the rejection characteristics which would be expected from a polymer membrane having carboxylic acid groups of pK value 3,5; 3,83; 5,45. The rejection increased sharply at pH 2 to 3,5 and then continued to increase slowly with rise of pH to 7, due to the successive ionizations of the acid groups present.

(b) Membranes MA/IA-4 and -5

were produced from polymers which were expected to be of higher molecular mass (no viscosity or GPC work was done due to insolubility of the polymers in 0,5 M sodium sulphate solution). These polymers showed rather low rejections which fell towards the end of the formation period. At the same point in the formation process the fluxes of these membranes increased. This is interpreted as a loss of membrane material. The polymers were probably of too high a molecular mass to fully penetrate the sublayer pore structure and failed to "pore-fill" correctly. A surface layer, poorly bonded to the substrate, formed in the

initial stages but dissolved as the pH rose and the acid groups ionized. Insolubilization of the polyelectrolyte occurred only by chelation to the zirconia sublayer and a surface gel was quickly dissolved at higher pH values.

(4) MA/VSA membrane

The vinyl sulphonic acid group has a pK_a of 3,0 and the maleic acid group a pK_a of 3,5. Over the pH range 2 to 3,5 membrane rejection rose sharply and flux decreased, as expected. Both flux and rejection now remained fairly stable as pH rose, with a gradual reduction in flux due to membrane compaction. The performance was consistent with the known polymer structure.

(5) Polyacrylic acid membrane

This particular polymer membrane was formed very rapidly at low pH as evidenced by the high rejection values obtained at pH below 3, where little polymer ionization or swelling occurred (pK_a = 4,25). The molecular mass of this polymer (148 000) would appear to be close to the optimum for the pore-filling process. Increasing polymer ionization between pH 3 and pH 7 resulted in a steady increase in rejection.

Evidence of rapid pore-filling is seen in the flux values for this membrane, flux being relatively stable at pH 2 to 5. Above pH 5, charge density became high and swelling of the polymer within the zirconia pore structure led to an increasingly "tighter" membrane with lower flux values.

5.2.4 MEMBRANE PERMANENCE

5.2.4.1 Introduction

One of the objectives of this research work was to produce polyelectrolytes having greater chelation to hydrous zirconia substrates. This improved chelation would be expected to lead to

greater membrane permanence, that is, better retention of properties with time. The zirconia/polyacrylic acid membranes in current use show a slow increase in flux and reduction in rejection with time, partially due to loss of material from the membrane.

Evaluation time was limited to 20 hours after formation, which was insufficient to determine any long-term trends, but it did enable some comparisons to be made between polymers, and served to eliminate those polymers which did not chelate effectively.

The general trend during the first few hours of operation of a membrane was for a slight reduction in flux to occur, together with a minor increase in rejection, resulting from membrane compaction under pressure.

5.2.4.2 Changes in membrane properties with time

The single most useful measure of performance is the Lonsdale figure of merit (FOM) and the change in this value with a longer evaluation time.

Figures of merit (A^2/B) are summarized for all membranes in table 5.5 below. Property changes are defined as

$$\Delta FOM = \frac{FOM\ (20\ h) - FOM\ (0,5\ h)}{FOM\ (0,5\ h)} \times 100\%$$

Positive values indicate property improvement with time.

Table 5.5 Figure of merit-changes with time

MEMBRANE REFERENCE	$FOM^{0,5}$	FOM^{20}	Δ FOM (%)
MA/VA-1.1	0,68	0,66	-2,9
-2.1	0,72	0,78	+8,3
-3.1	1,31	1,68	+28,2
-3.2	1,37	1,04	-24,1
-4.1	0,79	0,86	+8,7
MA/VOH-1.1	1,29	1,01	-21,7
-3.1	1,10	0,98	-10,9
-4.1	2,69	2,82	+4,8
-4.2	1,01	1,22	+22,0
MA/AA-1.1	0,55	0,53	-3,6
-2.1	0,38	0,48	+26,3
-3.1	0,97	0,81	-16,5
-4.1	0,85	0,73	-14,1
-4.2	1,13	1,28	+13,3
MA/IA-1.1	1,05	0,86	-18,1
-1.2	0,75	0,81	+8,0
-2.1	0,78	0,76	-2,6
-3.1	1,30	1,00	-23,1
-4.1	0,31	0,22	-29,0
-5.1	0,36	0,39	+8,3
MA/VSA-3.1	0,47	0,35	-25,5
PAA-5(C).1	0,66	0,51	-22,7
-5(C).2	0,80	0,75	-6,3

5.2.4.3 Discussion

Interpretation of the results presented in Table 5.2.10 in absolute terms is difficult due to the small number of evaluations performed and the variability which would appear to be inherent in results obtained with dynamic membranes. Only broad conclusions will be drawn, therefore, by comparison of experimental data with the results for the "control" poly(acrylic acid membrane) ref PAA-5(c).

(1) MA/VA copolymer membranes

The performance of these membranes is generally better than that of the control membrane and appears to be an optimum at the molecular mass of MA/VA-3. The poor result for MA/VA-3.2 is associated with a loss of rejection coupled with an increase in flux, and may indicate the development of a flaw in the membrane surface. There does appear to be a distinct molecular mass effect in this case, in line with that expected for the pore-filling model of membrane rejection discussed in Section 3.5.2. The improved permanence properties of these membranes compared with the properties of poly(acrylic acid) may be a result of the formation of a stronger chelate complex.

(2) MA/VOH copolymer membranes

These membranes again show good stability and high overall FOM figures with the lower intrinsic viscosity polymer MA/VOH-4 showing better performance. The general performance is rather similar to that of membranes formed from the parent MA/VA copolymers. The MA/VOH copolymers are expected to have higher charge densities than those of the MA/VA copolymers from which they were derived, as both carboxylic acid groups are neutralized during alkaline hydrolysis yielding, in theory, twice the charge density. In practice, the much greater swelling of these polymers during formation means that polymers of lower molecular

mass are likely to have the optimum hydrodynamic size to enable pore-filling to occur.

The MA/VOH copolymers have potential for enhanced chelation due to the presence of the hydroxyl group and membrane permanence appears to be significantly better than that of PAA.

(3) MA/AA copolymer membranes

No very marked trends were apparent in this membrane series, except that increase in molecular mass (intrinsic viscosity) appears to result in improved overall values of FOM. Permanence properties appeared to be of the same general level as of PAA.

(4) MA/IA copolymer membranes

The polymers from which these membranes were formed are of a random structure containing about 50-60 mole% maleic anhydride. The lack of a regular copolymer repeat group would be expected to result in fewer chelation properties and this appears to be confirmed by the permanence results. Copolymers MA/IA-4 and MA/IA-5, which would be expected to be of high molecular mass, produced rather low overall FOM values. Polymers of lower molecular mass would be expected to have rather high hydrodynamic volumes at pH 7, due to the presence of three carboxylate anions per repeat unit, and this may account for their comparatively good performance.

(5) MA/VSA copolymer membranes

A single polymer in this group was evaluated; it had a low intrinsic viscosity, indicating a low molecular mass. The permanence of the membranes evaluated were generally poor. Composition analysis showed that the copolymer contained only 27% MA with few opportunities for chelation.

5.2.5 pH EFFECTS ON MEMBRANE PERFORMANCE

5.2.5.1 Introduction

The composite membranes under consideration are anionic, the membrane charge density increasing with increase in ionization. The increase in ionization would be expected to lead to higher rejection as a result of the higher charge density, and lower flux due to polymer swelling and more efficient pore-filling. Ionization will increase with increasing pH until full neutralization of the acid groups has occurred, at a pH rather higher than the pK_a value of the acid group concerned. The pK_a is in fact defined, in a simple way, as the pH at which the acid group is one-half ionized (α = 0,5). The pK_a values of acid groups in the copolymers are listed below in Table 5.6. It should be noted that pK_as may be affected by the presence of neighbouring groups in some cases and the figures quoted should be treated as approximations.

Table 5.6 pK_as of carboxylic acid groups

Acid group	pK_a^1	pK_a^2
Maleic	3,5	6,5 (in alternating copolymers)
Acrylic	4,25	
Itaconic	3,85	5,45
Vinyl sulphonic	3,0	

5.2.5.2 Results

Table 5.7 Effects of pH on membrane performance

MEMBRANE	FLUX (X 1000)			R_{obs} (%)			$A^2/B \times 10^{-5}$		
	pH 7	pH 8	pH 9	pH 7	pH 8	pH 9	pH 7	pH 8	pH 9
MA/VA-1.1	2,40	2,08	1,95	89,2	91,0	90,7	0,66	0,69	0,63
-3.1	8,28	7,43	6,77	85,9	85,5	91,2	1,68	1,74	1,89
-3.2	6,92	6,01	5,38	81,6	86,0	87,6	1,04	1,25	1,30
MA/VOH-1.1	4,20	3,56	3,50	87,6	89,5	90,0	1,01	1,05	1,09
-4.2	4,41	3,93	2,92	88,2	90,3	91,1	1,22	1,44	1,42
MA/AA-1.1	5,83	5,58	5,07	73,4	76,7	80,3	0,53	0,60	0,68
-3.1	9,15	7,66	6,07	72,1	78,6	84,6	0,81	0,96	1,11
-4.1	5,08	4,74	4,98	80,9	84,2	81,2	0,73	0,83	0,65
-4.2	9,52	8,34	7,11	79,8	85,6	89,4	1,13	1,28	1,69
MA/IA-1.1	11,33	10,45	9,48	69,5	72,7	74,4	0,86	0,93	0,92
-1.2	8,34	7,70	6,98	74,4	76,6	78,5	0,81	0,83	0,85
-2.1	6,95	6,89	6,31	76,7	79,3	81,4	0,76	0,80	0,84
-3.1	10,93	11,78	10,21	69,4	76,0	77,8	1,00	1,22	1,31
-5.1	10,57	10,19	9,24	52,6	57,5	60,9	0,39	0,46	0,48
MA/VSA-3.1	7,42	7,37	7,28	58,3	61,5	62,3	0,35	0,39	0,40
PAA-5(c).2	2,02	1,63	1,65	91,4	93,5	94,1	0,75	0,83	0,83

5.2.5.3 Discussion

(1) MA/VA membranes:

The copolymers from which these membranes were made contain two carboxylic acid groups having pK values of about 2,5 and 6,5. When the first acid group has ionized, the second carboxylic acid group is prevented from ionizing, under normal conditions, by hydrogen-bonding interaction with the carboxylate anion. However, if the ionization of the first carboxylate group is suppressed by addition of a suitable simple electrolyte, or the hydrogen-bonding effect reduced by high temperatures, the second carboxylic acid can be neutralized.

The results for the MA/VA membranes show that, at pH 7 to 8 there is a fairly marked drop in flux, together with an increase in rejection and in figure of merit. The changes at pH 8 to 9 are generally less marked. These results indicate that charge density increases with pH, particularly at pH 7 to 8, and this can only be as a result of the neutralization of some of the second carboxylic acid groups (pK_a about 6,5). The test conditions used involve the use of about 0,03 mole.dm^{-3} sodium nitrate solution at a temperature of 35°C and it is conceivable that some carboxylate groups may be formed under these conditions. Strauss and Andrechak[149] have investigated similar alternating MA copolymers and have shown that the titration behaviour of maleic acid groups at the ends of chains is significantly different from that of "interior" groups, and this is a possible explanation for the observed behaviour.

(2) MA/VOH membranes

These membranes have a significantly higher charge density than that of the parent MA/VA polymers as they are fully neutralized with no fixed steric relationship between adjacent carboxylate

groups as exists in the MA/VA copolymers. It would be expected at pH 7, however, that some functional groups would be present in the carboxylic acid form due to the effects of inter- and intra-molecular hydrogen bonding. These carboxylic acid groups would perform in a manner identical to that postulated for the MA/VA copolymers, and this could lead to modest improvements in rejection and FOM figures at high pH.

These effects have, in fact, been demonstrated, but to a smaller degree than with the MA/VA polymers. The mechanism postulated of partial neutralization of hindered carboxylic acid groups under operating conditions is therefore supported.

(3) MA/AA membranes

The copolymers from which these membranes were formed also contain "hindered" or "blocked" carboxylic acid groups as in the case of the MA/VA copolymers. The same general trends in membrane properties are observed and the same explanation applies.

(4) MA/IA membranes

The MA/IA copolymers have four carboxylic acid groups, with pK values varying from 3,5 to 6,5 (the last value referring to the hindered maleic acid group). Interactions between these functionalities would be expected to produce a complex spread of ionization behaviour. The membrane performance results showed a fairly marked increase in rejection and a reduction in flux over the pH range 7 to 9 indicating an increase in charge density. It would appear that both itaconic acid groups and hindered maleic acid groups may account for these changes.

(5) MA/VSA membranes

These membranes exhibited a modest increase in rejection with increasing pH, but flux and FOM figures were changed very little.

The major ionization of the MA/VSA polymer occurs at low pH (pK_a VSA at 3,0, pK_a MA at 3,5). The charge density produced in the vicinity of the second maleic acid group appears to be sufficiently high to prevent any ionization.

(6) Poly(acrylic acid) membrane

This membrane showed a flux reduction with pH increase, but rejection and FOM figures increased slightly. It could be expected that this polymer would be completely ionized at pH 7, and no increase in charge density is expected with an increase in pH. It is possible that ionization is suppressed by the presence of high concentrations of counterions (Na^+ ions) in the membrane from the feed solution. In addition, the presence of high concentrations of carboxylate anions in the membrane will tend to suppress ionization to a certain extent.

5.2.6 MOLECULAR MASS EFFECTS

5.2.6.1 Introduction

In the only study published, Johnson et al[43] determined that a molecular mass in the range of 50 000 to 150 000 for polyacrylic acid gave the most favourable values of composite membrane rejection. No comprehensive study of this phenomenon has been made in this research work, but sufficient data are available, to indicate trends in some cases.

In this study Lonsdale's figure of merit has been used as the primary basis for comparison of membranes as it combines a number of different variables into a single quantitative factor. The variations of FOM with polymer intrinsic viscosities (IV) for a number of membranes have been presented in graphical form.

5.2.6.2 Results

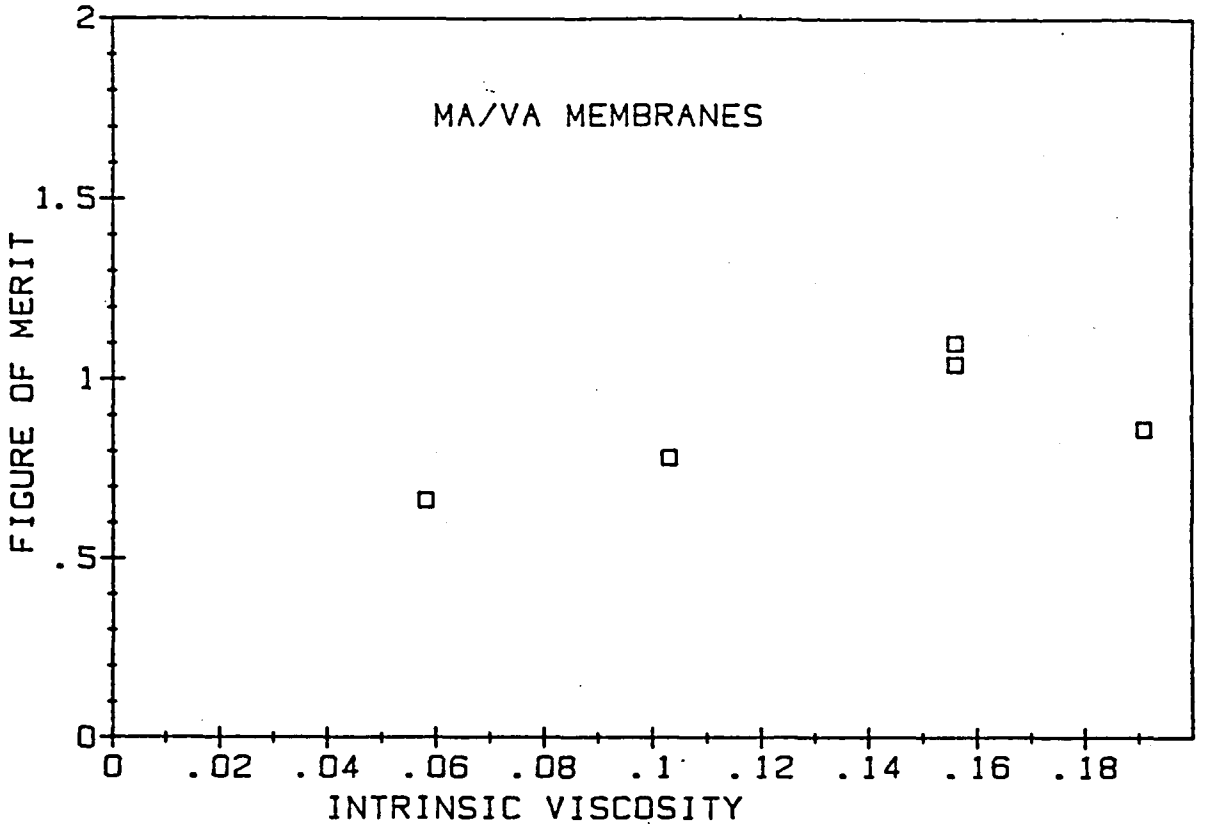

Fig. 5.9 IV vs Figure of merit for MA/VA membranes

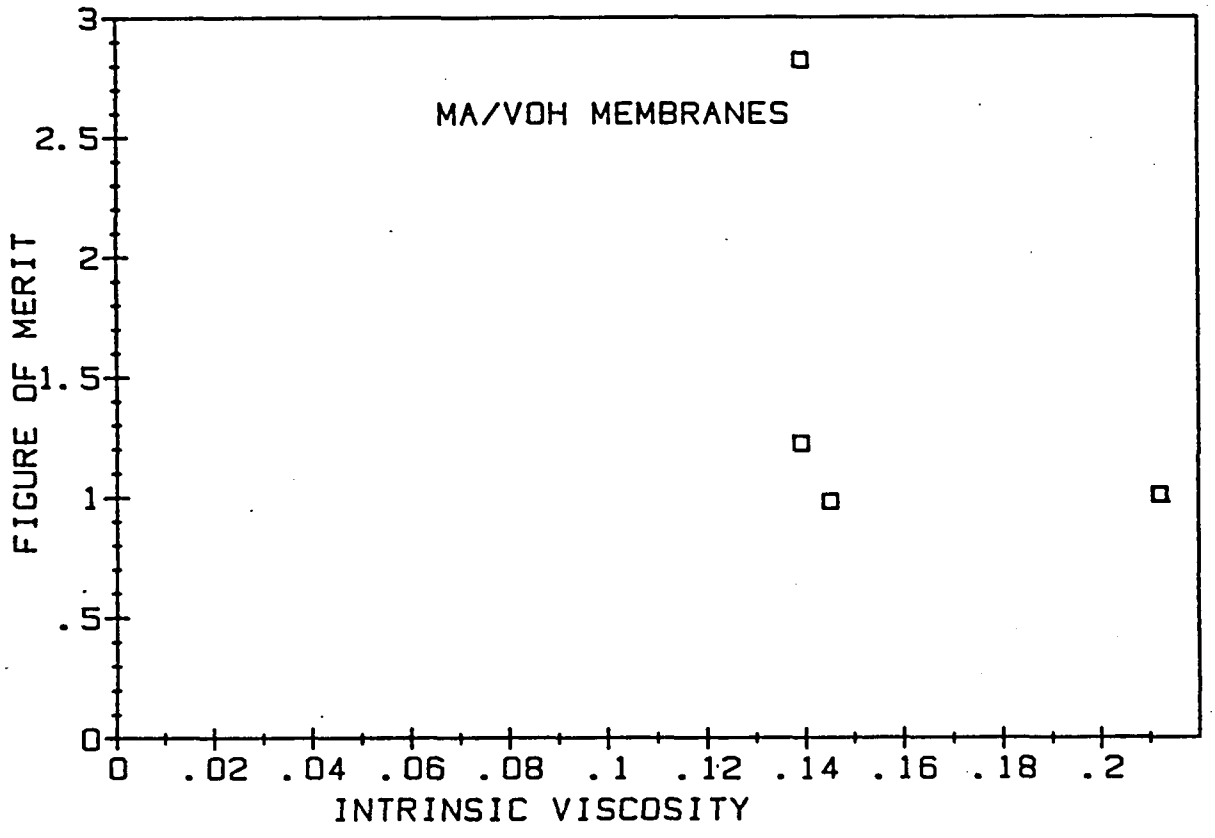

Fig. 5.10 IV vs Figure of merit for MA/VOH membranes

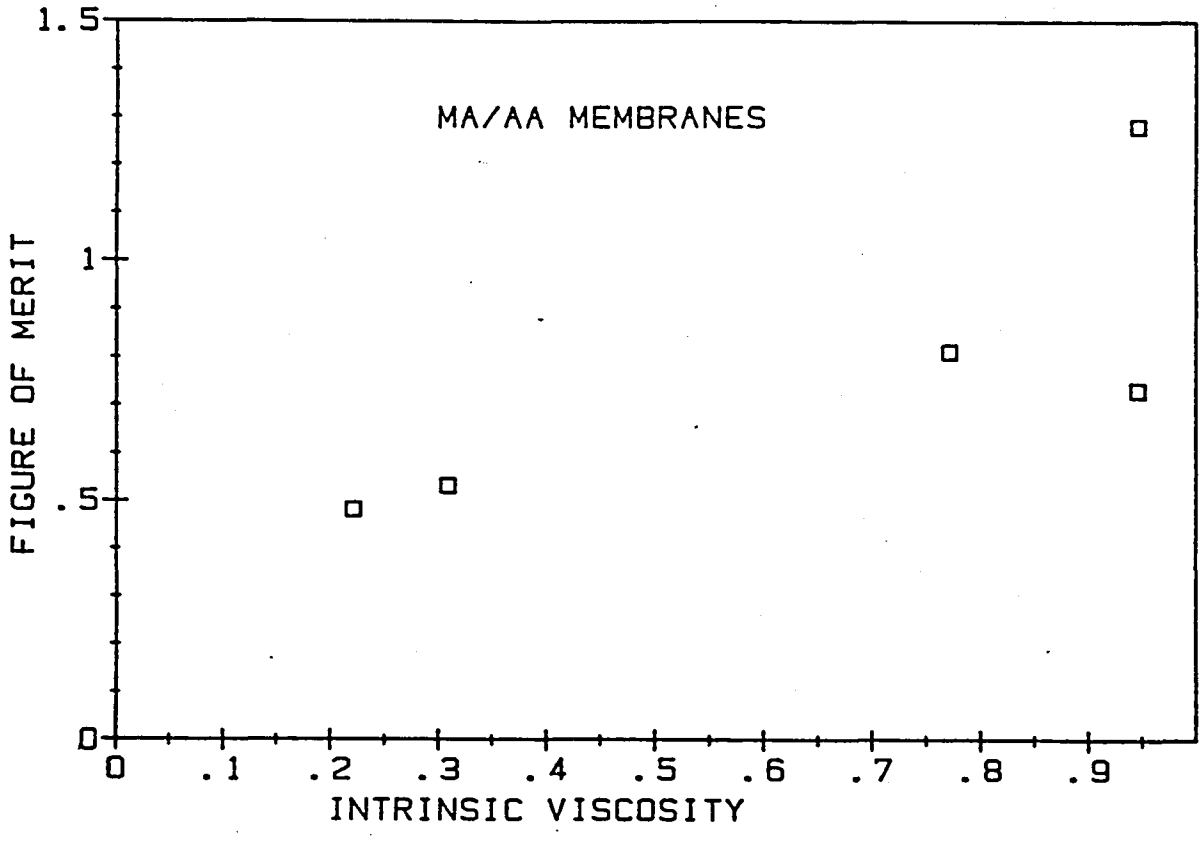

Fig. 5.11 IV vs Figure of merit for MA/AA membranes

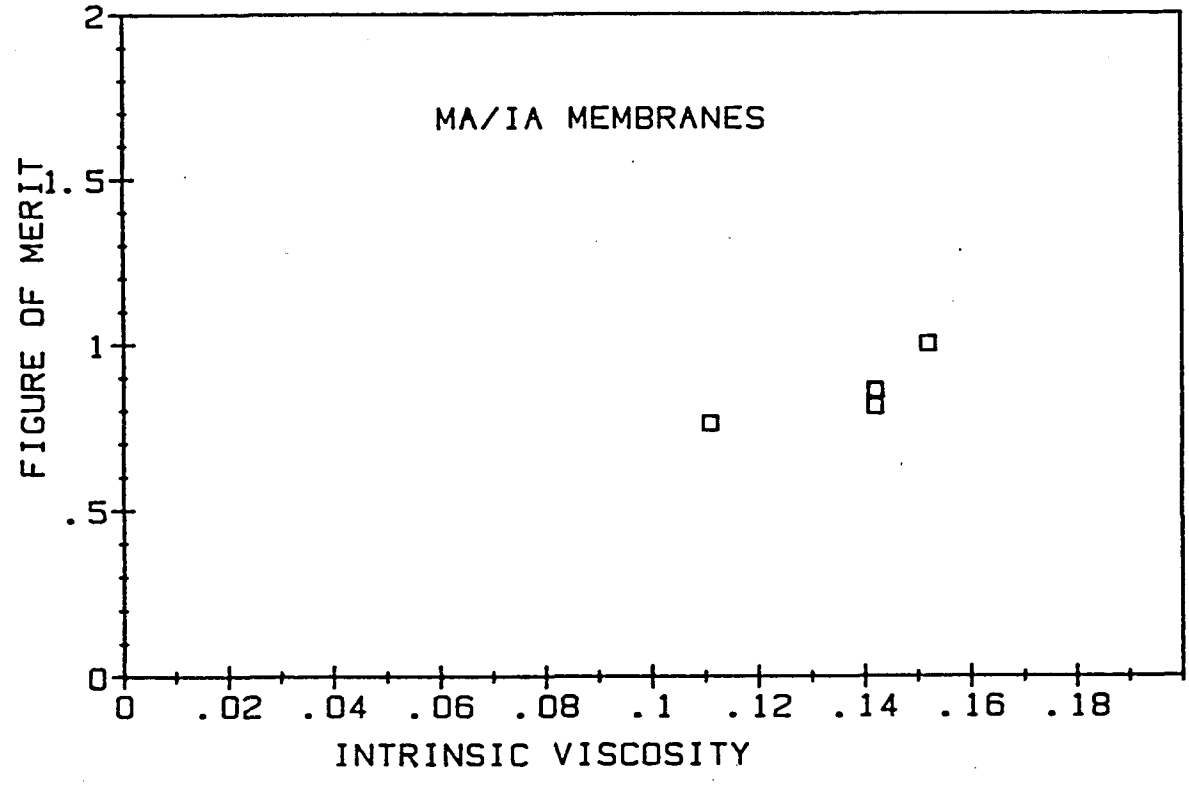

Fig. 5.12 IV vs Figure of merit for MA/IA membranes

5.2.6.3 Discussion

(1) MA/VA membranes

Some evidence of a peak in performance at an IV of about 0,16 is shown here, with quite good reproducibility between the results of two trials undertaken with this particular polymer (MA/VA-3).

(2) MA/VOH membranes

No trends can be discerned for these membranes. The large difference between observed values of FOM in two successive trials of the same polymer highlights the problem of non-reproducibility which is a marked feature of research on dynamic membranes.

(3) MA/AA membranes

A tendency for FOM to rise with increasing IV is evident in this graph; reproducibility is again a problem.

(4) MA/IA membranes

A complete plot is not presented for these membranes as IV values for MA/IA-4 and -5 are not available. If we make the reasonable assumption that the IV's of these polymers are higher than those for the earlier members of the polymer series then some tendency to reach a peak is indicated, since the FOM values for MA/IA-4 and -5 are low at 0,32 and 0,39, respectively.

5.2.7 MEMBRANE PERFORMANCE AS A FUNCTION OF SALT CONCENTRATION

5.2.7.1 Introduction

Discussions of the results presented in the previous sections of this chapter have been broad and qualitative. Quantitative comparisons can be made only if results are normalized to a

common salt concentration, as discussed in Section 3.6.3. To enable this to be done one copolymer from each group was selected for a second trial involving evaluation of properties over a range of concentrations. Those polymers which appeared to form the most satisfactory membranes in the first trial were chosen for re-assessment. The full results of these trials are given in Appendix C.1 and the related plots of log solute flux(s) against log feed concentration (m) in Appendix C.2.

The values of fixed-charge molality ($\bar{M}$) obtained from the intercepts are low compared with those quoted by Spencer[146]. In the case of the maleic acid copolymers used in our study the answer lies in a consideration of the hydrophilic nature of the polymer. The charge densities quoted are in units of moles per unit mass of the water in the swollen membrane, and the degree of swelling will affect this figure. Copolymers such as MA/IA which have more ionizable groups per unit length of chain in the dry form (compared with PAA) are also more hydrophilic and are greatly swollen when in the membrane form, accounting for the low molality of fixed charges. The high water content of the maleic acid copolymers is reflected in the high water flux values compared with PAA membranes.

Further discussions of the variables ($\bar{M}$) and (b) will be found in Section 5.2.10 in which an attempt is made to correlate these variables with membrane performance.

5.2.7.2 Results and discussions

Table 5.8 contains values of slope (E) intercept (H) and correlation coefficient (r) for the plots of log m against log s in Appendix C2, together with calculated values for fixed-charge index ($\bar{M}$) and fixed charge micro-homogeneity index (b) for the polymer membranes examined.

A value of B = 2,424 was used in the calculations.

Table 5.8 Membrane charge density and micro homogeneity indices

MEMBRANE	E	H	r	$\bar{M}$	b
MA/VA-3.2	0,723	0,328	0,996	1,14	0,86
MA/VOH-4.2	0,937	0,404	0,976	0,96	0,97
MA/AA-4.2	0,492	0,025	0,963	2,29	0,75
MA/IA-1.2	0,735	0,407	0,999	0,95	0,87
PAA-5(c).2	0,992	0,383	0,998	1,00	0,99
PAA*	0,40	-0,36	-	5,81	0,70

(PAA* refers to results drawn from the publication by Spencer[146])

E slope of log m vs log s plot
H intercept of log m vs log s plot
r correlation coefficient of regression line
$\bar{M}$ molality of free fixed charges in the active membrane
b Fixed charge micro-homogeneity index

The results marked PAA*, quoted by Spencer, are drawn from publications on earlier work in which sodium chloride was used in the feed. The results which have been obtained in the present research work, in which sodium nitrate was used as feed, are substantially different. The nature of the anion in the salt should not cause differences of this magnitude and the reasons for the discrepancies between these sets of results are not known. The results obtained for PAA-5(c) give a slope (E) very close to ideal (E = 1). The ideal ion-exchange membrane would

have E = b = 1 in a solution of a 1:1 electrolyte. The value of 0,99 for b in the case of PAA-5(c) can be interpreted as a nearly perfectly regular distribution of charge throughout the membrane. The values of (b) less than unity calculated for the other membranes indicate a more heterogeneous membrane structure. The areas of these membranes where charge density is low have a low exchange capacity and are not as concentration sensitive. Lower values of (b) therefore identify membranes in which rejection falls less markedly with increasing concentration than occurs with PAA-5(c).

5.2.8 NORMALIZED MEMBRANE RESULTS

5.2.8.1 Introduction

The effect of salt concentration on rejections of membranes is substantial. In order to compare membranes realistically, rejection values must be adjusted to a common value of salt concentration as discussed in Section 3.6.3. Flux, rejection and FOM values for the five membranes selected for the second trial were normalized to 2 000 ppm salt concentration (0,0235 mole.dm^{-3}) and are shown in Table 5.9.

5.2.8.2 Results

Table 5.9 Normalized membrane results

MEMBRANE	FLUX (l/m^2/d x 1000)	REJECTION %	FOM$\times 10^5$
MA/VA-3.2	7,094	85,8	1,42
MA/VOH-4.2	4,684	91,8	1,73
MA/AA-4.2	10,084	83,3	1,66
MA/IA-1.2	7,402	79,4	0,94
PAA-5(c).2	2,446	94,1	1,29

5.2.8.3 Discussion

The membranes, for which results are presented above, were produced from copolymers which had previously been shown to form membranes having the best overall properties within each copolymer group. The copolymer intrinsic viscosity ranges were not sufficiently wide to ensure that optimum molecular masses were selected for the second trials. The values presented are therefore not necessarily representative of the maximum performance which may be achieved from these copolymer types. Optimization procedures involving molecular mass adjustments, copolymer composition variation and alterations to formation conditions would be expected to produce some improvement.

The MA/VSA copolymer membranes have not been included in this comparison as performance of these membranes is below the level which is technologically useful. The MA/IA membrane has a FOM below that of PAA, which is the chosen standard of comparison. The remaining three membranes have substantially higher figures of merit than that of PAA, and are characterized by higher fluxes and rather lower rejections than the control. These membranes show a useful gradation of properties from the high flux/low rejection MA/AA-4.2 membranes to the high rejection/lower flux MA/VOH-4.2. The MA/VA-3.2 membrane has moderate flux and rejection properties.

5.2.9 CHARGE DENSITY DETERMINATION

5.2.9.1 Introduction

An electrolytic cell was used to determine the thermodynamically effective membrane charge density (ϕX). The method used was developed by researchers examining inorganic cation exchange membranes, and the theory and practical aspects of the method are discussed in Section 3.6.4 and Section 4.5.2 respectively.

5.2.9.2 Results

The five membranes previously selected for a second trial were removed from the test cells and evaluated by membrane potential measurements; basic data are listed in Appendix D.1, together with the calculated values of apparent co-ion transference number (T_{app}). The plots of $1/T_{app}$ vs $^{1}/_{Cl}$, are given in Appendix D.2, with their respective regression equations and correlation coefficients. Values of ϕX derived from this information are listed in Table 5.10. The corresponding values of free fixed-charge molality ($\bar{M}$), as determined in Section 5.2.7, are quoted for purposes of comparison.

Table 5.10 Membrane charge densities

MEMBRANE	ϕX (mole.dm^{-3})	$\bar{M}$ (mole.kg^{-1})
MA/VA-3.2	0,48 X 10^{-2}	1,14
MA/VOH-4.2	1,90 X 10^{-2}	0,96
MA/AA-4.2	0,69 X 10^{-2}	2,29
MA/IA-1.2	0,13 X 10^{-2}	0,95
PAA-5(c).2	0,69 X 10^{-2}	1,00

5.2.9.3 Discussion

The value of ϕX is not easy to interpret in practice. X is defined as the stoichiometric charge density in the membrane in equivalents/litre and ϕ represents the fraction of counter-ions not tightly bound to the membrane. The product ϕX therefore represents an effective rather than a total membrane charge density. The value of ϕX will vary with the type of salt used due to differing counter-ion binding equilibrium coefficients.

Both ϕX and $\bar{M}$ should be representative of the effective charge densities in the membrane and the wide disrepancies in both the absolute values and the ranking of membranes, is unsatisfactory.

No values for ϕX in sodium nitrate solutions are available in the literature, but values for ϕX in sodium chloride electrolyte vary from $2,7 \times 10^{-2}$ for cobalt sulphide membranes[133], to $9,1 \times 10^{-2}$ for poly(styrene sulphonic acid) membranes [132]. The values obtained in this study are therefore rather low by a simple comparison.

The values of membrane potential obtained by other researchers[132] using similar equipment and electrolytes with poly(styrene sulphonic acid) membranes, were an order of magnitude greater than those obtained in this work. The explanation to the problem lies in a consideration of the nature of the membranes used. In the electrolytic cell work referred to above, dense, compact membranes with low water content were used. These membranes would therefore have low water fluxes. The method depends on equilibration of ions in the external solutions with ions in the membrane, with a fixed ratio of concentrations ($C_2/C_1 = 10$) across the membrane. With the dynamic membranes used in this study, which have high water contents and high water fluxes, water flowed through the membrane from the dilute side to the concentrated side by the normal osmotic process and changed the relative solution concentrations. This phenomenon was, in fact, observed during the evaluation, when the solution level rose on the concentrated side and dropped on the dilute side, but the significance of the observation was not realized at the time.

It was also observed that when fresh solutions were added to the cell the value of the membrane potential rose sharply by an order of magnitude, and then fell slowly. The effect of this osmotic transport was to tend to equalize salt concentrations on each side of the membrane, leading to an observed potential much lower than the correct value. The membranes studied by other researchers would have solvent fluxes many orders of magnitude

lower than those of the dynamic membranes and this difficulty would not have arisen within the time period of their experiments.

It would appear, therefore, that this technique is not suitable for use with high-flux membranes using the present equipment, and the values of ϕX obtained would seem to have no real meaning.

The values of $\bar{M}$ obtained for the same membranes, and quoted in Section 5.2.7, are self-consistent in the context of charge densities quoted in the relevant source publication.[146]

5.2.10 CONSOLIDATION OF MEMBRANE DATA

5.2.10.1 Introduction

A large amount of membrane performance data has been presented in the previous sections of Chapter 5. These data include performance-oriented figures, in particular values for normalized flux, rejection and FOM; and also values of "structural" variables such as of charge density and membrane micro-homogeneity. The objective to be pursued in this section is to identify the "structural" variables that have the most significant effect on performance. It is expected that by this means an understanding will be gained of the way in which chemical structure effects membrane performance. Normalized performance data are available for only four maleic acid copolymer membranes and a PAA control membrane and it is clear this is too small a sample for any firm quantitative conclusions to be drawn. Reference will therefore be made to trends, where applicable, as a guide to areas of possible further investigation.

5.2.10.2 Results

Table 5.11 contains normalized membrane performance data for the five selected membranes together with the relevant "structural"

variables.

Table 5.11 Membrane data and structural variables

MEMBRANE	R_{obs}	Flux (x 1000)	FOM×10^5	b	$\bar{M}$	ϕX
MA/VA-3.2	85,8	7,09	1,42	0,81	1,44	0,48
VA/VOH-4.2	91,8	4,68	1,73	0,97	0,96	1,90
MA/AA-4.2	83,3	10,08	1,66	0,84	1,36	0,69
MA/IA-1.2	79,4	7,40	0,94	0,87	0,95	0,13
PAA-5(c).2	94,1	2,45	1,29	0,99	1,00	0,69

Robs Normalized observed rejection in %

Flux Normalized flux in $l/m^2/d$

FOM Lonsdale figure of merit calculated from normalized data

b Membrane micro-homogeneity index (max. value 1,00)

$\bar{M}$ Membrane charge density (Section 5.2.7) in $mole.kg^{-1}$

ϕX Thermodynamically effective charge density (Section 5.2.7) in $mole.dm^{-3}$

5.2.10.3 Discussion

An examination of the figures presented shows that both flux and rejection are strong functions of the membrane micro-homogeneity index b. The relationship is shown in Figs. 5.13 and 5.14.

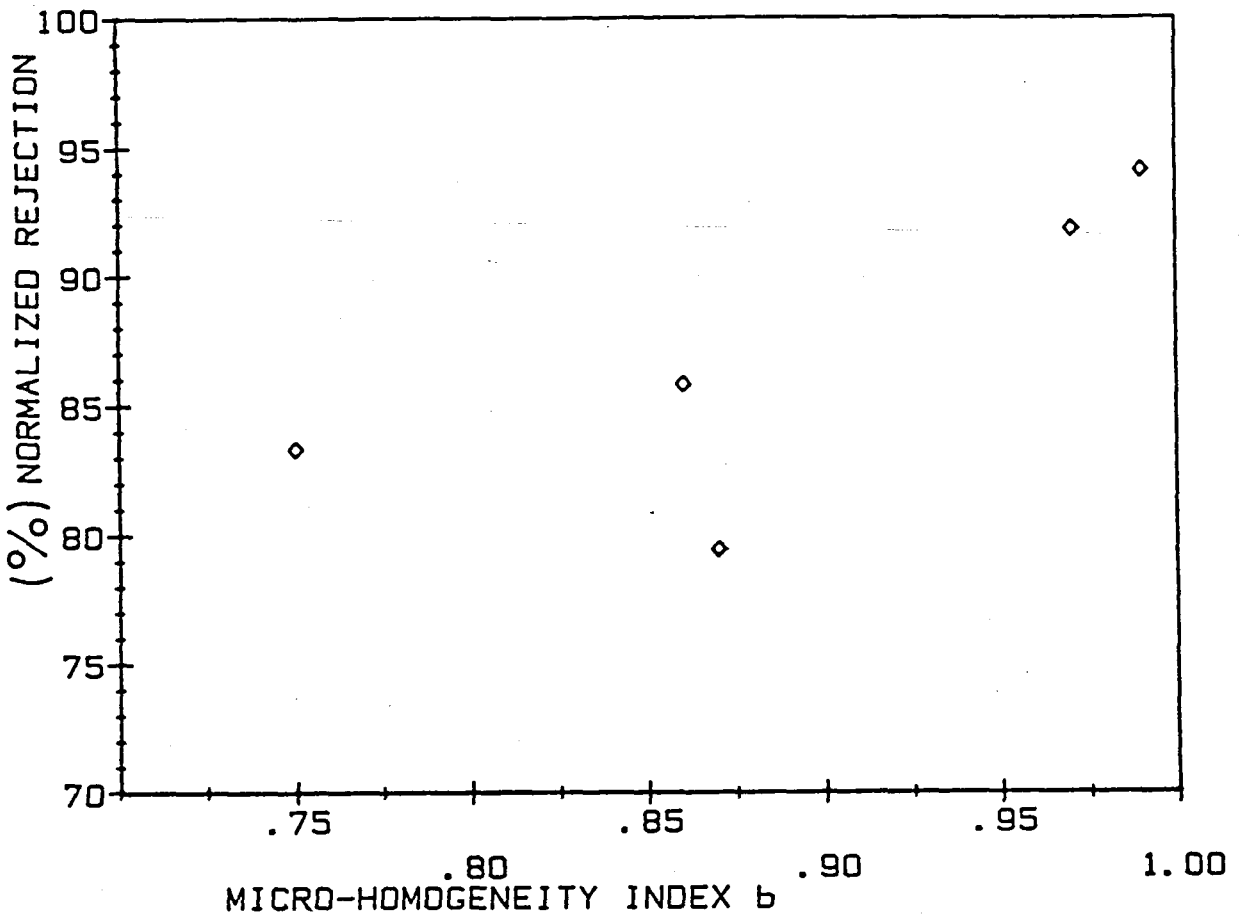

Fig. 5.13 Plot of rejection vs micro-homogeneity index

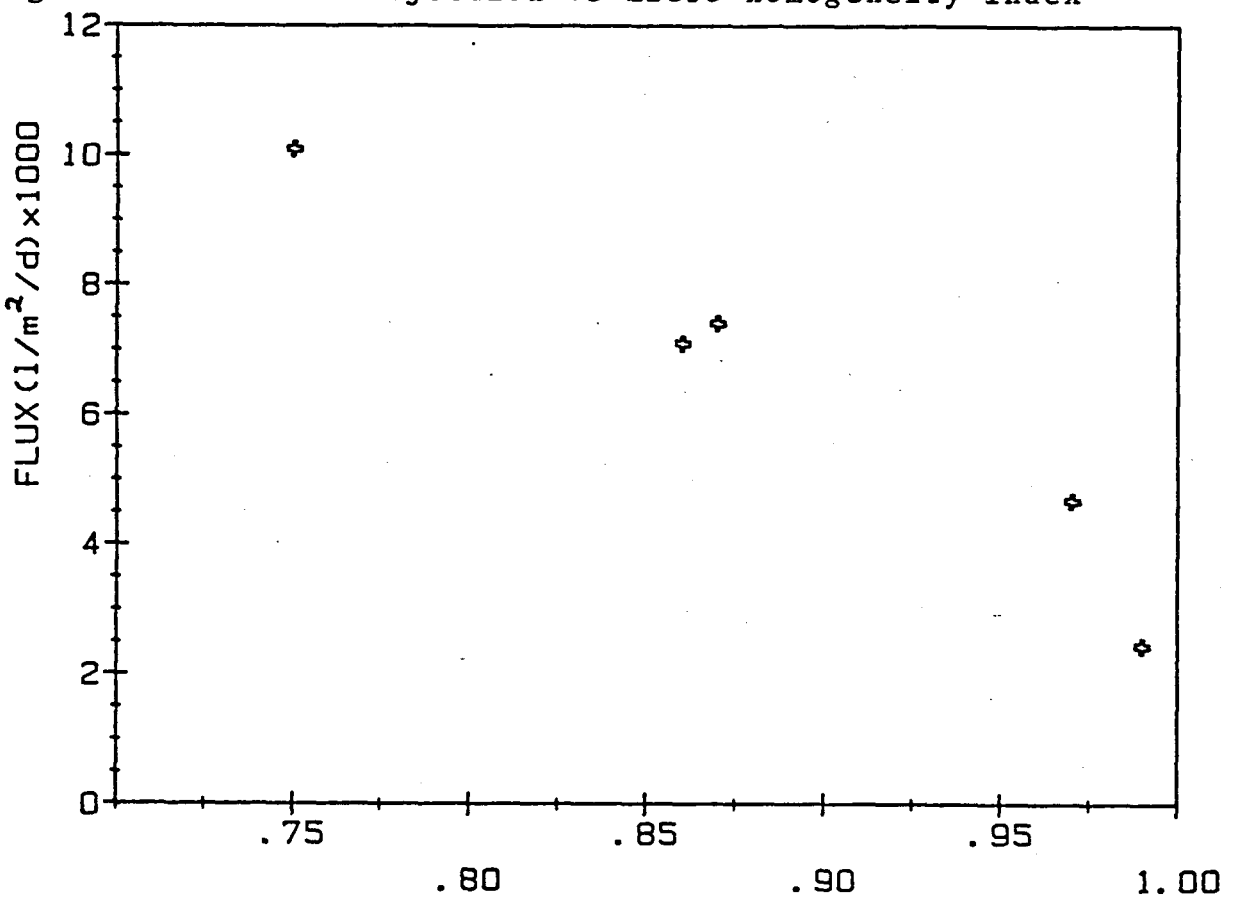

Fig. 5.14 Plot of flux vs micro-homogeneity index

The heterogeneity may be associated with the phenomenon of "ionic clustering" which appears to be associated with ionomeric copolymers having more than about 6% ionic content, when in the partially or fully neutralized form. A thorough review of this topic has been made by Eisenberg and King.[150] The evidence for cluster formation in solid ionomers is strong, but no evidence is available regarding the probabilities of cluster formation in a swollen gel. The occurrence of microphase separation in ethylene ionomers has been demonstrated by a Du Pont working group,[151] which observed grain structures of 100 - 1 000 Å diameter by electron microscopy of neutralized samples cast from solution. Marx et al[152] showed that neutralized copolymers of butadiene and methacrylic acid (7 - 18% acid content) also showed phase separation with periodicities of 13 and 25 Å. The evidence points to the conclusion that ionic clustering takes place and involves heterogeneities which are quite large in comparison with membrane pore sizes.

It is conceivable that the heterogeneities introduced by ionic clustering phenomena could contribute to the observed heterogeneous nature of certain of these membranes. The ionic cluster is perceived as an aggregation of neutralized acid groups surrounded by a hydrophobic shell.

An alternative but closely associated explanation is embodied in the concept of "micelle" formation where heterogeneous domains of a hydrophobic character are enclosed within an ionic shell. This structure is the inverse of the ionic cluster concept and which of these structures are present would greatly depend on the hydrophilic/hydrophobic balance, the polymer structure and the environment of the polymer species.

Partially hydrophobic polyacids (specifically, maleic anhydride-alt-alkyl vinyl ethers) have, when partially neutralized, been shown to form "polysoap" structures in water solution. Barbieri and Strauss[153] estimated that micellar structures containing 19 cooperative units were formed in the case of the butyl vinyl

ether copolymer. Schmitt et al[154] examined cross-linked membranes formed from polymers of this type and found clear evidence of organized structures within the membrane; the size of these structures varied with external salt concentration. They concluded that, at degrees of neutralization exceeding 0,5, the polymers formed micellar structures and a two-phase texture resulted.

The MA/VA alternating copolymers which have been studied are similar in a number of respects to the copolymers discussed above, and it is postulated that similar micellar structures are formed, particularly in the MA/VA copolymers membranes, resulting in a non-homogeneous texture, reflected by the value of (b), the micro-homogeneity index, obtained on evaluation of these membranes.

CHAPTER 6

CONCLUSIONS

6.1 INTRODUCTION

The objectives of this study, as set out in Chapter 1, were to (i) synthesize a number of polyelectrolytes which contain maleic acid functionality in aqueous solution and to characterize these polymers; (ii) evaluate these polymers in terms of their ability to form composite dynamic membranes in conjunction with hydrous zirconia membranes; (iii) determine the properties of the membranes formed in terms of rejection and flux properties as functions of (a) time i.e., membrane permanence,

(b) variation in pH,

(c) salt concentration,

and to derive values for membrane effective charge density and homogeneity index; (iv) explain the properties determined in (iii) above in terms of the chemistry and structures of the polymers concerned, (v) identify polymers having improved properties when compared with those of poly(acrylic acid) which is the currently accepted polymer for this application.

A brief review of the results obtained, related to these objectives, is given below.

6.2 POLYMERS

6.2.1 SYNTHESIS

No useful homopolymers of maleic anhydride were synthesized; only oligomeric products were formed. The following copolymers were produced:

(a) Poly(maleic anhydride-alt-vinyl acetate): four copolymers having different molecular masses.

(b) Poly(maleic anhydride-alt-vinyl alcohol) four copolymers by hydrolysis of the corresponding vinyl acetate copolymers.

(c) Poly(maleic anhydride-alt-acrylic acid): four copolymers prepared in organic solvent.

(d) Poly(maleic anhydride-co-itaconic acid): one copolymer polymerized in organic solvent.

(e) Poly(maleic acid-co-itaconic acid): four copolymers of different molecular masses polymerized in aqueous media.

(f) Poly(maleic acid-co-sodium vinyl sulphonate): three copolymers of low molecular mass.

(g) Poly(maleic anhydride-co-glycidyl methacrylate): one copolymer which crosslinked during polymerization.

The copolymers with itaconic acid, prepared in aqueous media, are novel. A terpolymer of maleic anhydride, itaconic acid and styrene, prepared in organic solvents is, however, described.

6.2.2 CHARACTERIZATION

With the exception of two MA/IA copolymers of high molecular mass and the cross-linked MA/GMA copolymers, all copolymers were characterized by solution viscometry using 0,5M sodium sulphate solution as solvent at 40°C. The intrinsic viscosities (IV's) were consistent with the predicted molecular mass progression. Attempts to determine M_w values by the use of GPC techniques were unsuccessful due to interactions of the polymers with the column packing. The compositions of a number of representative copolymers were determined by pH titration.

6.2.3 EVALUATION OF PROPERTIES

The copolymers which were water-soluble were used to form composite dynamic membranes in combination with hydrous zirconia membranes, using "Millipore" ultrafiltration membranes as supports. Insights were gained into the mechanism of dynamic membrane formation, and into the role of molecular mass and chemical structure on the development of properties during formation.

The permanence properties of the membranes were evaluated and explained in terms of chelation properties of the copolymers, and the effects of pH on properties were determined and discussed with reference to chemical structures.

A number of selected polymer membranes were further evaluated for property changes at various salt concentrations, which enabled variables such as effective charge density and micro-homogeneity index to be established for these membranes.

A theory was outlined to explain the differences in micro-structure observed in these membranes by reference to the chemistry of the copolymers concerned.

Three copolymers were identified as having performance properties which were significantly better than those of the hydrous zirconia poly(acrylic acid) combination.

These were (a) ZrO_2/MA/VA-3
(b) ZrO_2/MA/VOH-4
(c) ZrO_2/MA/AA-4

6.3 FURTHER RESEARCH DIRECTIONS

The results of the work reported in this thesis indicate that several possible areas remain for future research. These are discussed briefly below.

6.3.1 Molecular mass determination

The aqueous GPC technique proved to be unsatisfactory for determination of molecular mass. It is suggested that a method based on esterification followed by GPC work in an organic solvent be evaluated.

6.3.2 MA/IA copolymers

Copolymerization of MA and IA in aqueous solvent has not been reported previously. Further investigation is needed in to the copolymer ratios in this system, and the structure requires clarification.

6.3.3 MA/vinyl ester copolymers

Vinyl acetate is the only vinyl ester comonomer which has been reported in the literature, and other vinyl esters including aliphatic, cycloaliphatic and aromatic types could be investigated. This would have the effect of changing the copolymer hydrophilic/hydrophobic balance, and membranes formed from such copolymers would be expected to have properties markedly different from those of the vinyl acetate copolymer. It is expected that micelle formation would occur to a greater extent as the hydrophobicity of the vinyl ester comonomer is increased, and this effect could be studied by potentiometric titration techniques.

6.3.4 Membrane structure

Several of the copolymers investigated in this study appear to form membranes which are substantially heterogeneous. Direct observation of the texture of hydrated dynamic membranes has not been successful in the past, and the development of suitable techniques including, inter alia, cryoscopic electron microscope methods, would lead to a better understanding of both the mechanism of membrane formation and membrane microstructure.

APPENDIX A

A.1 SOLUTION VISCOSITY DATA

Graphical plots of n_{sp}/c vs. concentration for the range of copolymers synthesized are presented.

Key: Polymer XX/YY-1 +
-2 ×
-3 ◇
-4 □
-5 ○

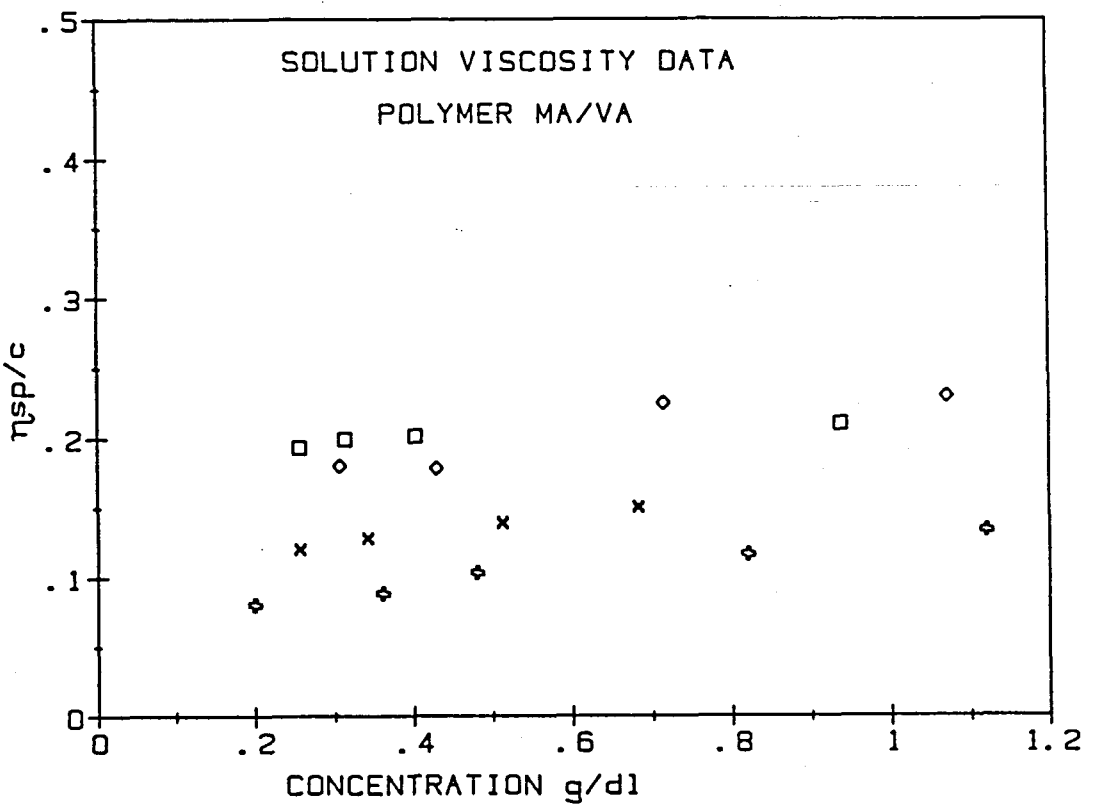

Fig. A.1.1 MA/VA polymers

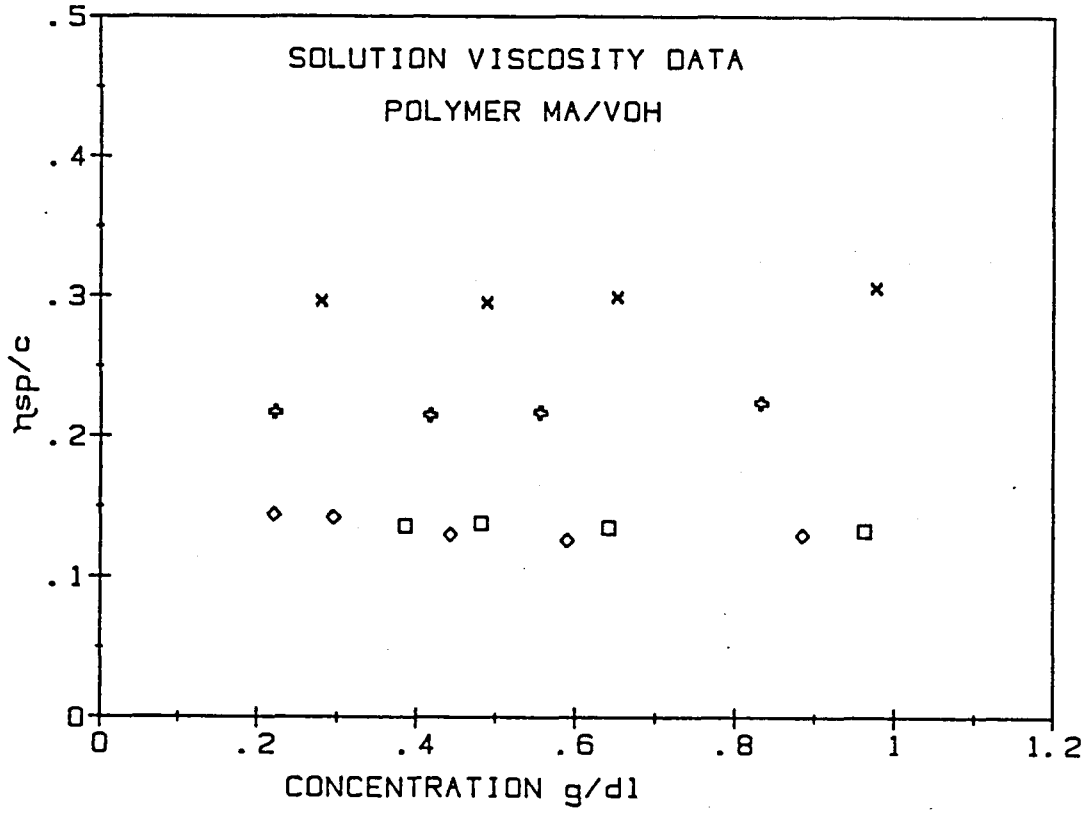

Fig. A.1.2 MA/VOH polymers

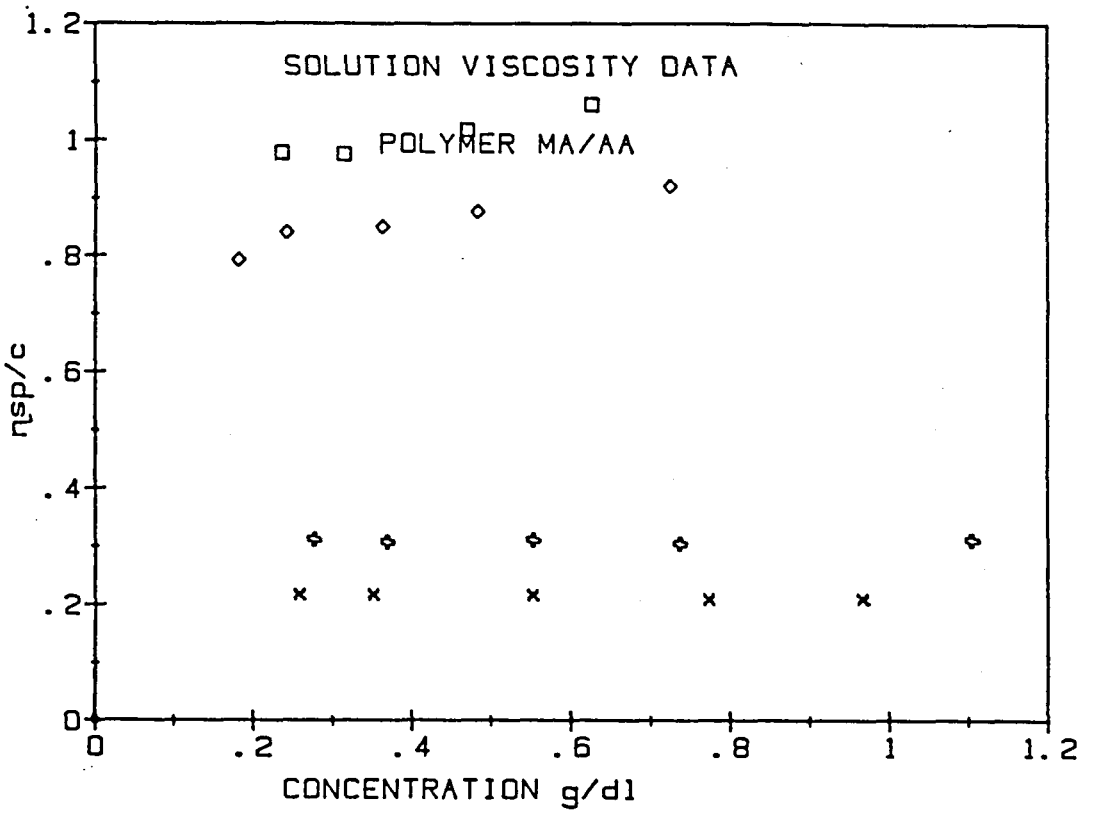

Fig. A.1.3 MA/AA polymers

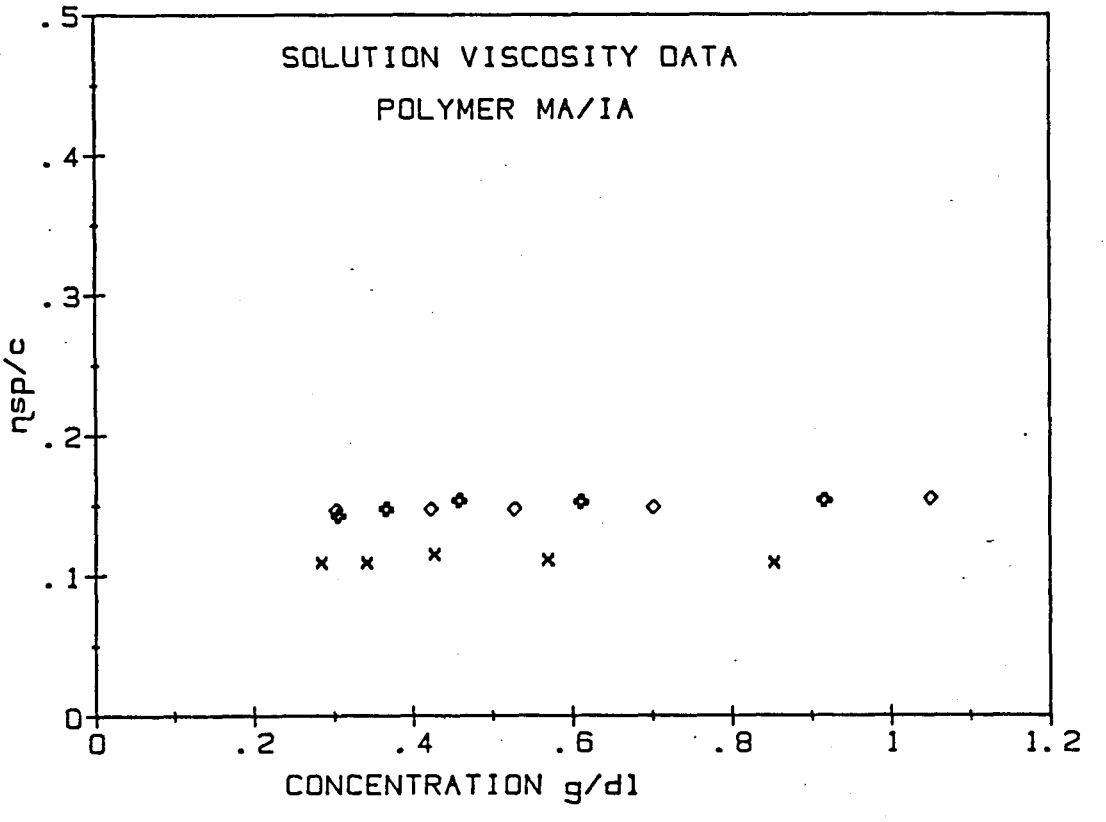

Fig. A.1.4 MA/IA polymers

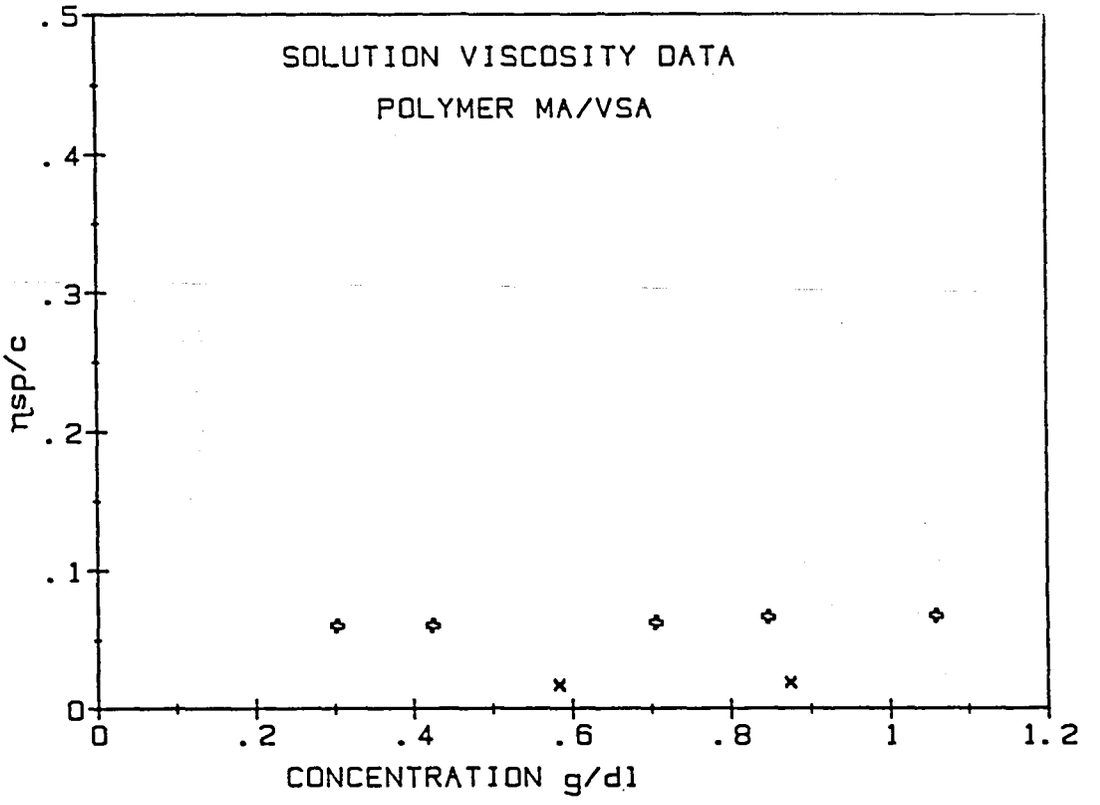

Fig. A.1.5 MA/VSA polymers

APPENDIX B

This Appendix contains the full performance data for all composite membranes evaluated. Values of flux, rejection and figure of merit are given during formation and after stabilisation.

Appendix B1. This contains rejection data during formation from pH2 to pH6, with rejection 30 minutes after formation being designated (pH 7,0). The rejection figure after 20 hours at pH7 is labelled pH $7,0^{20}$ and the values at pH 8 and pH 9, pH $8,0^{20}$ and pH $9,0^{20}$ respectively. The column labelled "ZrO_2" gives the rejection value for the zirconia base membrane before addition of polyelectrolyte and the final column labelled "Conc." defines the sodium nitrate concentration for the evaluation at pH 7, 8 and 9.

Figures of rejection for all cells evaluated in each trial are given. The legend "+" indicates that the membrane in that cell had a gross defect and the legend "-" indicates that no reading was taken under these conditions.

Appendix B2. This contains the flux data for the evaluation and has the same format as Appendix B1.

Appendix B3. This Appendix contains the figure of merit values (FOM) calculated from flux, rejection and concentration data obtained from Appendices B1 and B2.

Table B.1.1 Observed Rejection (Robs) % MA/VA Membranes

Polymer	Trial	Cell	pH 2,0	2,5	3,0	3,5	4,0	4,5	5,0	6,0	7,0	$7,0^{20}$	$8,0^{20}$	$9,0^{20}$	ZrO_2	Conc.
MA/VA-1	1	1	35,2	56,7	66,2	71,6	75,5	79,7	83,0	85,7	90,5	88,8	90,6	89,9	49,9	
		2	+	+	+	+	+	+	+	+	+	+	+	+	+	0,0342
		3	18,5	70,2	76,0	78,1	80,6	84,0	83,2	85,7	89,9	89,6	91,3	91,4	33,6	
	(Mean)		(26,9)	(63,5)	(71,1)	(74,9)	(78,1)	(81,9)	(83,1)	(85,7)	(90,2)	(89,2)	(91,0)	(90,7)	(41,8)	
MA/VA-2	1	1	16,5	35,2	45,4	52,0	-	56,6	61,7	65,6	72,5	77,4	-	-	42,0	
		2	14,0	46,4	51,6	60,8	-	65,4	72,2	74,8	77,3	80,2	-	-	22,0	0,0246
		3	22,7	39,7	50,6	53,5	-	61,0	71,9	75,4	79,7	80,3	-	-	44,0	
	(Mean)		(17,7)	(40,4)	(49,2)	(55,4)	-	(61,0)	(68,6)	(71,9)	(76,5)	(79,3)	-	-	36,0	
MA/VA-3	1	1	42,2	55,9	61,7	67,9	72,0	74,6	75,8	81,7	86,4	84,6	87,8	90,0	56,2	
		2	20,2	34,1	36,4	67,5	72,0	74,8	75,6	81,7	77,8	86,5	84,7	92,0	24,4	0,0249
		3	25,7	51,5	57,8	64,9	74,8	80,4	80,5	80,6	86,4	86,6	90,0	91,7	32,3	
	(Mean)		(29,4)	(47,2)	(52,0)	(66,7)	(72,9)	(76,6)	(77,3)	(81,3)	(83,5)	(85,9)	(85,5)	(91,2)	(37,6)	
MA/VA-3	2	1	15,0	39,6	49,3	56,0	61,0	65,5	70,8	76,2	83,1	79,3	83,6	85,9	47,9	
		2	20,6	44,1	54,0	60,9	66,2	70,8	76,1	82,8	90,0	93,8	88,1	90,0	54,9	0,0353
		3	8,8	65,0	69,2	70,3	72,1	73,7	73,8	80,6	88,0	81,8	86,2	87,0	51,0	
	(Mean)		(14,8)	(49,6)	(57,5)	(62,4)	(66,4)	(70,0)	(73,6)	(79,9)	(87,0)	(81,6)	(86,0)	(87,6)	(51,3)	
MA/VA-4	1	1	28,8	51,0	59,8	62,0	67,8	75,0	-	79,9	81,3	81,1	-	-	55,0	
		2	+	+	+	+	+	+	+	+	+	+	+	+	+	0,0292
		3	17,9	51,2	58,1	63,2	67,1	75,0	-	80,0	81,3	81,1	-	-	53,5	
	(Mean)		(23,4)	(51,1)	(59,0)	(62,5)	(67,5)	(75,0)	-	(80,0)	(81,3)	(81,1)	-	-	(54,3)	

Table B.1.2 Observed Rejection (Robs) % MA/VOH Membranes

Polymer	Trial	Cell	pH 2,0	2,5	3,0	3,5	4,0	4,5	5,0	6,0	7,0	$7,0^{20}$	$8,0^{20}$	$9,0^{20}$	ZrO_2	Conc.
M/VOH-1	1	1	17,4	39,2	51,2	60,3	69,8	75,7	77,0	84,3	89,6	86,1	87,2	87,8	52,0	
		2	19,4	39,8	53,5	63,6	73,3	78,9	80,9	87,7	92,4	89,3	90,7	91,2	55,8	0,0386
		3	13,8	35,8	50,0	60,3	70,9	77,3	81,0	87,7	91,8	87,6	90,5	90,9	48,3	
	(Mean)		(16,9)	(38,3)	(51,6)	(61,4)	(71,3)	(77,3)	(79,6)	(86,6)	(91,3)	(87,6)	(89,5)	(90,0)	(52,0)	
MA/VOH-3	1	1	7,0	34,0	54,6	64,3	69,1	76,6	84,3	88,0	93,5	90,4	-	-	57,2	
		2	0	9,3	41,1	64,1	70,2	76,2	83,4	87,1	93,0	91,2	-	-	18,3	0,0361
		3	0	32,9	43,2	61,3	66,5	75,1	82,8	86,7	92,7	91,0	-	-	53,7	
	(Mean)		(2,3)	(25,4)	(46,3)	(63,2)	(68,6)	(75,6)	(83,5)	(87,3)	(93,1)	(90,9)			(43,1)	
MA/VOH-4	1	1	26,5	51,3	63,4	71,7	75,3	81,1	87,5	91,7	97,1	95,9	-	-	53,4	
		2	0	7,2	54,4	-	71,2	76,8	83,4	87,4	91,2	94,9	-	-	6,1	0,0271
		3	11,4	51,9	63,9	70,3	74,3	79,6	87,4	91,5	98,0	96,1	-	-	30,1	
	(Mean)		(12,6)	(36,8)	(60,6)	(71,0)	(73,6)	(79,2)	(86,1)	(90,2)	(95,4)	(95,6)			(29,9)	
MA/VOH-4	2	1	8,0	33,1	46,9	55,2	64,6	72,9	82,3	88,0	83,9	85,9	88,1	89,0	53,2	
		2	13,4	39,6	53,6	61,0	69,4	76,9	85,1	90,6	89,3	91,4	93,1	93,8	55,8	0,0386
		3	3,4	56,5	62,3	65,0	69,2	75,0	81,2	87,3	85,5	87,4	89,7	90,5	50,8	
	(Mean)		(8,3)	(43,1)	(54,3)	(60,4)	(67,7)	(74,9)	(82,9)	(88,6)	(86,2)	(88,2)	(90,3)	(91,1)	(53,3)	

Table B.1.3 Observed Rejection (Robs) % MA/AA Membranes

			pH												
Polymer	Trial	Cell	2,0	2,5	3,0	3,5	4,0	4,5	5,0	6,0	7,0	$7,0^{20}$	$8,0^{20}$	$9,0^{20}$	ZrO_2	Conc.
MA/AA-1	1	1	37,6	44,5	49,0	53,3	55,5	57,8	53,5	63,1	73,0	74,8	77,9	81,9	58,4	
		2	32,0	38,6	44,1	48,3	51,3	54,9	50,2	60,9	71,4	72,3	75,2	78,4	58,6	0,0378
		3	31,1	39,0	45,6	50,3	52,4	55,7	53,7	63,6	73,8	73,0	76,9	80,5	56,0	
	(Mean)		(33,6)	(40,7)	(46,2)	(50,6)	(53,1)	(56,1)	(52,5)	(62,5)	(72,7)	(73,4)	(76,7)	(80,3)	(57,7)	
MA/AA-2	1	1	35,5	51,6	58,8	66,1	71,0	74,4	77,0	80,4	84,8	88,9	-	-	31,1	
		2	27,4	54,0	62,4	69,0	73,1	75,0	78,4	81,5	86,2	*	-	-	31,1	0,0318
		3	22,9	52,4	60,1	63,9	72,0	75,1	77,6	81,2	85,1	89,2	-	-	25,6	
	(Mean)		(28,6)	(52,7)	(60,4)	(66,3)	(72,0)	(74,8)	(77,7)	(81,0)	(85,4)	(89,1)	-	-	(29,3)	
MA/AA-3	1	1	36,5	48,6	55,4	60,1	62,5	65,0	61,9	68,7	77,5	66,6	74,9	83,2	59,1	
		2	29,1	47,2	55,2	60,0	62,3	57,7	61,4	68,7	*	*	*	*	31,5	0,0347
		3	16,6	44,7	52,5	68,7	68,2	67,8	61,7	68,7	77,6	77,6	82,3	85,9	26,4	
	(Mean)		(27,2)	(46,8)	(54,4)	(62,9)	(64,3)	(63,5)	(61,7)	(68,7)	(77,6)	(72,1)	(78,6)	(84,6)	(39,0)	
MA/AA-4	1	1	16,9	31,2	36,3	44,0	52,6	60,2	62,6	76,9	83,8	80,1	83,3	84,8	42,9	
		2	17,2	34,2	40,6	48,8	57,4	64,3	66,2	79,5	85,6	82,2	84,5	75,4	43,2	0,0415
		3	14,8	29,3	36,2	60,9	64,4	68,1	65,5	78,6	85,0	81,6	84,7	83,3	35,2	
	(Mean)		(16,3)	(31,6)	(37,7)	(51,2)	(58,1)	(64,2)	(64,8)	(78,3)	(84,8)	(81,3)	(84,2)	(81,2)	(40,4)	
MA/AA-4	2	1	+	+	+	+	+	+	+	+	+	+	+	+	+	
		2	24,5	36,7	46,8	52,1	57,4	59,7	64,9	73,1	80,9	82,9	88,2	91,4	54,7	0,0353
		3	19,8	31,2	41,0	45,9	50,2	52,2	59,6	66,5	74,8	76,7	83,0	87,4	50,3	
	(Mean)		(22,2)	(34,0)	(43,9)	(49,0)	(53,8)	(56,0)	(62,3)	(69,8)	(77,9)	(79,8)	(85,6)	(89,4)	(52,5)	

Table B.1.4 Observed Rejection (Robs) % MA/IA Membranes

Polymer	Trial	Cell	pH 2,0	2,5	3,0	3,5	4,0	4,5	5,0	6,0	7,0	$7,0^{20}$	$8,0^{20}$	$9,0^{20}$	ZrO_2	Conc.
MA/IA-1	1	1	-	26,6	33,9	38,8	44,5	50,1	58,3	64,5	70,4	67,4	70,5	72,1	47,4	
		2	-	28,5	34,7	39,4	44,7	51,4	59,3	66,2	71,9	70,9	73,1	74,9	56,8	0,0393
		3	-	19,8	30,3	32,1	36,9	44,2	56,6	64,5	73,1	70,2	74,5	76,3	49,6	
	(Mean)		-	(24,9)	(33,0)	(36,8)	(42,0)	(48,6)	(58,1)	(64,1)	(71,8)	(69,5)	(72,7)	(74,4)	(51,3)	
		1	+	+	+	+	+	+	+	+	+	+	+	+	+	
		2	7,4	31,3	49,9	50,7	56,4	60,8	66,4	70,9	73,5	75,1	76,9	79,0	49,4	0,0424
		3	2,1	26,4	55,2	61,9	62,5	63,5	65,5	70,0	72,6	74,2	76,2	78,2	46,2	
	(Mean)		(4,8)	(28,9)	(52,6)	(56,3)	(59,5)	(62,2)	(66,0)	(70,5)	(73,1)	(74,7)	(76,6)	(78,5)	(47,8)	
MA/IA-2	1	1	28,1	46,3	52,4	56,4	59,2	61,7	64,6	69,2	74,9	75,4	78,2	80,5	40,3	
		2	30,9	48,7	56,1	59,6	62,4	65,0	67,8	72,4	78,2	77,1	79,9	81,9	42,9	0,0381
		3	20,9	46,1	67,1	67,4	67,2	67,6	68,3	73,2	78,7	77,6	79,9	81,8	41,0	
	(Mean)		(26,6)	(47,0)	(58,5)	(61,1)	(62,9)	(64,8)	(66,9)	(71,6)	(77,3)	(76,7)	(79,3)	(81,4)	(41,4)	
MA/IA-3	1	1	5,6	22,5	30,6	35,8	40,0	45,2	53,1	58,7	73,2	67,4	73,9	75,8	56,2	
		2	7,9	25,7	34,5	39,9	44,8	50,4	57,9	64,1	78,1	71,6	77,8	79,6	59,1	0,0404
		3	3,2	20,8	29,7	59,1	58,7	58,2	55,7	61,7	76,2	69,3	76,2	78,0	54,2	
	(Mean)		(5,6)	(24,9)	(31,6)	(44,9)	(47,8)	(51,3)	(55,6)	(61,5)	(75,8)	(69,4)	(76,0)	(77,8)	(56,5)	
MA/IA-4	1	1	19,3	40,5	40,7	38,9	36,3	33,7	33,8	32,3	45,1	45,3	-	-	37,4	0,0308
MA/IA-5	1	1	35,5	44,2	49,3	50,9	51,9	51,2	40,9	41,5	47,4	52,5	57,5	61,2	54,4	
		2	27,0	44,7	49,8	51,8	52,6	52,1	40,9	41,5	47,4	52,5	57,1	60,4	53,4	0,0308
		3	33,5	38,7	43,9	48,4	49,3	48,8	41,5	42,1	48,3	52,9	57,8	61,2	38,2	
	(Mean)		(32,0)	(42,5)	(47,7)	(50,4)	(51,3)	(50,7)	(41,1)	(41,7)	(47,7)	(52,6)	(57,5)	(60,9)	(48,7)	

Table B.1.5 Observed Rejection (Robs) % MA/VSA Membranes

Polymer	Trial	Cell	pH 2,0	2,5	3,0	3,5	4,0	4,5	5,0	6,0	7,0	$7,0^{20}$	$8,0^{20}$	$9,0^{20}$	ZrO_2	Conc.
MA/VSA-3	1	1	27,6	41,5	50,0	48,6	50,5	50,9	50,9	44,6	49,1	55,4	58,2	59,1	51,4	
		2	30,5	43,9	49,1	51,4	53,7	54,2	54,7	48,7	53,8	59,6	63,1	63,6	54,1	0,0372
		3	25,3	38,6	58,0	56,8	55,7	54,9	54,9	50,0	55,3	60,0	63,1	64,3	52,6	
	(Mean)		(27,8)	(41,1)	(52,4)	(52,3)	(53,3)	(53,3)	(53,5)	(47,8)	(52,7)	(58,3)	(61,5)	(62,3)	(52.7)	

Table B.1.6 Observed Rejection (Robs) (%) PAA-5(C) Membranes

Polymer	Trial	Cell	pH 2,0	2,5	3,0	3,5	4,0	4,5	5,0	6,0	7,0	$7,0^{20}$	$8,0^{20}$	$9,0^{20}$	ZrO_2	Conc.
PAA-5(C)	1	1	-	-	-	61,6	-	77,7	77,7	90,7	96,0	92,7	-	-	-	
		2	-	-	-	-	-	74,8	-	83,6	93,3	94,0	-	-	-	0,0318
		3	-	-	-	-	-	73,6	-	85,6	92,3	91,7	-	-	-	
	(Mean)		-	-	-	(61,6)	-	(75,4)	(77,7)	(86,6)	(93,9)	(92,8)	-	-	-	
	2	1	23,6	32,4	43,4	50,2	58,3	64,4	74,6	82,4	88,7	88,8	91,4	92,5	43,0	
		2	26,3	37,0	49,5	57,1	65,7	71,6	80,8	88,2	94,6	93,2	95,1	95,3	48,0	0,0335
		3	18,6	59,4	65,2	69,0	73,8	77,1	79,8	87,4	93,9	92,1	94,1	94,4	44,4	
	(Mean)		(22,8)	(49,9)	(52,7)	(58,8)	(65,9)	(71,0)	(78,4)	(86,0)	(92,4)	(91,4)	(93,5)	(94,1)	(45,1)	

Table B.2.1 Membrane Flux $l/m^2/d$ x 1000 MA/VA Membranes

Polymer	Trial	Cell	pH 2,0	2,5	3,0	3,5	4,0	4,5	5,0	6,0	7,0	$7,0^{20}$	$8,0^{20}$	$9,0^{20}$	ZrO_2	Conc.
MA/VA-1	1	1	3,1	3,1	3,5	3,4	3,3	2,7	2,6	2,4	2,174	2,356	2,083	1,902	17,4	
		2	+	+	+	+	+	+	+	+	+	+	+	+	+	0,0342
		3	10,9	3,3	3,7	3,6	3,4	2,9	2,8	2,4	2,265	2,446	2,083	1,993	29,0	
	(Mean)		(7,0	(3,2)	(3,6)	(3,5)	(3,4)	(2,8)	(2,7)	(2,4)	(2,220)	(2,401)	(2,083)	(1,948)	(23,2)	
MA/VA-2	1	1	-	9,1	9,1	8,1	7,9	7,6	7,1	6,7	6,160	5,707	-	-	11,8	
		2	-	8,0	9,2	8,3	8,1	7,9	7,4	6,8	6,795	6,342	-	-	14,0	0,0246
		3	-	11,3	11,3	8,9	8,5	8,1	7,4	6,8	6,614	6,342	-	-	13,6	
	(Mean)		-	(9,5)	(9,9)	(8,4)	(8,2)	(7,9)	(7,3)	(6,8)	(6,523)	(6,130)	-	-	(13,1)	
MA/VA-3	1	1	9,1	9,1	6,2	9,2	9,3	9,2	8,2	7,6	7,066	7,071	6,976	6,342	26,5	
		2	-	-	-	11,6	11,6	10,1	9,2	9,1	8,607	9,513	8,607	7,792	68	0,0249
		3	10,9	9,1	8,8	8,4	9,2	9,1	8,3	7,3	6,885	7,610	6,704	6,161	30,4	
	(Mean)		(10,0)	(9,1)	(7,5)	(9,7)	(10,0)	(9,5)	(8,6)	(8,0)	(7,519)	(8,275)	(7,429)	(6,765)	(42,0)	
	2	1	10,0	8,2	8,7	8,4	8,2	7,7	7,1	6,4	5,436	6,342	5,527	4,983	24,7	
		2	10,3	9,1	9,9	9,7	9,3	8,8	8,2	7,4	6,161	7,429	6,433	5,708	32,0	0,0353
		3	11,4	8,7	9,1	9,1	8,8	8,2	7,7	7,1	5,798	6,976	6,070	5,436	32,0	
	(Mean)		(10,6)	(8,7)	(9,2)	(9,1)	(8,8)	(8,2)	(7,7)	(7,0)	(5,798)	(6,916)	(6,010)	(5,376)	(29,6)	
MA/VA-4	1	1	6,2	6,3	6,1	7,4	6,9	6,7	6,6	5,7	5,255	5,708	-	-	15,6	
		2	+	+	+	+	+	+	+	+	+	+	+	+	+	0,0292
		3	7,8	7,2	6,6	7,7	7,4	7,2	7,0	6,2	5,708	6,342	-	-	15,8	
	(Mean)		(7,0)	(6,8)	(6,4)	(7,6)	(7,2)	(7,0)	(6,8)	(6,0)	(5,482)	(6,025	-	-	(15,7)	

Table B.2.2 Membrane Flux $l/m^2/d$ x 1000 MA/VOH Membranes

Polymer	Trial	Cell	pH 2,0	2,5	3,0	3,5	4,0	4,5	5,0	6,0	7,0	$7,0^{20}$	$8,0^{20}$	$9,0^{20}$	ZrO_2	Conc.
MA/VOH-1	1	1	11,4	6,2	6,3	5,5	5,2	4,6	4,1	3,1	2,809	3,171	2,718	2,718	36,2	
		2	17,6	7,6	8,0	7,2	7,0	6,3	5,5	4,3	3,805	4,530	3,805	3,715	37,5	0,0386
		3	15,6	7,4	7,8	7,3	7,2	6,6	5,9	4,5	4,168	4,892	4,168	4,077	41,9	
	(Mean)		(14,9)	(7,1)	(7,4)	(6,7)	(6,5)	(5,6)	(5,2)	(4,0)	(3,594)	(4,198)	(3,564)	(3,503)	(38,5)	
MA/VOH-3	1	1	7,6	5,0	5,4	5,0	4,7	4,1	3,7	2,9	2,356	2,899	-	-	19,9	
		2	-	21,8	7,4	6,1	-	4,6	4,1	3,3	2,627	3,262	-	-	67,9	0,0361
		3	24,7	5,2	6,1	5,0	4,7	4,1	3,6	2,9	2,265	2,718	-	-	18,8	
	(Mean)		(16,2)	(10,7)	(6,3)	(5,4)	(4,7)	(4,3)	(3,8)	(3,0)	(2,416)	(2,960)	-	-	(35,5)	
MA/VOH-4	1	1	15,0	5,3	6,0	5,5	5,4	4,7	4,3	3,6	2,718	3,805	-	-	20,1	
		2	-	36,2	6,8	-	5,9	5,1	4,6	3,7	2,809	4,077	-	-	13,5	0,0271
		3	15,1	4,8	5,4	5,2	5,1	4,3	4,1	3,3	2,537	3,715	-	-	19,4	
	(Mean)		(15,1)	(15,4)	(6,1)	(5,4)	(5,5)	(4,7)	(4,3)	(3,5)	(2,688)	(3,866)	-	-	(17,7)	
MA/VOH-4	2	1	6,9	5,8	6,4	6,3	6,2	5,6	4,9	3,8	4,530	4,530	4,258	3,805	29,0	
		2	6,6	5,7	6,5	6,3	6,3	5,8	5,2	4,0	4,711	4,711	4,439	3,895	30,4	0,0386
		3	6,1	5,8	6,6	6,6	6,3	5,8	5,2	4,1	4,801	4,801	4,530	4,077	28,3	
	(Mean)		(6,5)	(5,8)	(6,5)	(6,4)	(6,3)	(5,7)	(5,1)	(4,0)	(4,681)	(4,681)	(4,409)	(3,926)	(29,2)	

Table B.2.3 Membrane Flux $l/m^2/d$ x 1000 MA/AA Membranes

			pH												
Polymer	Trial	Cell	2,0	2,5	3,0	3,5	4,0	4,5	5,0	6,0	7,0	$7,0^{20}$	$8,0^{20}$	$9,0^{20}$	ZrO_2	Conc.
MA/AA-1	1	1	8,3	7,8	7,1	7,2	7,0	7,1	6,8	6,3	5,436	5,074	4,892	4,439	16,0	
		2	8,4	8,8	8,2	8,3	8,2	8,2	7,9	7,3	6,523	6,070	5,798	5,345	17,0	0,0378
		3	7,1	8,8	8,2	8,4	8,2	8,3	8,1	7,6	6,614	6,342	5,960	5,436	14,3	
	(Mean)		(7,9)	(8,5)	(7,8)	(8,0)	(7,8)	(7,9)	(7,6)	(7,1)	(6,191)	(5,829)	(5,557)	(5,073)	(15,8)	
MA/AA-2		1	-	3,2	3,4	3,4	3,4	3,1	2,8	2,5	1,993	1,812	-	-	22,5	
		2	-	3,3	3,4	3,4	3,5	3,4	2,9	2,5	1,993	+	-	-	26,1	0,318
		3	-	3,3	3,4	3,4	3,4	3,2	2,8	2,4	1,903	1,721	-	-	25,0	
	(Mean)		-	(3,3)	(3,4)	(3,4)	(3,4)	(3,2)	(2,8)	(2,5)	(1,963)	(1,767)	-	-	(24,5)	
MA/AA-3	1	1	11,2	12,3	11,6	12,7	12,0	11,6	11,4	10,1	8,698	9,966	7,882	5,708	29,0	
		2	18,1	14,9	14,3	14,3	13,1	15,4	12,7	11,1	+	+	+	+	38,8	0,0347
		3	-	12,7	12,5	12,7	12,0	11,8	11,4	10,0	8,335	8,335	7,429	6,433	32,6	
	(Mean)		(14,7)	(13,3)	(12,8)	(13,2)	(12,4)	(12,9)	(11,8)	(10,4)	(8,517)	(9,151)	(7,656)	(6,071)	(33,5)	
MA/AA-4	1	1	10,9	10,9	10,0	10,0	9,1	8,9	7,8	5,7	4,530	4,989	4,621	4,256	18,8	
		2	-	11,2	11,2	10,3	9,4	9,2	8,5	5,9	4,621	-	4,802	5,074	21,0	0,0415
		3	10,9	10,9	10,3	10,3	9,4	9,1	8,3	5,9	4,711	5,164	4,802	5,617	24,6	
	(Mean)		(10,9)	(11,0)	(10,5)	(10,2)	(9,3)	(9,1)	(8,2)	(5,8)	(4,621)	(5,077)	(4,742)	(4,963)	(21,5)	
MA/AA-4	2	1	+	+	+	+	+	+	+	+	+	+	+	+	+	
		2	22,2	15,4	15,1	15,0	14,9	14,3	14,0	11,2	9,422	9,422	8,062	6,885	36,2	0,0358
		3	17,9	15,2	14,9	15,0	14,5	14,0	14,0	11,4	9,603	9,603	8,607	7,339	32,6	
	(Mean)		(20,1)	(15,3)	(15,0)	(15,0)	(14,7)	(14,2)	(14,0)	(11,3)	(9,513)	(9,523)	(8,335)	(7,112)	(34,4)	

Table B.2.4 Membrane Flux $l/m^2/d$ x 1000 MA/IA Membranes

Polymer	Trial	Cell	pH 2,0	2,5	3,0	3,5	4,0	4,5	5,0	6,0	7,0	$7,0^{20}$	$8,0^{20}$	$9,0^{20}$	ZrO_2	Conc.
MA/IA-1	1	1	-	15,4	14,9	13,6	13,4	13,6	13,2	12,5	11,788	10,872	10,147	9,241	40,2	
		2	-	15,2	15,0	14,5	14,1	14,5	14,0	13,6	13,046	11,868	10,872	9,875	34,0	0,0393
		3	-	15,0	14,7	14,0	13,8	13,6	13,4	12,9	12,322	11,234	10,328	9,332	31,1	
	(Mean)		-	(15,2)	(14,9)	(14,0)	(13,8)	(13,9)	(13,5)	(13,0)	(12,382)	(11,325)	(10,449)	(9,483)	(35,1)	
	2	1	+	+	+	+	+	+	+	+	+	+	+	+	+	
		2	18,8	12,0	11,1	10,2	10,2	9,2	9,5	9,3	8,335	8,335	7,701	6,976	29,0	0,0424
		3	18,8	11,4	10,9	9,7	10,0	8,9	9,5	9,1	8,335	8,335	7,701	6,976	30,1	
	(Mean)		(18,8)	(11,7)	(11,0)	(10,0)	(10,1)	(9,1)	(9,5)	(9,2)	(8,335)	(8,335)	(7,701)	(6,976)	(32,9)	
MA/IA-2	1	1	5,9	6,9	6,8	6,5	6,8	6,4	6,3	6,7	6,070	5,889	5,436	4,892	16,9	
		2	6,7	7,3	8,0	7,7	8,1	7,7	7,7	8,0	7,067	7,248	6,614	6,070	20,1	0,0381
		3	8,0	8,3	8,3	8,1	8,4	8,1	8,0	8,3	7,067	7,520	6,885	6,251	20,9	
	(Mean)		(6,9)	(7,5)	(7,7)	(7,4)	(7,8)	(7,4)	(7,3)	(7,7)	(6,947)	(6,886)	(6,312)	(5,738)	(19,3)	
MA/IA-3	1	1	14,5	11,6	9,1	11,2	10,9	11,2	10,9	10,3	9,603	10,147	8,698	8,335	24,6	
		2	17,8	16,3	14,5	14,0	13,9	14,1	13,8	13,1	11,959	13,046	11,234	10,872	30,8	0,0404
		3	17,8	14,5	13,4	13,1	13,0	13,1	12,7	12,1	11,234	12,140	10,691	10,328	30,0	
	(Mean)		(16,7)	(14,1)	(12,3)	(12,8)	(12,6)	(12,8)	(12,5)	(11,8)	(10,932)	(11,778)	(10,208)	(9,845)	(28,5)	
MA/IA-4	1	1	8,8	9,1	9,5	9,5	9,3	9,8	9,6	10,2	9,513	7,882	-	-	14,7	0,0308
MA/IA-5	1	1	10,5	10,5	10,9	10,5	11,8	11,1	11,3	12,3	11,325	10,419	10,057	9,060	17,6	
		2	26,5	12,6	12,3	12,1	12,0	12,3	11,9	13,0	12,321	10,872	10,419	9,332	18,1	0,0308
		3	11,2	12,7	12,9	11,8	11,6	11,2	11,9	12,1	12,050	10,419	10,057	9,332	30,4	
	(Mean)		(16,1)	(11,9)	(12,0)	(11,5)	(11,8)	(11,5)	(11,7)	(12,5)	(11,899)	(10,570)	(10,178)	(9,241)	(22,0)	

Table B.2.5 Membrane Flux $l/m^2/d$ x 1000 MA/VSA Membranes

			pH												
Polymer	Trial	Cell	2,0	2,5	3,0	3,5	4,0	4,5	5,0	6,0	7,0	$7,0^{20}$	$8,0^{20}$	$9,0^{20}$	ZrO_2	Conc.
MA/VSA-3	1	1	16,5	12,0	13,8	12,9	12,5	12,1	11,8	11,8	11,053	6,613	6,613	6,523	18,1	
		2	18,8	15,0	16,2	15,0	14,7	14,3	14,0	13,6	12,648	7,429	7,429	7,248	20,9	0,0372
		3	21,7	18,8	17,6	16,7	16,0	15,5	14,9	14,5	13,590	8,245	8,064	8,064	24,2	
	(Mean)		(19,0)	(15,3)	(15,9)	(14,9)	(14,4)	(14,0)	(13,6)	(13,3)	(12,430)	(7,429)	(7,369)	(7,728)	(21,1)	

Table B.2.6 Membrane Flux $l/m^2/d$ x 1000 PAA-5(C) Membranes

Polymer	Trial	Cell	pH 2,0	2,5	3,0	3,5	4,0	4,5	5,0	6,0	7,0	$7,0^{20}$	$8,0^{20}$	$9,0^{20}$	ZrO_2	Conc.
PAA/5(C)	1	1	2,7	2,3	2,1	2,0	2,0	2,0	2,2	1,5	1,268	1,359	-	-	-	
		2	3,2	2,4	2,3	2,3	2,3	2,1	1,9	1,8	1,268	1,087	-	-	-	0,0318
		3	2,5	2,1	2,0	2,0	2,0	1,9	2,0	1,4	0,997	1,087	-	-	-	
	(Mean)		(2,8)	(2,3)	(2,1)	(2,1)	(2,1)	(2,0)	(2,0)	(1,6)	(1,178)	(1,178)	-	-	-	
	2	1	4,1	3,6	3,5	3,4	3,3	3,3	3,0	2,3	1,812	1,903	1,540	1,450	16,9	
		2	4,4	3,9	3,8	3,8	3,7	3,7	3,4	2,5	1,812	2,084	1,721	1,540	22,3	0,0335
		3	4,2	3,9	3,8	3,7	3,6	3,6	3,3	2,5	1,721	2,084	1,631	1,540	22,8	
	(Mean)		(4,2)	(3,8)	(3,7)	(3,6)	(3,5)	(3,5)	(3,2)	(2,4)	(1,782)	(2,024)	(1,631)	(1,510)	(20,7)	

Table B.3.1

FIGURES OF MERIT (X 10^5)

MA/VA MEMBRANES

MEMBRANE	TRIAL	CELL	pH			
			7,0	$7,0^{20}$	$8,0^{20}$	$9,0^{20}$
MA/VA-1	1	1	0,68	0,62	0,66	0,56
		2	+	+	+	+
		3	0,67	0,70	0,72	0,70
(mean)			(0,68)	(0,66)	(0,69)	(0,63)
MA/VA-2	1	1	0,54	0,65	+	-
		2	0,76	0,85	-	-
		3	0,86	0,85	-	-
(mean)			(0,72)	(0,78)		
MA/VA-3	1	1	1,48	1,40	1,66	1,89
		2	1,00	2,02	1,57	2,96
		3	1,45	1,63	1,99	2,25
(mean)			(1,31)	(1,68)	(1,74)	(2,37)
MA/VA-3	2	1	0,88	0,80	0,93	1,00
		2	1,83	1,27	1,57	1,70
		3	1,41	1,04	1,25	1,20
(mean)			(1,37)	(1,04)	(1,25)	(1,30)
MA/VA-4	1	1	0,76	0,81	-	-
		2	+	+	+	+
		3	0,82	0,91	-	-
(mean)			(0,79)	(0,86)		

Table B.3.2

FIGURES OF MERIT (X 10^5)

MA/VOH MEMBRANES

MEMBRANE	TRIAL	CELL	pH 7,0	pH $7,0^{20}$	pH $8,0^{20}$	pH $9,0^{20}$
MA/VOH-1	1	1	0,80	0,65	0,61	0,65
		2	1,53	1,25	1,23	1,27
		3	1,54	1,14	1,31	1,35
(mean)			(1,29)	(1,01)	(1,05)	(1,09)
MA/VOH-3	1	1	1,19	0,90	-	-
		2	1,15	1,12	-	-
		3	0,95	0,91	-	-
(mean)			(1,10)	(0,98)		
MA/VOH-4	1	1	3,00	2,94	-	-
		2	0,96	2,51	-	-
		3	4,10	3,02	-	-
(mean)			(2,69)	(2,82)		
MA/VOH-4	1	1	0,78	0,91	1,04	1,02
		2	1,30	1,65	1,98	1,95
		3	0,94	1,10	1,30	1,28
(mean)			(1,01)	(1,22)	(1,44)	(1,42)

Table B.3.3

FIGURES OF MERIT (X 10^5)

MA/AA MEMBRANES

MEMBRANE	TRIAL	CELL	pH 7,0	pH $7,0^{20}$	pH $8,0^{20}$	pH $9,0^{20}$
MA/AA-1	1	1	0,49	0,50	0,57	0,66
		2	0,54	0,52	0,58	0,64
		3	0,62	0,57	0,66	0,74
(mean)			(0,55)	(0,53)	(0,60)	(0,68)
MA/AA-2	1	1	0,37	0,48	-	-
		2	0,41	+	-	-
		3	0,36	0,47	-	-
(mean)			(0,38)	(0,48)		
MA/AA-3	1	1	0,99	0,66	0,78	0,93
		2	+	+	+	+
		3	0,95	0,95	1,14	1,29
(mean)			(0,97)	(0,81)	(0,96)	(1,11)
MA/AA-4	1	1	0,77	0,66	0,76	0,78
		2	0,91	0,77	0,86	0,52
		3	0,88	0,75	0,88	+
(mean)			(0,85)	(0,73)	(0,83)	(0,65)
MA/AA-4	2	1	+	+	+	+
		2	1,32	1,51	1,99	2,41
		3	0,94	1,04	1,39	1,65
(mean)			(1,13)	(1,28)	(1,69)	(2,03)

Table B.3.4

FIGURES OF MERIT (X 10^5)

MA/IA MEMBRANES

MEMBRANE	TRIAL	CELL	pH 7,0	pH $7,0^{20}$	pH $8,0^{20}$	pH $9,0^{20}$
MA/IA	1	1	0,93	0,74	0,80	0,79
		2	1,10	0,96	0,98	0,97
		3	1,11	0,87	1,00	0,99
(mean)			(1,05)	(0,86)	(0,93)	(0,92)
MA/IA-1	2	1	+	+	+	+
		2	0,76	0,83	0,85	0,87
		3	0,73	0,79	0,81	0,83
(mean)			(0,75)	(0,86)	(0,83)	(0,85)
MA/IA-2		1	0,60	0,60	0,64	0,67
		2	0,84	0,81	0,87	0,91
		3	0,90	0,86	0,90	0,93
(mean)			(0,78)	(0,76)	(0,80)	(0,84)
MA/IA-3		1	+	+	+	+
		2	1,41	1,09	1,30	1,40
		3	1,19	0,91	1,13	1,21
(mean)			(1,30)	(1,00)	(1,22)	(1,31)
MA/IA-4		1	0,26	0,22	-	-
		2	+	+	+	+
		3	0,35	+	+	+
(mean)			(0,31)	(0,22)		
MA/IA-5		1	0,34	0,38	0,45	0,47
		2	0,37	0,40	0,46	0,47
		3	0,37	0,39	0,46	0,49
(mean)			(0,36)	(0,39)	(0,46)	(0,48)

Table B.3.5

FIGURES OF MERIT (X 10^5)

MA/VSA MEMBRANES

MEMBRANE	TRIAL	CELL	pH			
			7,0	$7,0^{20}$	$8,0^{20}$	$9,0^{20}$
MA/VSA-3	1	1	0,35	0,27	0,30	0,31
		2	0,49	0,36	0,42	0,42
		3	0,56	0,41	0,46	0,48
(mean)			(0,47)	(0,35)	(0,39)	(0,40)

Table B.3.6

FIGURES OF MERIT (X 10^5)

PAA-5(C) MEMBRANES

MEMBRANE	TRIAL	CELL	pH			
			7,0	$7,0^{20}$	$8,0^{20}$	$9,0^{20}$
PAA-5(c)	1	1	1,01	0,57	-	-
		2	0,58	0,56	-	-
		3	0,39	0,40	-	-
(mean)			(0,66)	(0,51)		
	2	1	0,47	0,50	0,54	0,59
		2	1,05	0,94	1,10	1,03
		3	0,88	0,80	0,86	0,86
(mean)			(0,80)	(0,75)	(0,83)	(0,83)

APPENDIX C

Appendix C.1

REJECTION CHANGES WITH CHANGE OF FEED CONCENTRATION

Key:

M	feed concentration in mole/dm^3
Robs	observed rejection in %
S	solute flux = (1 - Robs/100)

Table C.1.1 MA/VA-3.2 MEMBRANE

Conc. of feed (M)	(Robs)			Solute flux (S)					
	CELL 1	CELL 2	CELL 3	S1	S2	S3	Mean S	Log S	Log M
0,0353	79,3	83,8	81,8	0,207	0,162	0,182	0,184	-0,735	-1,452
0,0395	77,5	81,9	79,9	0,225	0,181	0,201	0,202	-0,695	-1,403
0,0497	72,4	76,7	74,8	0,276	0,233	0,252	0,254	-0,595	-1,304
0,0596	69,4	73,5	71,8	0,306	0,265	0,282	0,284	-0,547	-1,225
0,0690	66,5	70,9	68,8	0,335	0,291	0,312	0,313	-0,505	-1,161
0,0784	64,1	68,4	66,0	0,359	0,316	0,340	0,338	-0,471	-1,106
0,0882	60,6	65,1	65,4	0,394	0,349	0,346	0,363	-0,440	-1,055
0,0979	58,9	63,3	61,2	0,411	0,367	0,388	0,389	-0,410	-1,009
0,1070	56,2	60,8	58,8	0,438	0,392	0,412	0,414	-0,383	-0,971

Table C.1.2 MA/VOH-4.2 MEMBRANE

Conc. of feed (M)	(Robs)			Solute flux (S)					
	CELL 1	CELL 2	CELL 3	S1	S2	S3	Mean S	Log S	Log M
0,0386	85,9	91,4	87,4	0,141	0,086	0,126	0,118	-0,928	-1,413
0,0498	82,3	88,8	84,6	0,177	0,112	0,154	0,148	-0,830	-1,303
0,0599	78,9	85,5	80,8	0,211	0,145	0,192	0,183	-0,783	-1,223
0,0698	75,9	82,8	78,1	0,241	0,172	0,219	0,211	-0,676	-1,156
0,0795	73,1	80,4	75,3	0,269	0,196	0,246	0,237	-0,625	-1,100
0,0888	71,3	78,8	75,1	0,287	0,212	0,249	0,249	-0,604	-1,052
0,0978	69,2	76,8	71,3	0,308	0,232	0,287	0,276	-0,559	-1,100
0,1068	67,5	75,3	69,3	0,325	0,247	0,304	0,292	-0,535	-0,971

Table C.1.3 MA/AA-4.2 MEMBRANE

Conc. of feed (M)	(Robs)			S = Solute flux(s)					
	CELL 1	CELL 2	CELL 3	S1	S2	S3	Mean S	Log S	Log M
0,0353	+	82,9	76,7	+	0,171	0,233	0,202	-0,695	-1,452
0,0467	+	81,5	75,4	+	0,185	0,246	0,216	-0,667	-1,331
0,0575	+	78,0	71,4	+	0,220	0,286	0,253	-0,597	-1,240
0,0680	+	75,2	68,5	+	0,248	0,315	0,282	-0,551	-1,168
0,0782	+	72,8	65,6	+	0,272	0,344	0,308	-0,511	-1,107
0,0882	+	70,3	62,9	+	0,297	0,371	0,334	-0,476	-1,055

Table C.1.4 MA/IA-1.2 MEMBRANE

Conc. of feed (M)	(Robs)			S = Solute flux(s)					
	CELL 1	CELL 2	CELL 3	S1	S2	S3	Mean S	Log S	Log M
0,0369	+	78,2	77,5	+	0,218	0,225	0,222	-0,654	-1,433
0,0424	+	75,1	74,2	+	0,249	0,258	0,254	-0,595	-1,373
0,0535	+	71,0	69,7	+	0,290	0,303	0,297	-0,527	-1,272
0,0639	+	66,5	65,5	+	0,335	0,345	0,340	-0,469	-1,195
0,0742	+	62,4	61,5	+	0,376	0,385	0,381	-0,419	-1,130
0,0843	+	59,1	58,2	+	0,409	0,418	0,414	-0,383	-1,074
0,0941	+	56,2	55,1	+	0,438	0,449	0,444	-0,353	-1,026

Table C.1.5 PAA-5(c).2 MEMBRANE

Conc. of feed (M)	(Robs)			S = Solute flux(s)					
	CELL 1	CELL 2	CELL 3	S1	S2	S3	Mean S	Log S	Log M
0,0299	90,3	94,3	93,3	0,097	0,057	0,067	0,074	-1,133	-1,524
0,0335	88,8	93,2	92,1	0,112	0,068	0,079	0,086	-1,064	-1,475
0,0449	87,6	91,0	89,7	0,124	0,090	0,103	0,106	-0,976	-1,348
0,0553	83,4	88,3	86,8	0,166	0,117	0,132	0,138	-0,859	-1,257
0,0654	80,6	85,8	84,3	0,194	0,142	0,157	0,164	-0,784	-1,184
0,0749	78,2	83,8	82,2	0,218	0,162	0,178	0,186	-0,731	-1,126
0,0843	76,0	81,9	80,3	0,240	0,181	0,197	0,206	-0,686	-1,074

APPENDIX C.2

LOG/LOG PLOTS OF FEED CONCENTRATION VS SOLUTE FLUX

Graphical plots of log s (solute flux) vs log m (feed concentration) are presented, the values being extracted from Appendix C.1. Error bars are used to indicate the spread of data between cells. The equations of the regression lines are given below:

Fig. C.2.1 MA/VA-3.2 $\log s = 0{,}629 \log m + 0{,}224$ ($r = 0{,}999$)

Fig. C.2.2 MA/VOH-4.2 $\log s = 0{,}937 \log m + 0{,}404$ ($r = 0{,}991$)

Fig. C.2.3 MA/AA-4.2 $\log s = 0{,}686 \log m + 0{,}249$ ($r = 0{,}999$)

Fig. C.2.4 MA/IA-1.2 $\log s = 0{,}735 \log m + 0{,}407$ ($r = 0{,}999$)

Fig. C.2.5 PAA-5(c).2 $\log s = 0{,}992 \log m + 0{,}383$ ($r = 0{,}998$)

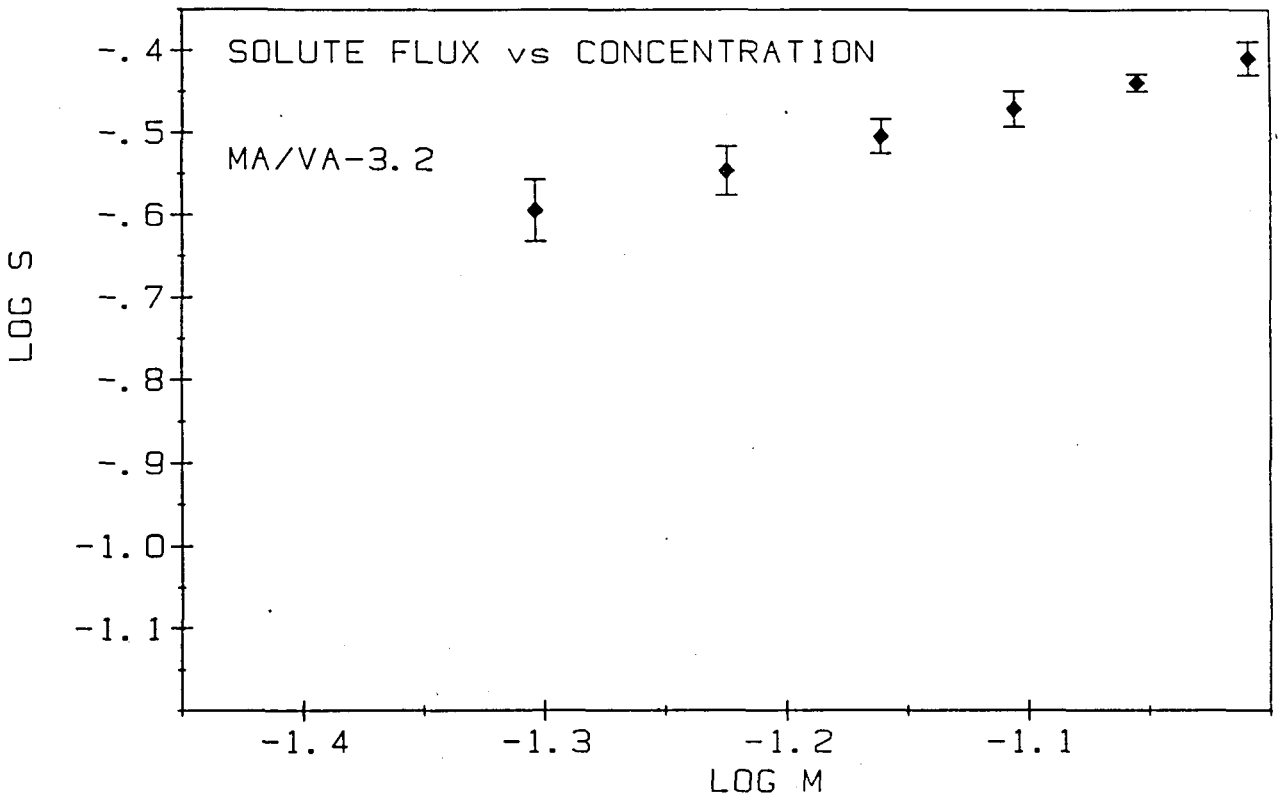

Fig. C.2.1

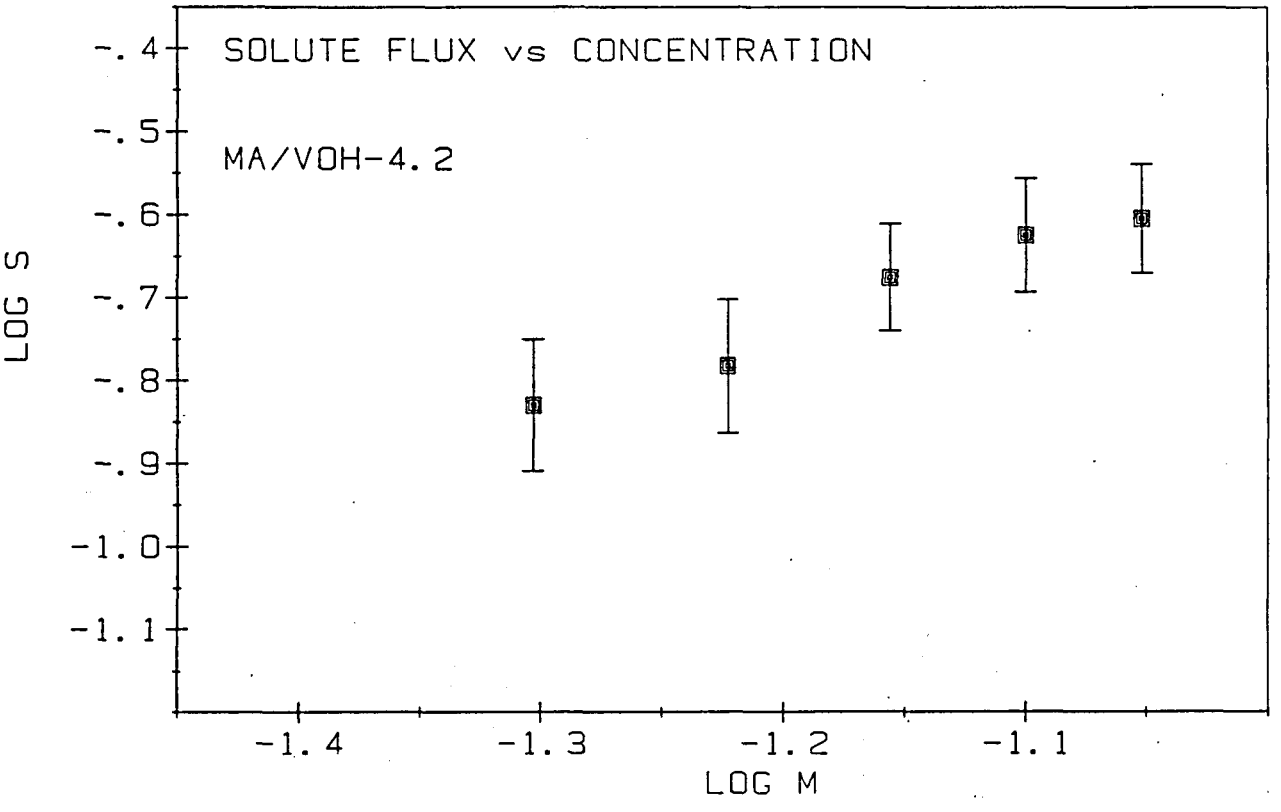

Fig. C.2.2

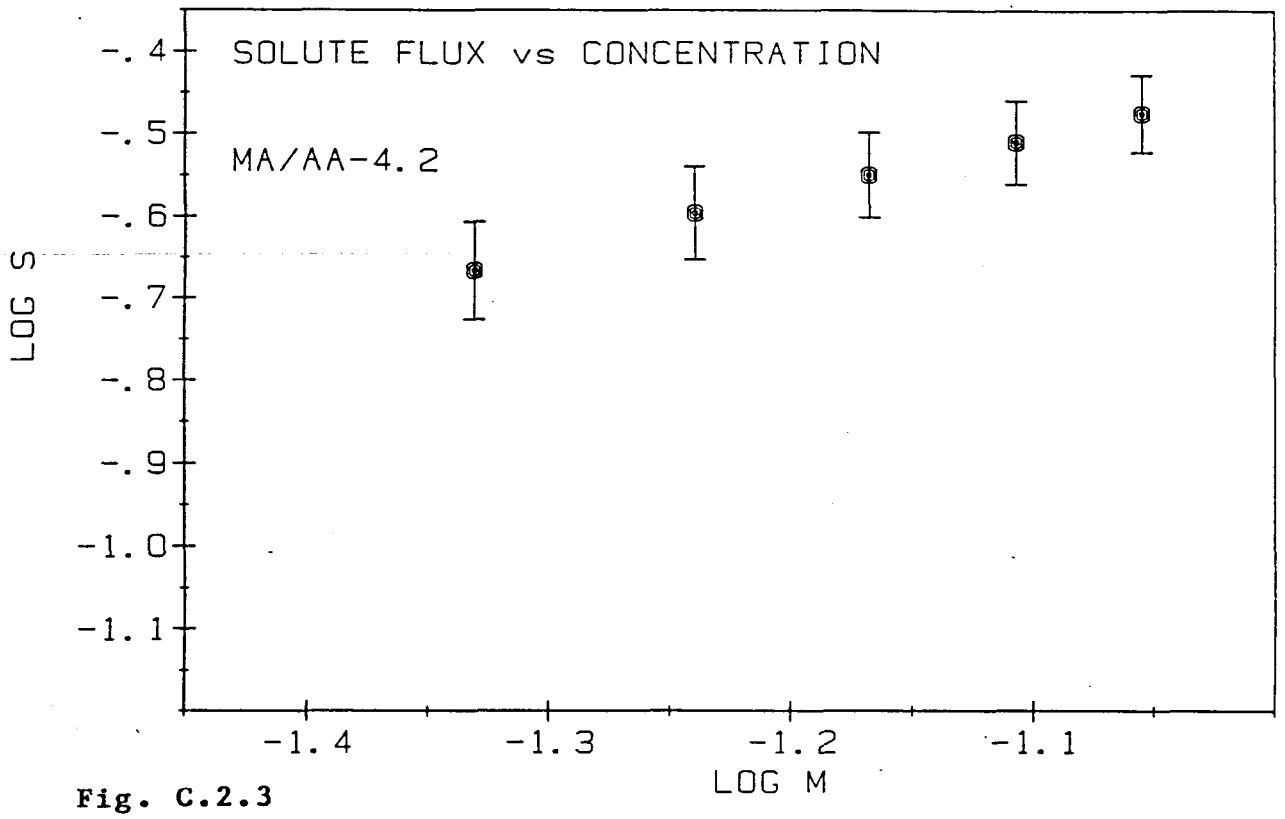

Fig. C.2.3

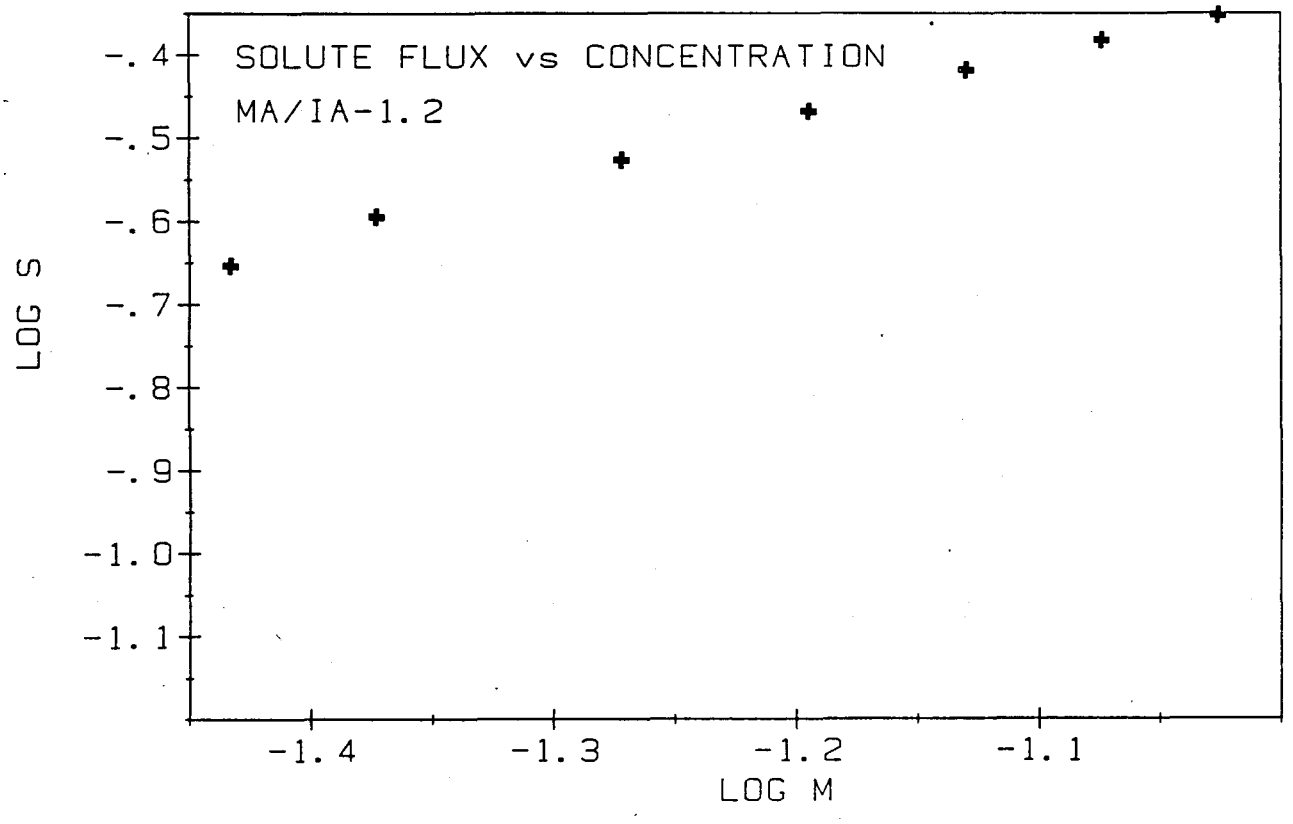

Fig. C.2.4

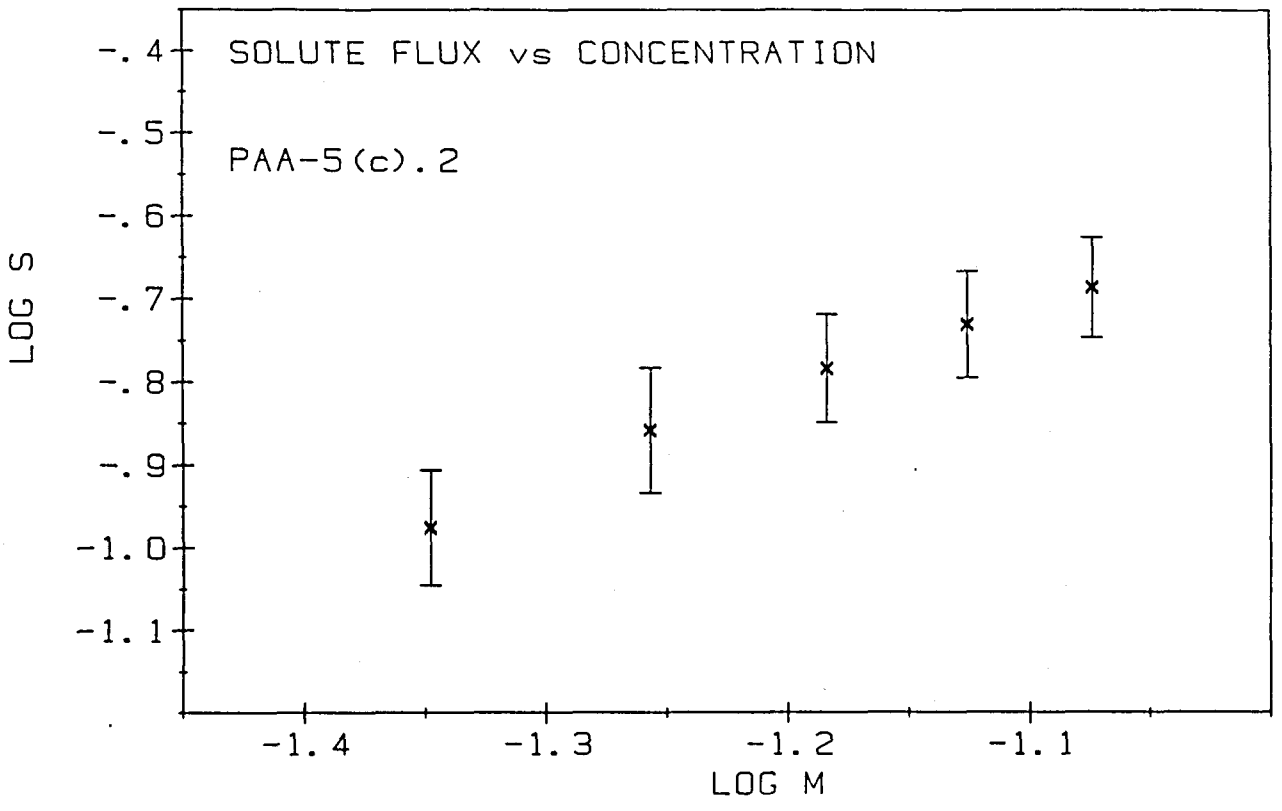
SOLUTE FLUX vs CONCENTRATION
PAA-5(c).2
LOG S
-.4
-.5
-.6
-.7
-.8
-.9
-1.0
-1.1
-1.4
-1.3
-1.2
-1.1
LOG M

Fig. C.2.5

APPENDIX D.1

ELECTROLYTIC CHARGE DENSITY DATA IN TABLE FORM

Values EMF (Em) obtained from electrolytic cell measurements are given, with the values of C_1 (C_2/C_1 in each case). The calculated values of apparent co-ion Transference number Tapp, calculated as described in Section 3.6.4 are also given.

Table D.1.1 - MA/VA-3.2 membrane EMF

C_1 (mole.dm^{-3})	Em (mV)	Tapp
0,1	1,4	0,550
0,05	0,85	0,530
0,01	-0,20	0,493
0,005	-0,90	0,468

Table D.1.2 - MA/VOH-4.2 membrane EMF

C_1 (mole.dm^{-3})	Em (mV)	Tapp
0,1	0,5	0,518
0,05	0,35	0,512
0,01	-2,1	0,426
0,005	-5,0	0,323

Table D.1.3 - MA/AA-4.2 membrane EMF

C_1 (mole.dm^{-3})	Em (mV)	Tapp
0,1	0,6	0,521
0,05	0,95	0,534
0,01	-0,1	0,497
0,005	-2,0	0,429

Table D.1.4 - MA/IA-1.2 membrane EMF

C_1 (mole.dm^{-3})	Em (mV)	Tapp
0,1	1,1	0,534
0,05	1,3	0,543
0,01	1,9	0,539
0,005	2,1	0,514

Table D.1.5 - PAA-5(c).2 membrane EMF

C_1 (mole.dm^{-3})	Em (mV)	Tapp
0,1	0,4	0,514
0,05	0,4	0,514
0,01	-0,6	0,479
0,005	-2,4	0,415

APPENDIX D.2

ELECTROLYTIC CHARGE DENSITY PLOTS

Plots of $^{1}/_{T_{app}}$ vs $^{1}/_{C_1}$ are presented here. The slopes and intercepts of these plots are used to calculate a value of ϕX, the thermodynamically effective charge density.

The equations of the regression lines relating to the plots are as follows:

Fig. D.2.1 MA/VA-3.2 $y = 1{,}575 \times 10^{-3} x + 1{,}838$ $(r = 0{,}976)$

Fig. D.2.2 MA/VOH-4.2 $y = 6{,}13 \times 10^{-3} x + 1{,}826$ $(r = 0{,}993)$

Fig. D.2.3 MA/AA-4.2 $y = 2{,}27 \times 10^{-3} x + 1{,}846$ $(r = 0{,}970)$

Fig. D.2.4 MA/IA-1.2 $y = 0{,}44 \times 10^{-3} x + 1{,}843$ $(r = 0{,}93)$

Fig. D.2.5 PAA-5(c).2 $y = 2{,}43 \times 10^{-3} x + 1{,}899$ $(r = 0{,}99)$

where $y = {}^{1}/_{T_{app}}$ and $x = {}^{1}/_{C_1}$

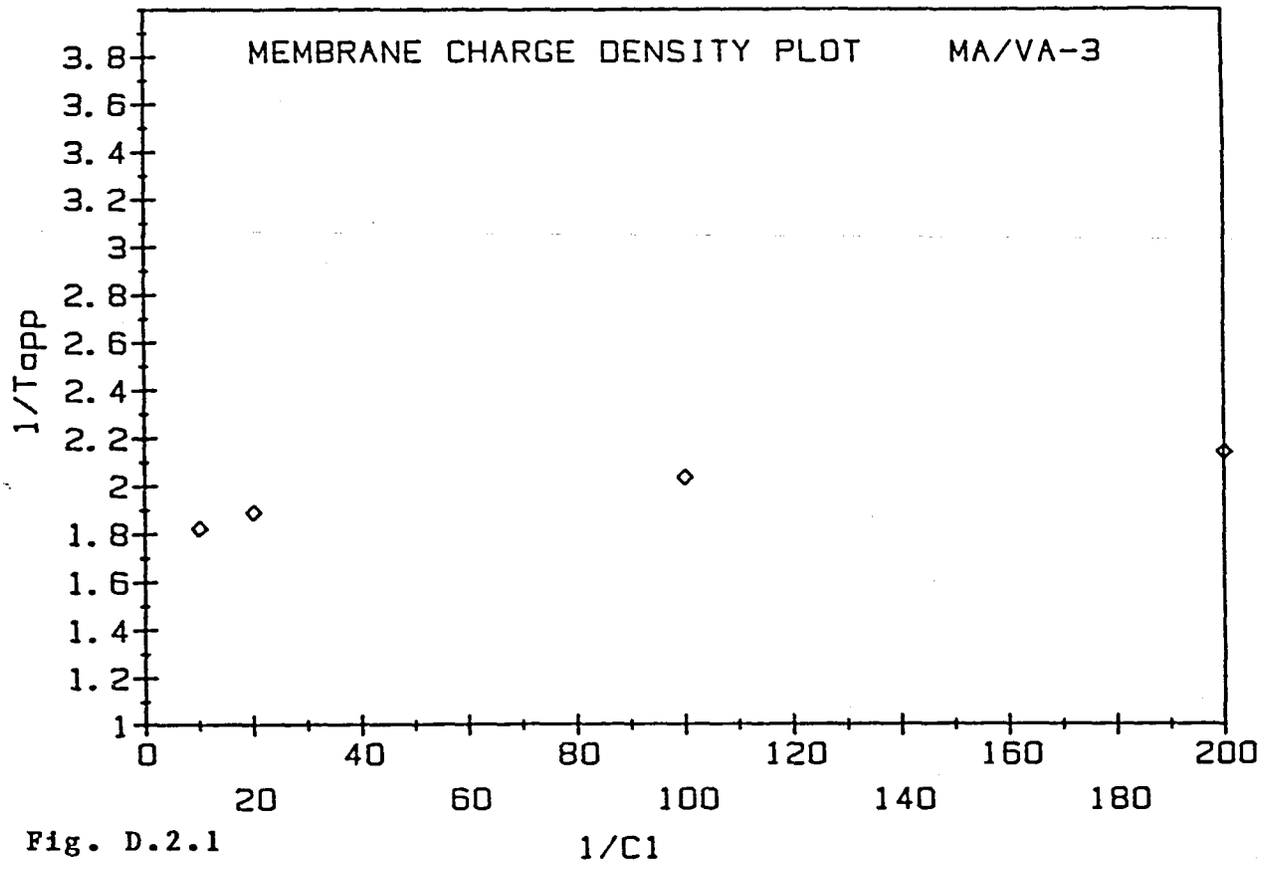

Fig. D.2.1

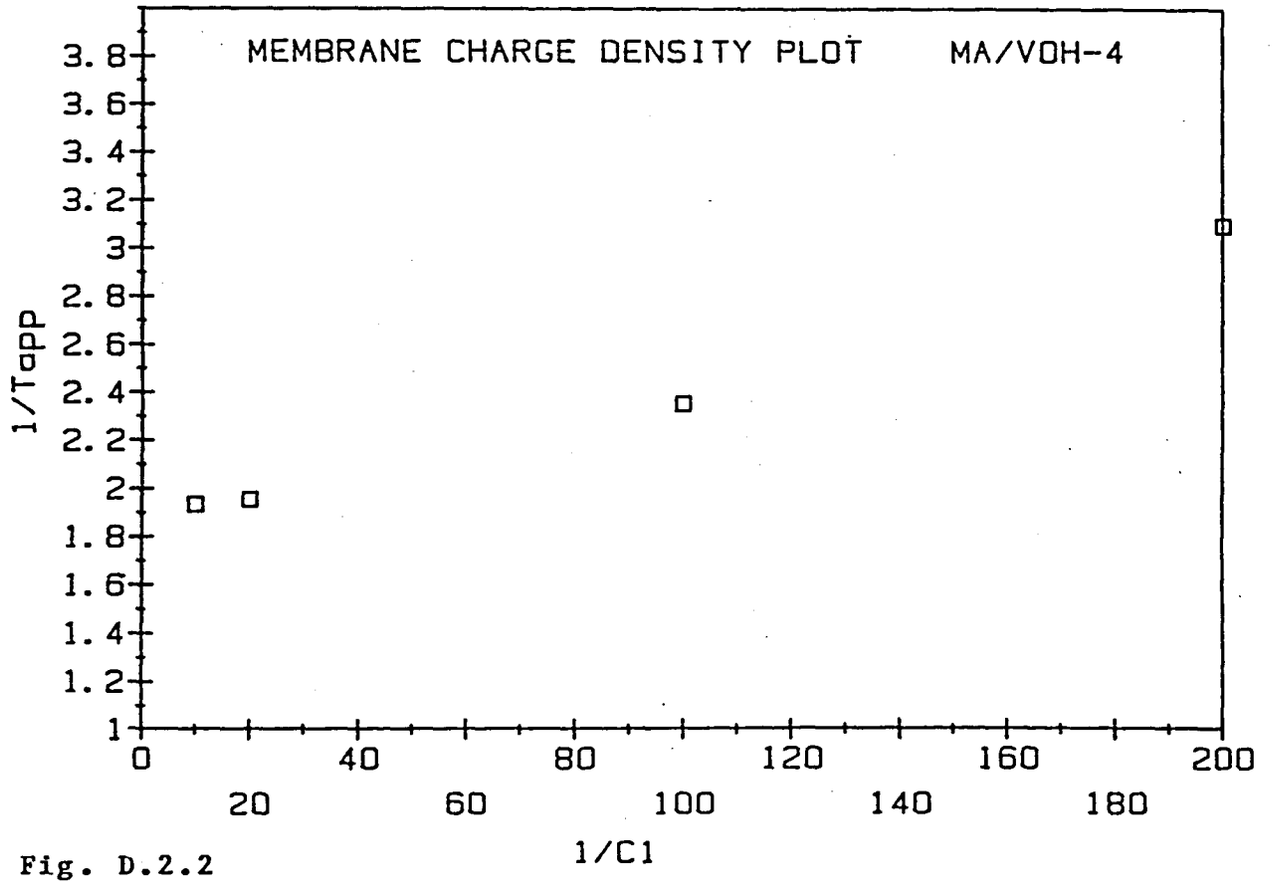

Fig. D.2.2

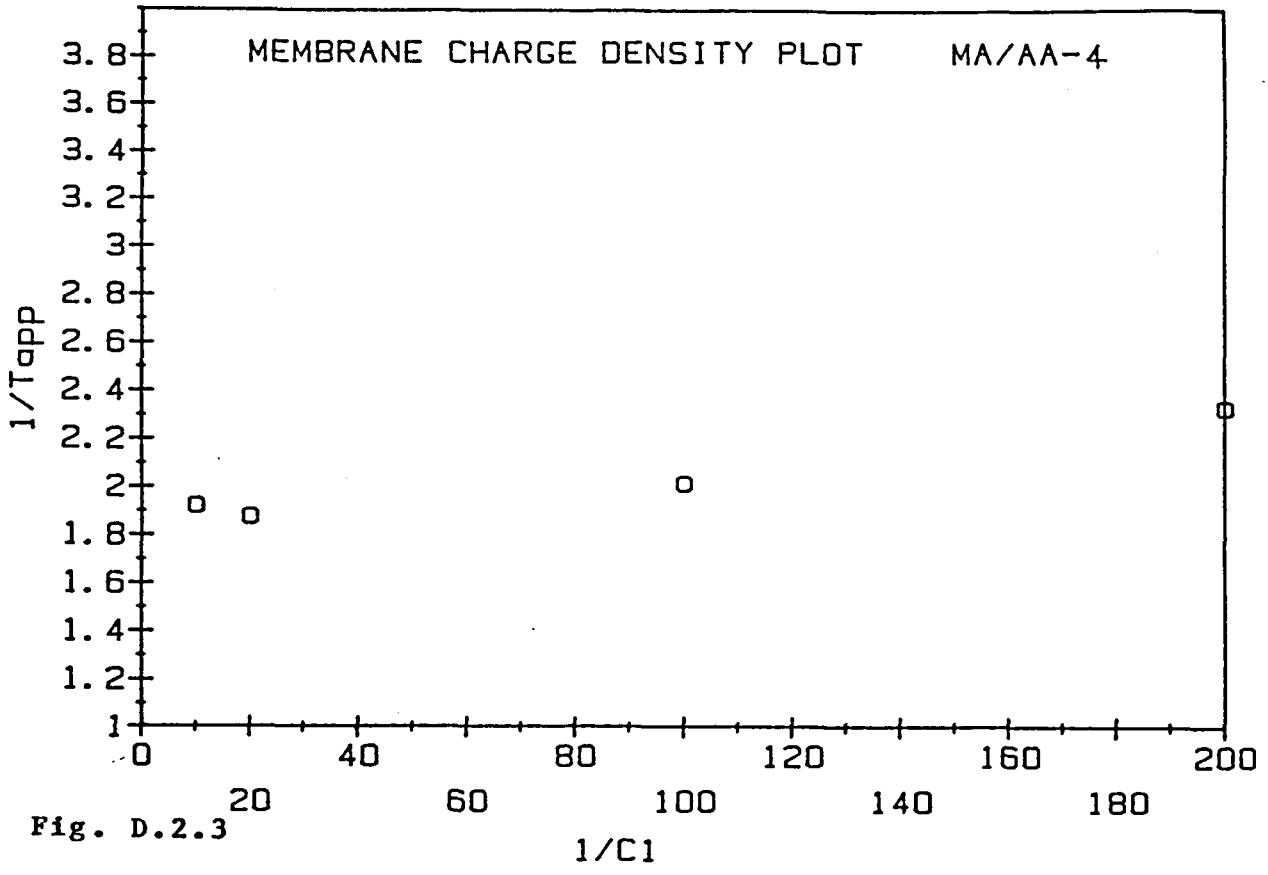

Fig. D.2.3

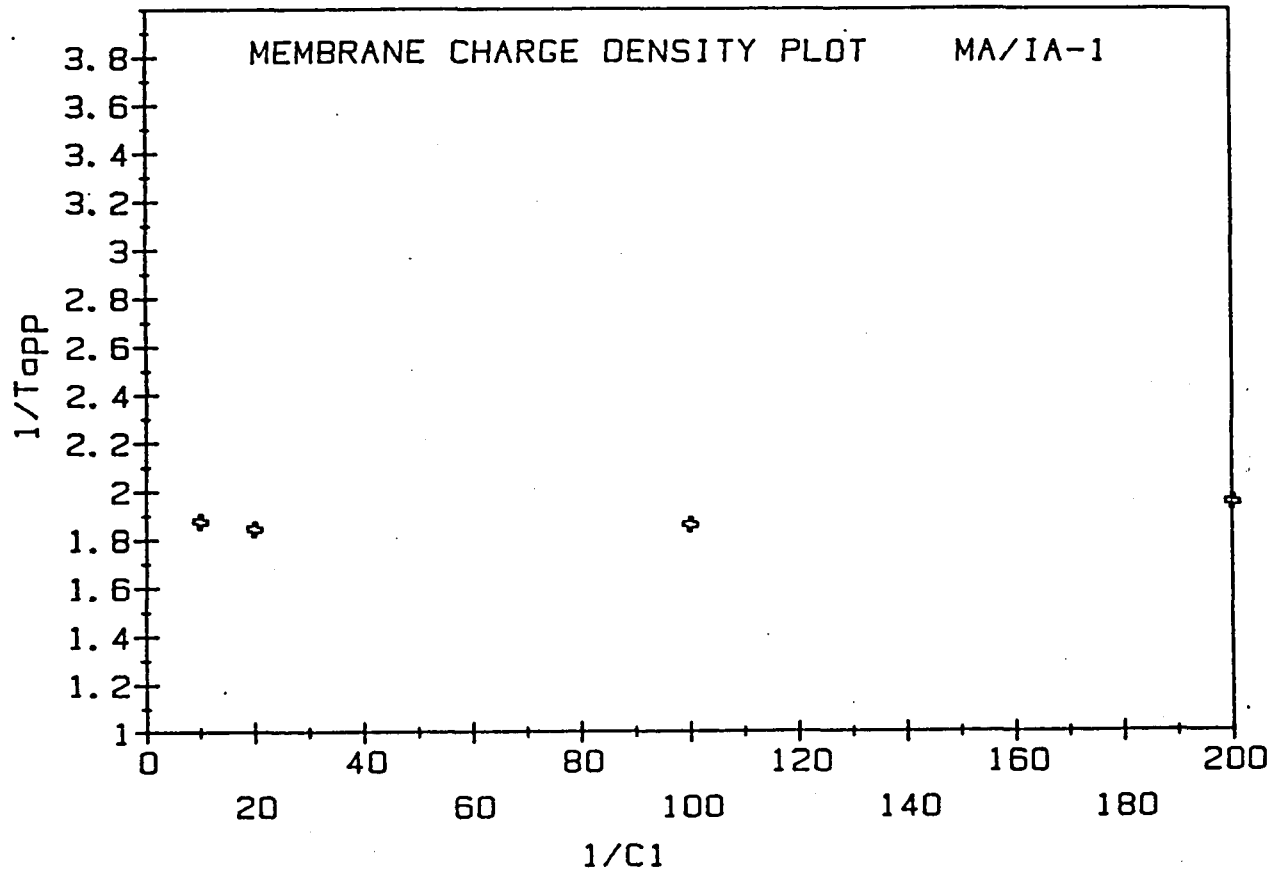

Fig. D.2.4

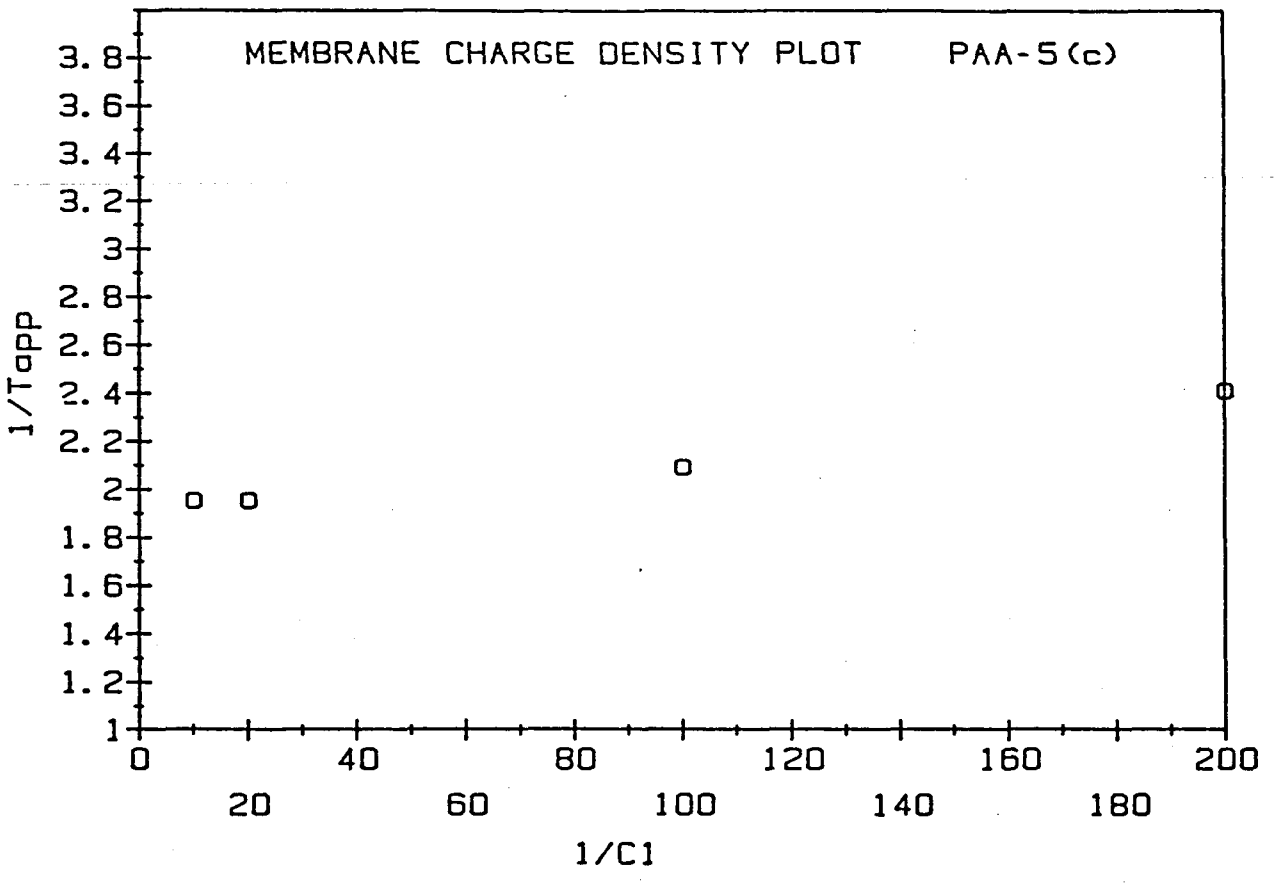
MEMBRANE CHARGE DENSITY PLOT PAA-5(c)
1/Tapp
3.8
3.6
3.4
3.2
3
2.8
2.6
2.4
2.2
2
1.8
1.6
1.4
1.2
1
0
20
40
60
80
100
120
140
160
180
200
1/C1

Fig. D.2.5

APPENDIX E - PHOTOGRAPHS

E.1 VACUUM POLYMERIZATION SYSTEM

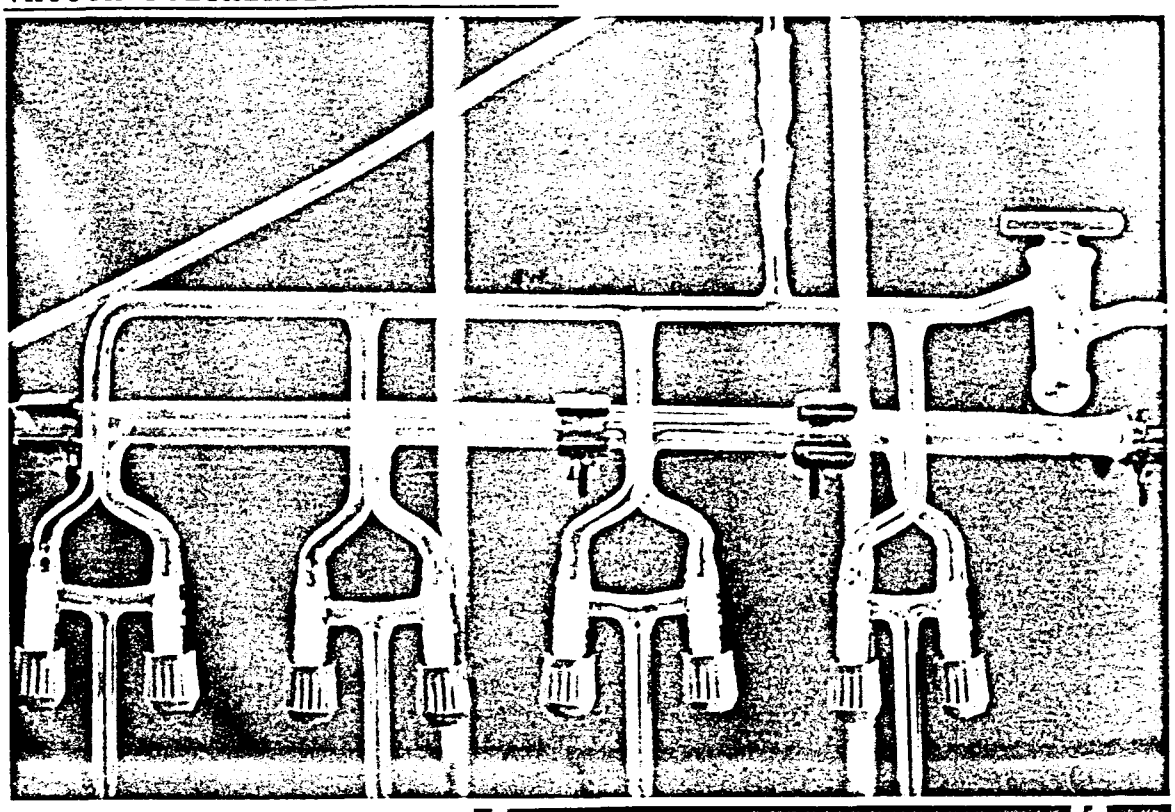

Fig. E.1.1 Vacuum and argon gas manifolds

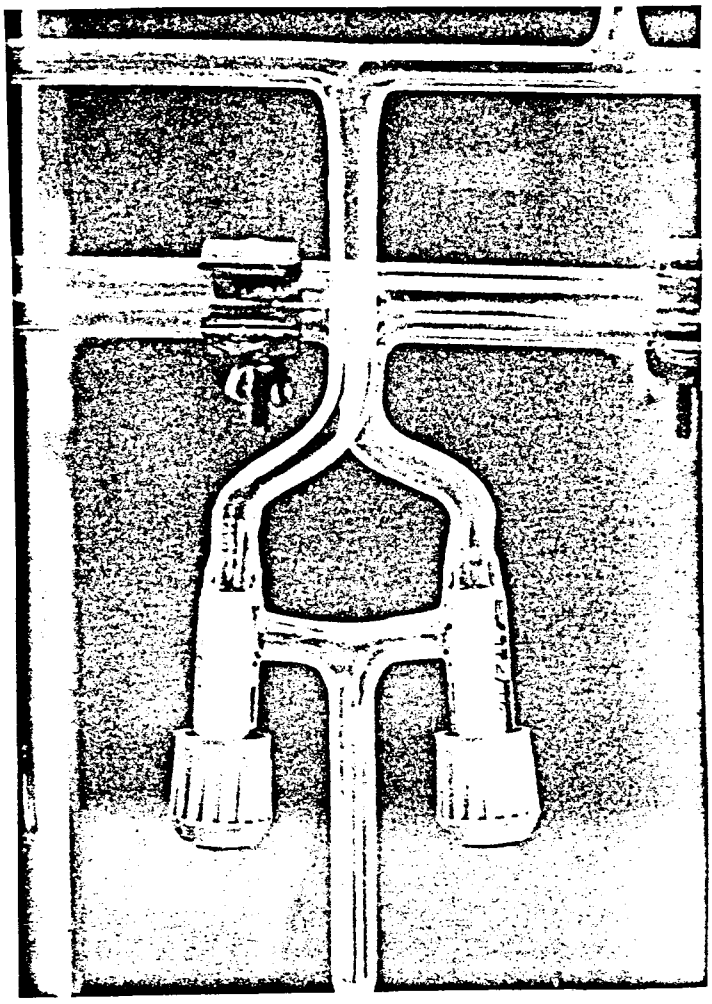

Fig. E.1.2 Detail of vacuum/gas changeover valves

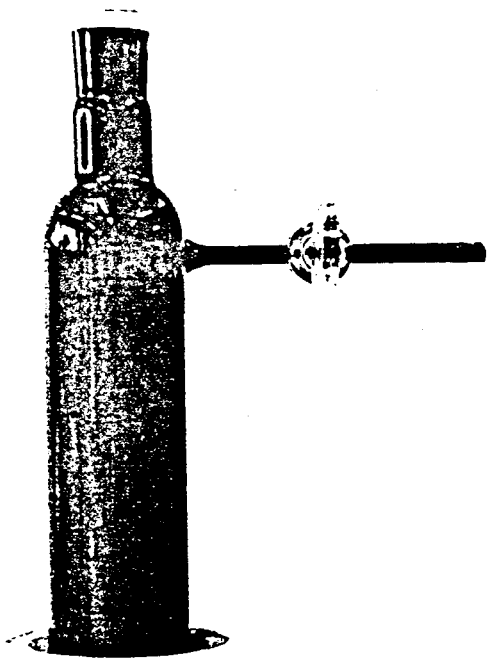

Fig. E.1.3 Reaction ampoule

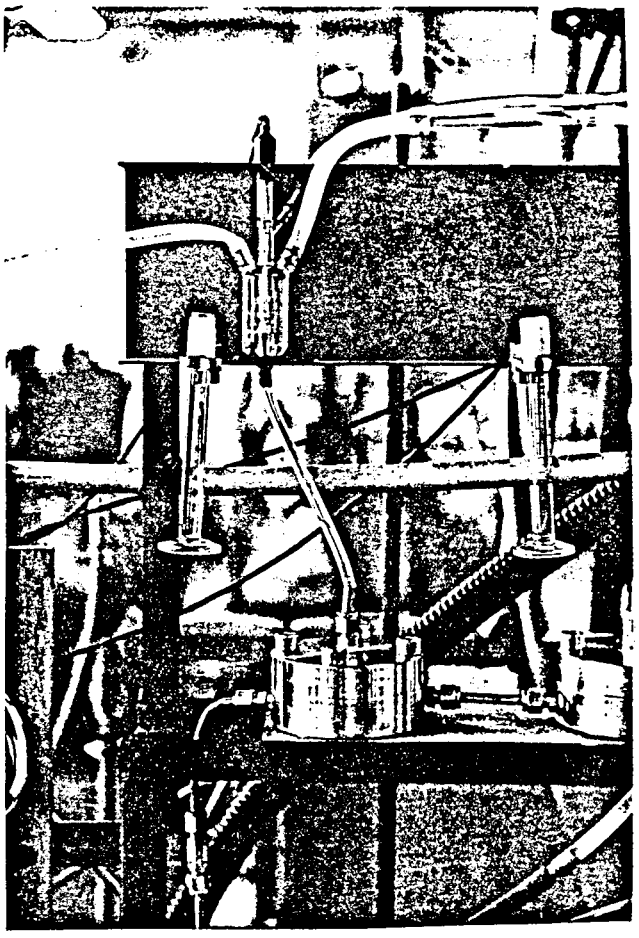

Fig. E.2.3 Single cell with conductivity measuring flow cell

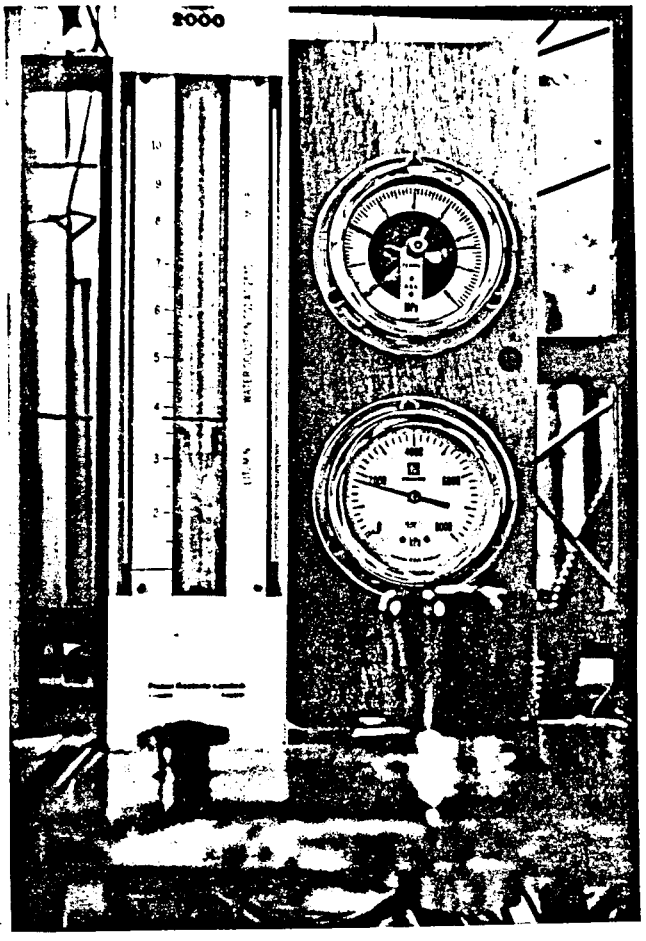

Fig. E.2.5 Inlet and outlet pressure gauges, flowmeter and valves

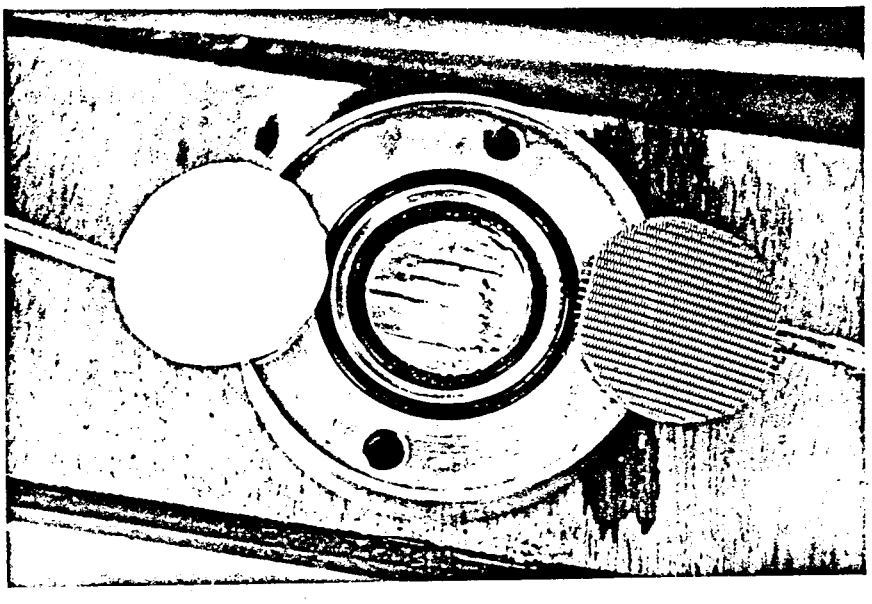

Fig. E.2.4 Test cell dismantled to show seals, turbulence promoting acrylic insert and s/s gauze backing disc

E.2 MEMBRANE FORMATION/EVALUATION EQUIPMENT

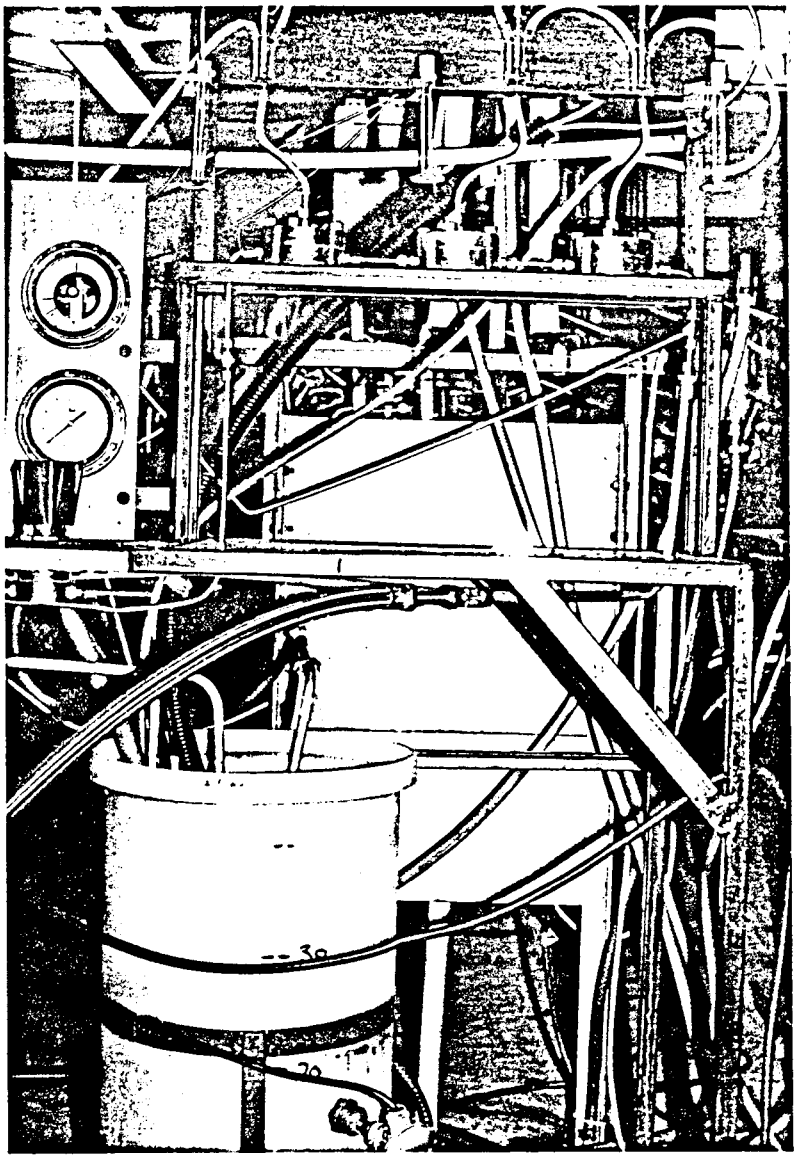

Fig. E.2.1
General view

Fig. E.2.2 Testcells connected to in-line conductivity measuring cells

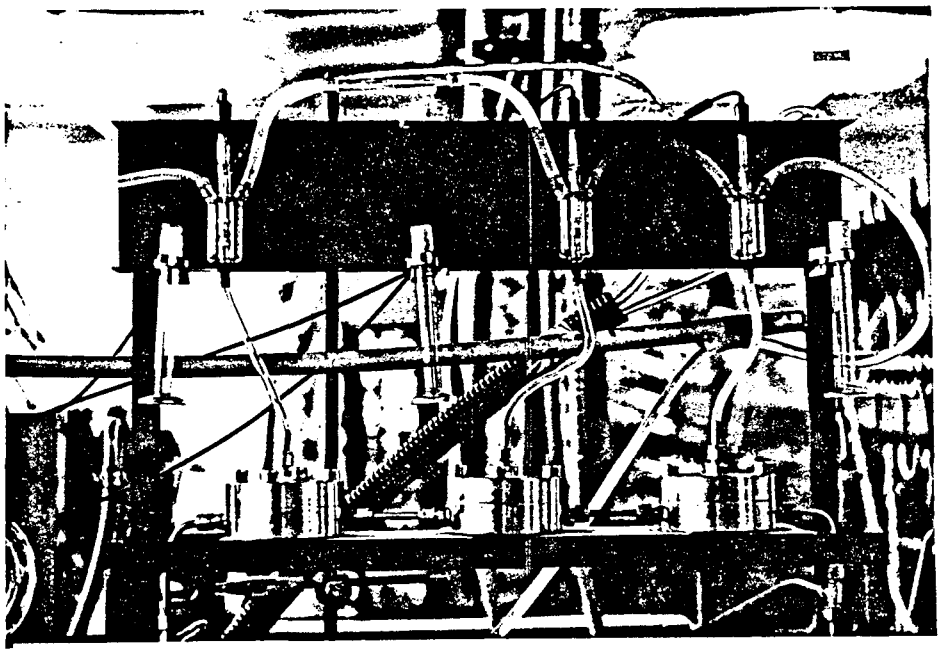

E.3 ELECTROLYTIC CELL FOR MEMBRANE POTENTIAL MEASUREMENTS

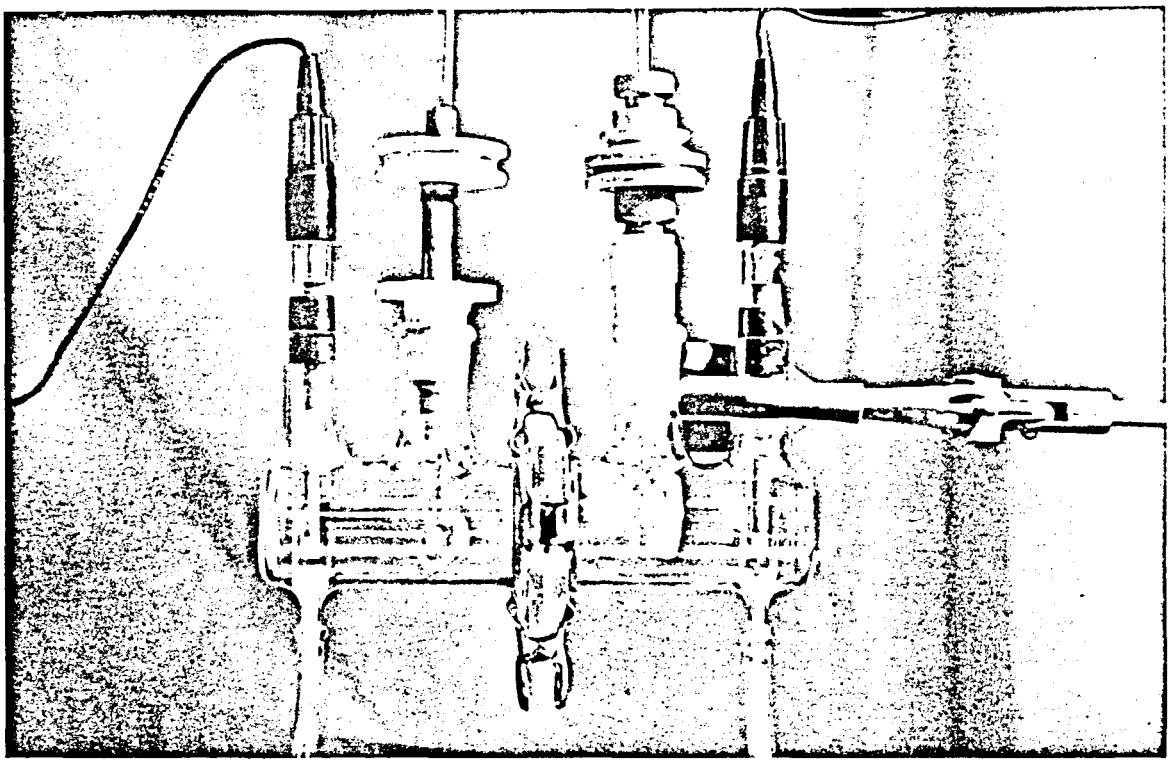

Fig. E.3.1 Assembled cell

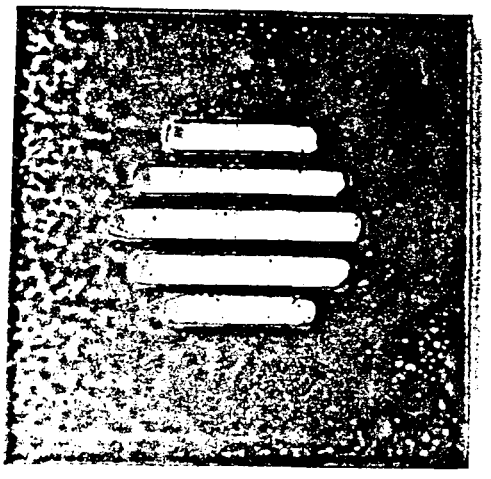

Fig. E.3.2 Acrylic "mask " for membrane clamping

BIBLIOGRAPHY

1. l'Hermite, M., **Ann. Chim. Phys.**, 43, 420, (1855).

2. Traube, M., **Archiv. fur anat., physiol., und wissench. medizin**, 87, (1867).

3. Findlay, A., **"Osmotic pressure"**, Longmans, London., (1913), p. 5.

4. Van't Hoff, J.H., **Ber.**, 27, 6, (1894).

5. McBain, J.W., Stuewer, J., **J. Phys. Chem.**, 40, 1153 (1936).

6. McBain, J.W., McClatchie, W.L., **J. Am. Chem. Sci.**, 55, 1315, (1933).

7. Reid, C.E., Breton, E.J., **J. Appl. Polymer Sci.**, 1, 133, (1959).

8. Breton, E.J., **Office of Saline Water Research and Development Progress Report, No. 16**, P B 161391 (1957).

9. Loeb, S., Sourirajan, S., **Advan. Chem. Ser.**, 38, 117, (1963).

10. Loeb, S., Sourirajan, S., **U.S. Patent, 3,133,132**, (May 12, 1964).

11. McKelvey, J.G., Spiegler, K.S., Wyllie, M.R.J., **J. Phys. Chem.**, 61, 174, (1957).

12. Berger, C., Hubata, R., Plizga, M., **Office of Saline Water Research and Development Progress Report No. 138**, (1965).

13. McKelvey, J.G., Milne, J.H., in "**Clays and Minerals**", (Bradley, W.F.-Ed.), 248, MacMillan, New York, (1962).

14. Srivastava, R.C., Yadav, S., **Indian J. Chem.**, 16A, 920, (1978).

15. Kraus, K.A., Marcinowski, A.E., Johnson, J.S., Schor, A.J., **Science**, 151, 194, (1966).

16. Elmer, T.H., **Am. Chem. Soc. Bull.**, 57 (11), (1978).

17. Sourirajan, S., "**Reverse Osmosis**", Academic press, (1970).

18. Dresner, L., Johnson (Jnr.), J.S., "**Principles of Desalination**", (Spiegler, K.S., Laird, A.D.K., Eds.), Academic Press, (1980).

19. Sachs, S.B., Lonsdale, H.K., **J. Appl. Polym. Sci.**, 15 (4), 797, (1971).

20. Sachs, S.B., Zisner, E., **Util. brackish water, Proc. Isr. Symp. Desalin.**, 9th, 70, (1972).

21. Banks, W., Sharpes, A., **J. Appl. Chem.**, 16, 28, (1966).

22. Kremen, S.S., **U.S. Patent 3 887 978**, (1975).

23. Tadahiro, U., Masaru, K., Inoue, T., **Eur. Pat. App., EP 72 002.**

24. Huang, R.Y.M., Gao, C.J., Kim, J.J., **J. Appl. Polym. Sci.**, 28 (10), 3063, (1983).

25. Toray Industries Inc., **Japan Kokai Tokkyo Koho 80 114 306.**

26. Dalton, G.L., Pienaar, H.S., Sanderson, R.D., **Desalination**, 24, 235, (1978).

27. Shteinberg, L.A., Yavorskaya, E.S., **USSR patent 449 918**, (1974).

28. Habert, A.C., Burns, C.M., Huang, R.Y.M., **J. Appl. Polym. Sci.**, 24 (3), 801, (1979).

29. Vasil'ev, A.A., Gershmann, M.B., Vasil'eva, T.A., **Zh. Prikl. Khim.**, 38 (12), 2869, (1965).

30. Wydeven, T., Katz, M.G., **U.S. Patent application, US 392** 092, (1983).

31. Gregor, H.P., **U.S. Publ. Pat. Appl. B433 930**, (1976).

32. Koyama, K., Okada, M., Nishimura, M., **J. Appl. Polym. Sci.**, 27 (8), 2783, (1982).

33. Mizrahi, S., Hsu, H.J., Gregor, H.P., Gryte, C.C., **Am. Chem. Soc. Div. Org. Coat. Plast. Chem. Pap.**, 35 (1), 468, (1975).

34. Gryte, C.C., Chen, J., Kevorkian, V., Gregor, H.P., **J. Appl. Polym. Sci.**, 23 (9), 2611, (1979).

35. Endoh, R., Tanaka, T., Kurihara, M., Ikeda, K., **Desalination**, 21 (1), 35, (1977).

36. Suminoe, T., Aotani, S., Kobayashi, Y., **Japan Kokai** 76 50 293 (1976).

37. Kuppers, J.R., Harrison, N., Johnson (Jnr), J.S., **J. Appl. Polym. Sci.**, 10, 969, (1966).

38. Dickson, J.M., Lloyd, D.R., Huang, R.Y.M., **J. Appl. Polym**

Sci., 24, 1341, (1979).

39. Marcinowsky, A.E., Kraus, K.A., Phillips, H.O., Johnson (Jnr.), J.S., Shor, A.J., **J. Am. Chem. Soc.**, 88(24), 5744, (1966).

40. Kraus, K.A., Phillips, H.O., Markinowsky, A.E., Johnson, J.S., Shor, A.J., **Desalination**, 1, 225, (1966).

41. Kraus, K.A., Shor, A.J., Johnson, J.S., **Desalination**, 2, 243, (1967).

42. Sachs, S.B., Baldwin, W.H., Johnson (Jnr.), J.S., **Desalination**, 6, 215, (1969).

43. Johnson (Jnr.), J.S., Minturn, R.E., Wadia, P.H., **J. Electroanal. Chem.**, 37, (1972).

44. Freilich, D., Tanny, G.B., **J. Coll. Interface. Sci.**, 64(2), 362, (1978).

45. Tanny, G.B., Johnson (Jnr.), J.S., **J. App. Polym. Sci.**, 22, 289, (1978).

46. Freilich, D., Tanny, G.B., **Desalination**, 27, 233, (1978).

47. Tanny, G.B., **Sep. and purif. methods**, 7(2), 183, (1978).

48. Igawa, M., Seno, M., Takahashi, H., Yamabe, T., **Desalination**, 22, 281, (1977).

49. Johnson (Jnr.), J.S., Kraus, K.A., Fleming, S.M., Cochran (Jnr) H.D., Perona, J.J., **Desalination**, 5(3), 359, (1968).

50. Spencer, H.G., Todd, D.K., McClellan, D.B., **Desalination**, 49, 193, (1984).

51. Ozari, Y., Tanny, G.B., Jagur-Grodzinski, J., **J. Appl. Polym. Sci.**, 21, 555, (1977).

52. Igawa, M., Seno, M., Takahashi, H., Yamabe, T., **J. Appl. Polym. Sci.**, 22, 1607, (1978).

53. Perona, J.J., Butt, F.H., Fleming, S.M., Mayer, S.T., Spitz, R.A., Brown, M.K., Cochran, H.D., Kraus, K.A., Johnson (Jnr.), J.S., **Environmental Science and Technology**, 1, 991, (1967).

54. Antoniou, S., Springer, J., Grohmann, A., **Desalination**, 32, 47, (1980).

55. El-Nashar, A.M., **Desalination**, 33, 21, (1980).

56. Minturn, R.E., Johnson (Jnr.) J.A., Schofield, W.M., Todd, D.K., **Water Research**, 8, 921, (1974).

57. El-Nashar, A.M., **Desalination**, 23, 1, (1977).

58. Brandon, C.A., Gaddis, J.L., **A.S.M.E. publication 75-ENAS-46**, (1975).

59. Groves, G.R., Buckley, C.A., Cox, J.M., Macmillan, C.D., Simpson, M.J., **Desalination**, 47, 305, (1983).

60. Lang, J.L., Pavelich, W.A., Clarey, H.C., **J. Polym. Sci.**, 55, 531, (1961).

61. Lang, J.L., Pavelich, W.A., Clarey, H.L., **J. Polym. Sci. A-1**, 1, 1123, (1963).

62. Heseding, C., Schneider, C., **Eur. Polym. J.**, 13, 387, (1977).

63. Bartlett, P.D., Nozaki, K., **J. Am. Chem. Soc.**, 68, 1497,

(1946).

64. General Aniline Film, US Patent 3 385 834 (1968).

65. Proctor and Gamble Co., Brit. Pat. 1 073 323 (1967).

66. Braun, D., El Sayed, I.A.A., Pomakis, J., Makromol. Chem., 124, 249, (1969).

67. Ordelt, Z., Collect. Czech, Chem. Commun., 38(7), 1930, (1967).

68. Gaylord, N.G., Maiti, S., J. Polym. Sci. Polym. Lett. Ed., 11, 253, (1973).

69. Gaylord, N.G., J. Macromol. Sci. Rev. Macromol. Chem., C13(2), 235, (1975).

70. Araki, M., Kato, K., Kayanagi, T., Machida, S., J. Macromol. Sci. Chem., A11(5), 1039, (1971).

71. Papisov, I.M., Garina, S., Kabanov, V.A., Kargin, V.A., Vysokomol. Soedin, B11, 614, (1969).

72. Du Plessis, T.A., Lustigand, A., Greyling, E., J. Macromol. Sci. Chem., A11(5), 1015, (1977).

73. Panasenko, A.A., Senchenko, O.G., Sultanova, V.S., Arbuzova, L.N., Minsker, K.S., Vysokomol. Soedin., B16(9), 645, (1974).

74. G.A.F. Corporation. Brit. Pat. 712 220 (1954).

75. Caze, C., Loucheux, C., J. Makromol. Sci. Chem., 7(4), 991, (1973).

76. Caze, C., Loucheux, C., **J. Makromol. Sci. Chem.**, A9(1), 29, (1975).

77. Ghesquiere, D., Arnaud, R., Caze, C., **J. Phys, Chem.**, 83(15), 2029, (1979).

78. Vinyl Products, **Brit. Pat. 887 356** (1962).

79. Hattori, K., Komeda, Y., **Kogyo Kagaku Zasschi.**, 68(9), 1729, (1965).

80. Ismailov, A.G., Rzaev, Z.M., Movsum-Zade, A.A., Rasulov, N.S., Bryksiva, L.V., **Azerb, Chim. Zh.**, 3, 114, (1973).

81. El Saied, A.A., Mirlina, S.Y., Kargin, V.A., **Vysokomol. Soedin.**, A11(2), 282, (1969).

82. Shantarovich, P.S., Sosnovskaya, L.N., Potapova, T.P., **Izv. Adak. Nauk. SSR Ser. Khim.**, 10, 2250, (1970).

83. Yakovleva, M.K., Sheinker, A.P., Abkin, A.D., **Radiats. Khim.**, 2, 251, (1972).

84. Coleman, L.E., Bork, J.F., Wyman, D.P., Hoke, D.I., **J. Polym. Sci.**, A3(4), 1601, (1965).

85. Kurdubov, Y.F., Baramboim, N.K., **Kozh. Obuvn. Prom. St.**, 22(8), 52, (1981).

86. Lion Fat and Oil Co., **Jap. Pat. 149 705** (1975).

87. Research Institute for Production development. **Jap. Pat. 56 776** (1973).

88. Gulf research corp. **Fr. Pat. 2 050 077** (1971).

89. Ford motor Co. **Jap. Pat. 48 490** (1976).

90. Dresner, L., Johnson (Jnr.), J.S., **in :Principles of desalination"**, 2nd Edition, part B. (Spiegler, K.S., Laird, A.D.K., -editors), **Academic press**, 1980, ISBN 0-12-656702-6 (V.2).

91. Johnson, J.S., Kraus, K.A., **J. Am. Chem. Soc.**, 78, 3937, (1956).

92. Clearfield, A., Vaughan, P.A., **Acta. Cryst.**, 9, 555, (1956).

93. Clearfield, A., **Rev. Pure and Appl. Chem.**, 14, 91, (1964).

94. Regel, W., Schneider, C., **Macromol. Chem. Phys.**, 182(1), 237, (1981).

95. Nakayama, Y., Hayashi, K., Okamura, S., **J. Appl. Polym. Sci.**, 18, 3633, (1974).

96. Nakayama, Y., Kondo, K., Takakura, K., Hayashi, K., Okamura, S., **J. Appl. Polym. Sci.**, 18, 3661, (1974).

97. Nakayama, K., Kondo, K., Takakura, K., Hayashi, K., Okamura, S., **J. Appl. Polym. Sci.**, 18, 3653, (1974).

98. Young, L.J., **in "Polymer Handbook"**,(Brandup, J. and Immergut, E.H., eds.), Wiley, New York (1975).

99. Mellville, H.W., Burnett, G.M., **J. Polym. Sci.**, 13, 417, (1954).

100. Alfrey (Jnr.), T., Price, C.C., **J. Polym. Sci.**, 2, 101, (1947).

101. Du Plessis, T.A., Lustigand, A., Greyling, E., **J. Macromol. Sci. Chem.**, A11(5), 1015, (1977).

102. GAF Corp., **Brit. Pat. 1 117 519** (1968).

103. Bevington, J.C., Nicora, C., **Polymer**, 13(6), 239, (1972).

104. Tsuchida, E., Tomono, T., **Makromol. Chem.**, 141, 265, (1972).

105. Tsuchida, E., Tomono, T., Sano, H., **Makromol. Chem.**, 151, 245, (1972).

106. Gaylord, N.G., **J. Makromol. Sci.**, A6, 259, (1972).

107. Nikolayev, A.F., Bordrenko, V.M., Shakalova, N.K., **Vysokomol. Soedin**, B16(1), 14, (1974).

108. Jedlinski, L., Maslinski-Solich, J., **J. Polym. Sci.**, C42, 411, (1971).

109. Pravednikov, A.N., Novikov, S.N., **Vysokomol. Soedin.**, A13, 1404, (1971).

110. Hirooka, M., **J. Polym. Sci.**, B10, 171, (1972).

111. Trivedi, B.C., Culbertson, B.M., in "**Maleic anhydride**", Plenum press, 1982, ISBN 0-306-40929-1.

112. Seymour, R.B., Garner, D.P., Sanders, L.J., **J. Macromol. Sci.**, A13(2), 173, (1979).

113. Grubisic, Z., Rempp. R., Benoit, H., **J. Polym. Sci.**, B5, 753, (1967).

114. Fox, T.G., Flory, P.J., **J. Am. Chem. Soc.**, 73, 1904, (1951).

115. Spatorico, A.L., Beyer, G.L., **J. Appl. Polym. Sci.**, 19, 2933, (1975).

116. Bose, A., Rollings, J.E., Caruthers, J.M., Okos, M.R., Tsao, G.T., J. Appl. Polym. Sci., 27, 795, (1982).

117. Waters Associates - Manual CU 84330 (1980).

118. Siebourg, W., Lundberg, R.D., Lenz, R.W., Macromolecules, 13, 1013, (1980).

119. Rinaudo, M., Desbrieres, J., Eur. Polym. J., 16, 849, (1980).

120. Waters Associates - private communication.

121. Thomas, D.G., Mixon, W.R., Desalination, 15, 287, (1974).

122. Nomura, T., Kimura, S., Desalination, 32, 57, (1980).

123. Hock, A.L., Chemistry and Industry, 2, 1, (1974).

124. Shor, A.J., phD Thesis, University of Tennessee, March 1968.

125. Lonsdale, H.K., Desalination, 13, 317, (1973).

126. Rosenfelt, J., Loeb, S., I and CE Process Design and Development, 6, 122, (1967).

127. Van Reenen, A., University of Stellenbosch, M.Sc. Thesis, (In print).

128. Toerell, T., Proc. Soc. Exptl. Biol., 33, 282, (1935).

129. Meyer, K.H., Sievers, J.F., Helv. Chim. Acta., 19, 649, 665, 987, (1936).

130. Kobatake, Y., Takeguchi, N., Toyoshima, Y., Fujita, H., J. Phys. Chem., 69(11), 3981, (1965).

131. Kobatake, Y., Yuasa, N., Fujita, H., **J. Phys. Chem.**, 72, 2871, (1972).

132. Kamo, N., Oikawa, M., Kobatake, Y., **J. Phys. Chem.**, 77(1), 92, (1973).

133. Beg, M.N., Siddiqi, F.A., Shyam, R., **Can. J. Chem.**, 55, 1680, (1977).

134. Kobatake, Y., Kamo, N., **Prog. Polym. Sci. Jpn.**, 5, 257 (1972).

135. Mason, F.A., **J. Chem. Soc.**, 700, (1930).

136. Brown, A.L., Ritchie, P.L., **J. Chem. Soc.**, C, 2007, (1968).

137. Merck index, (Windholtz, M.ed.), Rayway, N.J., 9th Ed., (1978).

138. Treurnicht, Ilse, **M.Sc. Thesis**, University of Stellenbosch, (1979).

139. Imoto, E., Horiuchi, H., **Chem. High Polymers Jap.**, 8, 463, (1951).

140. Cobianu, N., et. al., **Ind. Usoara: Text., Tricotaje, Confectii Text.**, 32(8), 348, (1981).

141. Heuck, C., Lederer, M., (Farb. Hoechst A-G), **U.S. Patent 3 457 240** (22 July 1969).

142. General Ainline and Film Corp., **Belgian Patent 672 161** (March 1 1966).

143. General Ainline and Film Corp., **U.S. Patent 3, 385, 843** (May 28, 1968).

144. Rzaev, Z.M., Dzhafarov, R.V., Ibragimova, D., Masterova, M.N., Zubov, V.P., **Vysokomol. Soedin. Ser. B.**, 24(10), 728, (1982).

145. Hahn, F.L., Weiler, G., **Z. Anal. Chem.**, 69, 417, (1926).

146. Spencer, H.G., **Desalination**, 52, 1, (1984).

147. Nakagawa, U., Edogawa, K., Kurihara, M., Tonomura, T., **"Solute Separation and Transport Characteristics through PEC-1000 Reverse Osmosis Membranes". Presented at the Symposium on Reverse Osmosis and Ultrafiltration**, ACS meeting, Philadelphia, August, 1984.

148. Dubin, P.L., Strauss, U.P., **J. Phys. Chem.**, 74(14), 2842, (1970).

149. Strauss, U.P., Andrechak, J.A., **J. Polym. Sci. Polym. Chem. Ed.**, 23, 1063 (1985).

150. Eisenberg, A., King, M., **in "Polymer Physics, vol. 2"**, (Stein R.S. Ed.), Academic Press, New York 1977. ISBN 0-12-235050-2.

151. Longworth, R., in **"Ionic Polymers"** (Holliday, L. ed.), ch II., Halstead Press, Wiley, New York, 1975.

152. Marx., C.L. Caulfield, D.F., Cooper, S.L., **Macromolecules**, 6, 344, (1973).

153. Macknight, W.J., **Am. Chem. Soc. Polym. Preprints**, 11, 504, (1970).

154. Barbieri, B.W., Strauss, U.P., **Macromolecules**, 18, 411, (1985).